

MESTRADO
TOXICOLOGIA E CONTAMINAÇÃO AMBIENTAIS

Bioactivity screening of cyanobacteria for the isolation of novel anticancer compounds using 2D and 3D cell culture models

Leonor do Amaral Silva Ferreira

M

2018

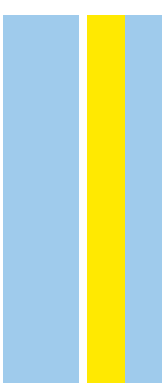
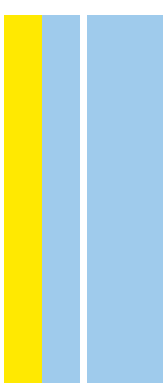
Leonor do Amaral Silva Ferreira. Bioactivity screening of cyanobacteria for the isolation of novel anticancer compounds using 2D and 3D cell culture models



M.I.C.B.A.S 2018

Bioactivity screening of cyanobacteria for the isolation of novel anticancer compounds using 2D and 3D cell culture models

Leonor do Amaral Silva Ferreira



Leonor do Amaral Silva Ferreira

Bioactivity screening of cyanobacteria for the isolation of novel anticancer compounds using 2D and 3D cell culture models

Dissertação de Candidatura ao grau de mestre em Toxicologia e Contaminação Ambientais submetida ao Instituto de Ciências Biomédicas de Abel Salazar da Universidade do Porto

Orientador – Doutor Ralph Urbatzka

Categoria – Investigador Pós-Doutoramento

Afiliação – Centro Interdisciplinar de Investigação Marinha e Ambiental

Coorientador – Professor Doutor Vitor Vasconcelos

Categoria – Professor Catedrático

Afiliação – Faculdade de Ciências da Universidade do Porto/Centro Interdisciplinar de Investigação Marinha e Ambiental

Acknowledgements

My deepest appreciation goes to my supervisor, Dr Ralph Urbatzka, for all the guidance and support and for all the insights and knowledge shared with me during this work, and to my co-supervisor, Professor Doctor Vitor Vasconcelos, for giving me such a great opportunity to work in this project and in this amazing team.

To Dr Marco Preto for all the time, knowledge and help he provided for the chemistry work and to Maria Lúcia Sousa for teaching me all about spheroids and for helping me work the results. Thank you so much.

To everyone on the BBE lab, thank you so much for welcoming me and helping me with anything I needed, especially to Dr Mariana Reis and Tiago Ribeiro for guiding me through the beginning of my work. I would also like to thank LEGE Culture Collection for providing the cyanobacterial strains used on this work.

To my friends and family, who put up with me despite all and still support me even in the toughest times. To all my friends and colleagues, André, Beatriz, Cristiana, Margarida, Mariana, Mário, Marlene, Natália, Pedro and Ricardo for the company and support throughout this work and for the movies, lunches and dinners and all the relaxation moments. To my sister, for always being there for me. To Luís, thank you so much for being my emotional support throughout all this work and for everything you do for me. To my parents for giving me the strength and the means to become someone better and to always push myself harder. I could not have done it without you all.

I would also like to thank Interdisciplinary Centre of Marine and Environmental Research (CIIMAR), Institute of Biomedical Sciences of Abel Salazar from the University of Porto (ICBAS) and Faculty of Sciences from the University of Porto (FCUP).

This work was supported by the project INNOVMAR - Innovation and Sustainability in the Management and Exploitation of Marine Resources (reference NORTE-01-0145-FEDER-000035, within the research line NOVELMAR, supported by North Portugal Regional Operational Program (NORTE 2020), under the PORTUGAL 2020 Partnership Agreement, through the European Regional Development Fund (ERDF).

Abstract

Cancer is one of the deadliest diseases of our time, responsible for killing over 9 million people in 2018, and it is believed that this number will increase in the future. New therapeutics are being studied in order to find more effective anticancer drugs, with different modes of action. Natural products have been, for a long time now, a reliable source of compounds with interesting properties for human health. Due to the ocean's biodiversity, marine organisms are seen more and more as a source of natural compounds with unique and diverse structures, with potential applications in various fields. Drugs like Trabectedin and Eribulin mesylate (commercially available as Yondelis and Halaven, respectively) are originated from marine organisms and are currently being used as anticancer drugs, with many more bioactive compounds yet to be found. Cyanobacteria are photosynthetic and ubiquitous microorganisms, known to produce potentially bioactive secondary metabolites.

In the work here presented, different cyanobacteria strains from the LEGE Culture Collection, of the BBE group at CIIMAR, were tested for anticancer bioactivity, either on 2D cell culture of the MG-63 cell line, where MTT assays were performed, as well as on 3D cell culture of HCT 116 spheroids, using both fluorescence microscopy and spectroscopy. In order to isolate the compound responsible for the activity, a bioassay-guided fractionation was followed. The crude extract from the cyanobacteria biomass was fractionated by vacuum liquid chromatography, according to a gradient of polarity. Further sub-fractionations of the active fractions were performed using different separation techniques, depending on the sample's characteristics, using column chromatography and HPLC, combined with NMR, LC-MS or fragmentation by ESI techniques to further elucidate the molecule responsible for the bioactivity.

Several fractions of the tested strains showed an interesting cytotoxic activity against cancer cells. Fractions E14031 E5D2, E15074 B4I and E18184 H, originated from the genus *Synechocystis* (*Synechocystis* sp. LEGE 07211, *Synechocystis salina* LEGE 06099 and *Synechocystis* sp. LEGE 06005, respectively) reduced the cell viability of MG-63 cell line after 48h of exposure. Fractions E17165 A7O2, E17165 A7O5, E17165 A7O8C, E17165 A7O8D, E17165 A7O8E and E17165 A7O8F, extracted from the biomass of *Nodosilinea nodulosa* LEGE 06102 diminished the mitochondrial activity of cells from the same cell line as before. These fractions have the potential to isolate new molecules with cytotoxic properties against cancer cells.

However, the assays made on 3D spheroids of the HCT 116 cell line showed bioactivity from different fractions in comparison to the results from the 2D culture model, unveiling selectivity for cell lines and possible differences in chemical properties of the bioactive compounds. As spheroids are a better model for solid tumours, these results are very promising, but this methodology still needs some improvement in order to obtain more

definitive results. Fractions E15074 H, E18179 F, E17165 D and E18184 H were the most bioactive in 3D assays.

In order to obtain chemical information about the components of the bioactive fractions, techniques like proton NMR spectroscopy, HPLC, LC-MS and fragmentation by ESI were decisive to help to create an idea of the molecule's properties and, in the future, to possibly elucidate the chemical structure of said compounds.

In summary, multiple fractions from cyanobacteria extracts displayed cytotoxic bioactivity on cancer cells, which further highlights that these microorganisms are a very interesting source of new anticancer compounds. More research is needed in order to fully assess all their potential, as well as to develop more physiologically sensitive and relevant methods for anticancer screening of cyanobacteria.

Keywords: Cyanobacteria metabolites, Bioassay-guided fractionation, Anticancer activity, 2D cell models, 3D cell models, MTT assay, fluorescence microscopy, NMR spectroscopy, LC-MS

Resumo

O Cancro é uma das principais causas de morte mundiais estando estimado que cause a morte de cerca de 9 milhões de pessoas em 2018. Estes valores justificam a necessidade de encontrar novos medicamentos, com diferentes modos de ação e mais eficazes. Produtos naturais têm sido ao longo de muitos anos fonte de vários compostos com propriedades biológicas interessantes para a saúde humana. O diverso e ainda desconhecido ambiente marinho tem sido visto como fonte de obtenção de novos produtos, nomeadamente os microrganismos, uma vez que possuem a capacidade de produzir metabolitos secundários com estruturas químicas únicas e diversas, e ainda com possíveis aplicações em várias áreas. A Trabectedin e Eribulin mesylate (de nome comercial Yondelis e Halaven, respetivamente) são medicamentos inspirados em compostos obtidos a partir de organismos marinhos e são atualmente usados no tratamento de alguns tipos de cancro. As cianobactérias são microrganismos fotossintéticos que são encontrados nos mais diversos ambientes e que são atualmente reconhecidos por produzirem metabolitos secundários bioativos.

No trabalho aqui apresentado, diferentes estirpes de cianobactérias pertencentes à coleção de cianobactérias LEGE Culture Collection do grupo BBE do CIIMAR, foram testadas para atividade anticancerígena, em modelos de cultura 2D da linha celular MG-63, por ensaios MTT, mas também em culturas em 3D, usando esferoides da linha celular HCT 116, analisados por microscopia e espectroscopia de fluorescência. Para isolar o composto responsável pela bioatividade, seguiu-se um fracionamento guiado pelos ensaios de bioatividade. O crude obtido da biomassa das cianobactérias foi fracionado por um gradiente de polaridade crescente, e os fracionamentos seguintes das frações bioativas realizaram-se por cromatografia em coluna e HPLC, combinados com técnicas como NMR, LC-MS e fragmentação para elucidação química dos compostos bioativos.

Das estirpes testadas, várias frações mostraram interferir com a viabilidade celular. Frações E14031 E5D2, E15074 B4I e E18184 H, todas de origem no género *Synechocystis* (*Synechocystis* sp. LEGE 07211, *Synechocystis salina* LEGE 06099 e *Synechocystis* sp. LEGE 06005, respetivamente) reduziram a viabilidade celular da linha MG-63, após 48h de exposição. Frações E17165 A7O2, E17165 A7O5, E17165 A7O8C, E17165 A7O8D, E17165 A7O8E e E17165 A7O8F, extraídas de biomassa de *Nodosilinea nodulosa* LEGE 06102, diminuíram a atividade mitocondrial da mesma linha celular. Todas estas frações têm potencial para isolar novas moléculas com propriedades citotóxicas contra células cancerígenas.

No entanto, os testes feitos em esferoides 3D da linha celular HCT 116, usando microscopia e espectrofotometria de fluorescência, mostraram resultados diferentes dos obtidos nos modelos 2D, apresentando uma possível seletividade no que toca à linha

celular e possíveis diferenças nas propriedades químicas dos compostos bioativos. Este ensaio é um modelo mais representativo para tumores sólidos, sendo os seus resultados promissores. No entanto, esta metodologia precisa ainda de ser aprimorada para se avaliar mais precisamente a bioatividade das frações às quais as células são expostas. As frações E15074 H, E18179 F, E17165 D e E18184 H foram as mais bioativas nos ensaios em 3D.

De forma a obter alguma informação no que toca aos componentes das frações bioativas, técnicas como ressonância magnética nuclear, HPLC, LC-MS e fragmentação por ESI, foram decisivas para se ter uma ideia das propriedades químicas das frações, e para que no futuro seja possível elucidar a estrutura química dos compostos.

Várias frações de extratos de diferentes cianobactérias apresentaram bioatividade anti cancro, provando que estes microrganismos são uma fonte interessante para isolar novos compostos, sendo necessária mais pesquisa de forma a avaliar todo o seu potencial, e também para desenvolver novos testes fisiologicamente mais sensíveis e pertinentes para rastreio de bioatividade de metabolitos secundários de cianobactérias.

Palavras-chave: metabolitos de cianobactérias, metabolitos secundários, atividade anti cancro, modelos celulares 2D, modelos celulares 3D, MTT, microscopia de fluorescência, RMN, LC-MS

Work dissemination

During the course of this work a poster communication entitled "**Bioactivity screening of cyanobacteria for the isolation of novel anticancer compounds using 2D and 3D cell culture models.**" Was presented at the *IMMR - International Meeting on Marine Research*, 5 and 6th of July 2018, Peniche, Leiria, Portugal (Appendix I)

Index

1. Introduction.....	1
1.1. Cancer.....	1
1.1.1. Causes of cancer.....	3
1.1.2. Cancer Statistics.....	4
1.1.3. Cancer treatment strategies and future perspectives.....	4
1.2. Natural products discovery.....	5
1.3. Cyanobacteria as a source of natural products.....	7
1.3.1. Cyanobacteria.....	7
1.3.2. Cyanobacteria bioactive compounds.....	8
1.3.3. Cyanobacteria anticancer compounds.....	9
2. Objectives.....	10
3. Materials and Methods.....	11
3.1. Cyanobacteria cultures.....	11
3.1.1. Biomass extraction and fractionation.....	11
3.2. Bioassay-guided fractionation.....	14
3.2.1. Sub-fractioning of E14031 E5D.....	14
3.2.2. Sub fractioning of E15074 B.....	15
3.2.3. Sub fractioning of E15074 B4.....	15
3.2.4. Sub fractioning of E17165 A.....	16
3.2.5. Sub fractioning of E17165 A7.....	17
3.2.6. Sub fractioning of E17165 A7O.....	19
3.2.7. Sub fractioning of E17165 A7O8.....	19
3.3. Cell culture and bioassays.....	20
3.3.1. MTT assays.....	20
3.3.2. Spheroids assays.....	21
4. Results.....	22
4.1. Biomass collection and fractionation.....	22
4.2. Bioassay-guided fractionations.....	23

4.2.1.	Screening and sub-fractionation of E14031 E5	23
4.2.2.	Screening and sub-fractionation of E15074	28
4.2.3.	Screening and sub-fractionation of E18179	33
4.2.4.	Screening and sub-fractionation of E17165	35
4.2.5.	Screening and sub-fractionation of E18184	41
4.3.	Spheroids of HCT-116 Cell Line – 3D cell model assays	42
4.3.1.	Screening of E15074	43
4.3.2.	Screening of E18179	45
4.3.3.	Screening of E17165	47
4.3.4.	Screening of E18184	49
5.	Discussion	51
5.1.	Bioactivity screening of cyanobacteria fractions	51
5.1.1.	Bioactivity in 2D.....	51
5.1.2.	Bioactivity in 3D.....	52
5.1.3.	Bioactive fractions in 2D vs 3D	54
5.2.	Difficulties in using the bioassay-guided fractionation of cyanobacteria fractions 57	
6.	Conclusion and future work	58
7.	References	59
8.	Appendix.....	67

Figure Index

Figure 1: Organic extraction of cyanobacterial biomass	12
Figure 2: VLC apparatus for the fractionation of cyanobacteria crude extracts.....	12
Figure 3: Sub-fractionation of E17165 A	17
Figure 4: TLC procedure and retention factor calculation	17
Figure 5: Cell viability after 24 and 48 hours of exposure to sub-fractions of E14031 E5 (top) and E14031 E5D (bottom), at a concentration of 20 µg/mL. Cells on Solvent Control were exposed to 0.5% DMSO, on Positive Control to 20% DMSO and on Control to culture medium only. All sub-fractions were exposed to at least 3 replicates and controls in 6 replicates, data are shown as mean +/- standard deviations.....	23
Figure 6: HPLC chromatogram of E14031 E5D	24
Figure 7: LC-MS data of sub-fraction E14031 E5D2. Sample was solubilized in MeOH. Peak at Rt = 13.02 minutes and the corresponding MS peak of [M + H] ⁺ = 623.289 m/z.....	25
Figure 8: ¹ H NMR spectrum of E14031 E5D2 at 600 MHz. Sample diluted in deuterated DMSO.....	26
Figure 9: Cell viability and standard deviation after 24 and 48 hours of exposure to VLC fractions of E15074 (top), sub-fractions of E15074 B (middle) and sub-fractions of E15074 B4 (bottom) at a concentration of 50 µg/mL. Cells on Solvent Control were exposed to 0.5% DMSO, on Positive Control to 20% DMSO and on Control to culture medium only. All sub-fractions were exposed to at least 3 replicates and controls in 6 replicates.....	28
Figure 10: Example of TLC of the collection tubes, to separate the sub-fractions	29
Figure 11: NMR spectrum of E15074 B4 at 400 MHz. Sample diluted in deuterated chloroform.....	30
Figure 12: LC-MS data from sample E15074 B4. Sample diluted in a mixture of CHCl ₃ : MeOH	30
Figure 13: Chromatogram of the sub-fractionation of E15074 B4.....	31
Figure 14: Cell viability after 24 and 48 hours of exposure to VLC fractions of E18179 (top), sub-fractions of E18179 DE (middle) and sub-fractions of E18179 DE3 (bottom) at a	

concentration of 50 µg/mL. Cells on Solvent Control were exposed to 0.5% DMSO, on Positive Control to 20% DMSO and on Control to culture medium only. All sub-fractions were exposed to at least 3 replicates and controls to 6 replicates, and data are shown as mean +/- standard deviations.....33

Figure 15: Cell viability after 24 and 48 hours of exposure to VLC fractions of E17165 (top, left), sub-fractions of E17165 A (top, right), sub-fractions of E17165 A7 (middle, left), E17165 A7O (middle, right) and E17165 A7O8 (bottom) at a concentration of 50 µg/mL. Cells on Solvent Control were exposed to 0.5% DMSO, on Positive Control to 20% DMSO and on Control to culture medium only. All sub-fractions were exposed to at least 3 replicates and controls to 6 replicates, and data are shown as mean +/- standard deviations.35

Figure 16: HPLC chromatogram of E17165 A7O37

Figure 17: ¹H NMR of E17165 A7O2 at 400 MHz. Sample was diluted in deuterated chloroform.....38

Figure 18: MS and MS/MS of E17165 A7O2. Sample was diluted in DCM. Peaks observed [M + H]⁺ = 441.405 m/z on the positive ionisation and [M + Cl]⁻ = 475.369 m/z on the negative ionization.38

Figure 19: HPLC chromatogram of E17165 A7O840

Figure 20: Cell viability after 24 and 48 hours of exposure to VLC fractions of E18184 at a concentration of 50 µg/mL. Cells on Solvent Control were exposed to 0.5% DMSO, on Positive Control to 20% DMSO and on Control to culture medium only. All fractions were exposed to at least 3 replicates and controls to 6 replicates, and data are shown as mean +/- standard deviations.41

Figure 21: ¹H NMR of E18184 H at 400 MHz. Sample was diluted in deuterated MeOH..42

Figure 22: Data analysis of the spheroids assay after 48 h exposure of E15074 fractions (30 µg/mL) to HCT 116 spheroids. For the fluorescence readings (left), a bottom read of the plate with an integration time of 500 ms at 340Ex/280Em for Hoechst 33342 and 535Ex/586Em for Propidium Iodide was used. For the microscopy imaging (right), filters for DAPI (for Hoechst 33342) and TRITC (for propidium iodide) were chosen at an integration time of 2 and 30 ms respectively. Solvent Control was 0.5% of DMSO and Doxorubicin (4µM) served as positive control. All tests were performed, at least, with triplicates.43

Figure 23: Microscopy imaging of HCT 116 spheroids after exposure to fraction E15074 H, Solvent Control (0.5% of DMSO) and Doxorubicin (4 μ M), as positive control. Filters for DAPI (for Hoechst 33342) and TRITC (for propidium iodide) were chosen, at an integration time of 2 and 30 ms respectively and 10x objective. All tests were performed, at least, with triplicates.44

Figure 24 Data analysis of the spheroids assay after 48 h exposure of E18179 fractions (30 μ g/mL) to HCT 116 spheroids. For the fluorescence readings (left), a bottom read of the plate with an integration time of 500 ms at 340Ex/280Em for Hoechst 33342, 485 Ex/538 Em for Calcein, and 535Ex/586Em for Propidium Iodide was used. For the microscopy imaging (right), filters for DAPI (for Hoechst 33342), FITC (for Calcein) and TRITC (for propidium iodide) were chosen, at an integration time of 1, 1 and 15 ms respectively. Solvent Control was 0.5% of DMSO and Paclitaxel (400 nM) served as positive control. All tests were performed, at least, with triplicates.45

Figure 25: Microscopy imaging of HCT 116 spheroids after exposure to fraction E18179 F, Solvent Control (0.5% of DMSO) and Paclitaxel (400 nM) as positive control. Filters for DAPI (for Hoechst 33342), FITC (for Calcein) and TRITC (for propidium iodide) were chosen, at an integration time of 1, 1 and 15 ms respectively and 10x objective. All tests were performed, at least, with triplicates.....46

Figure 26: Data analysis of the spheroids assay after 48 h exposure of E17165 fractions (30 μ g/mL) to HCT 116 spheroids. For the fluorescence spectroscopy readings (left), a bottom read of the plate with an integration time of 500 ms at 340Ex/280Em for Hoechst 33342, and 535Ex/586Em for Propidium Iodide was used. For the microscopy imaging (right), filters for DAPI (for Hoechst 33342) and TRITC (for propidium iodide) were chosen, at an integration time of 2 and 30 ms respectively. Solvent Control was 0.5% of DMSO and Doxorubicin (4 μ M) served as positive control. All tests were performed, at least, with triplicates.47

Figure 27: Microscopy imaging of HCT 116 spheroids after exposure to fraction E17165 D, Solvent Control (0.5% of DMSO) and Doxorubicin (4 μ M) as positive control. Filters for DAPI (for Hoechst 33342) and TRITC (for propidium iodide) were chosen, at an integration time of 2 and 30 ms respectively and 10x objective. All tests were performed, at least, with triplicates.48

Figure 28 Data analysis of the spheroids assay after 48 h exposure of E18184 fractions (30 μ g/mL) to HCT 116 spheroids. For the fluorescence readings (left), a bottom read of the plate, with an integration time of 500 ms, at 340Ex/280Em for Hoechst 33342, 485 Ex/538

Em for Calcein, and 535Ex/586Em for Propidium Iodide were used. For the microscopy imaging (right), filters for DAPI (for Hoechst 33342), FITC (for Calcein) and TRITC (for propidium iodide) were chosen, at an integration time of 0.5, 2 and 5 ms respectively. Solvent Control was 0.5% of DMSO and Paclitaxel (400 nM) and Mitomycin C (4 μ M) worked as positive control. All tests were performed, at least, with triplicates.49

Figure 29: Microscopy imaging of HCT 116 spheroids after exposure to fraction E18184 H and to Solvent Control (0.5% of DMSO), and as positive controls, Paclitaxel (400 nM) and Mitomycin C (4 μ M). Filters for DAPI (for Hoechst 33342), FITC (for Calcein) and TRITC (for propidium iodide) were chosen, at an integration time of 0.5, 2 and 5 ms respectively and 10x objective. All tests were performed, at least, with triplicates.50

Table Index

Table 1: Marine natural drugs approved by FDA and EMA	6
Table 2: Five main groups of cyanobacteria.....	8
Table 3: Gradients used in the VLC	13
Table 4: Separation conditions for the reverse phase semi-preparative HPLC of active fraction E14031 E5D.....	14
Table 5: Conditions for the SPE of the fraction E15074 B	15
Table 6: Conditions for the sub-fractionation of E17165 A7	18
Table 7: Sub-fractions obtained after sub-fractioning of E17165 A7.....	18
Table 8: Conditions for the HPLC separation of E17165 A7O	19
Table 9: Optimized conditions for the HPLC separation of E17165 A7O8.....	20
Table 10: Extraction and fractionation data for the strains used on this work	22
Table 11: Sub-fractions obtained after the separation of E14031 E5.....	24
Table 12: Sub-fractions obtained after SPE of E15074 B.....	29
Table 13: Sub-fractions obtained after HPLC of E15074 B4.....	31
Table 14: Data from the MS of fraction E15074 B4 and suggested hits for identification..	32
Table 15: Column chromatography results of the fractionation of E17165 A	36
Table 16: Sub-fractionation of E17165 A7.....	36
Table 17: Sub-fractions after sub-fractionation of E17165 A7O.....	37
Table 18: Sub-fractions after sub-fractionation of E17165 A7O8.....	40
Table 19: Summary of the bioactive fractions after all the assays on both models. 2D refers to the assays on cultures of MG-63, PI refers to propidium iodide and Cal to calcein, stains used on 3D cultures of HCT 116. Bioactivity is characterized as decrease in cell viability, assessed by three levels: +++ strong bioactivity, ++ medium bioactivity, + low bioactivity or – no bioactivity.	54

Abbreviations list

^1H NMR – Proton Nuclear Magnetic Resonance

ATP – Adenosine triphosphate

BBE – Blue Biotechnology and Ecotoxicology team

CHCl_3 – Chloroform

DCM - Dichloromethane

DMEM – Dulbecco's modified Eagle Medium

DMSO – Dimethyl Sulfoxide

DNA – Deoxyribonucleic acid

EMA – European Medicines Agency

ESI – Electrospray ionization

EtOAc – Ethyl Acetate

FBS – Fetal bovine serum

FDA – Food and Drug Administration (USA)

H_2O - Water

HCT 116 – Human colorectal carcinoma cell line

HO – Hoechst-33342

HPLC – High-Performance Liquid Chromatography

IARC – International Agency for Research on Cancer

LDH – Lactate dehydrogenase

MeCN - Acetonitrile

MeOH - Methanol

MG-63 – Human osteosarcoma cell line

MS – Mass spectrometry

MTT – 3-(4,5-dimethylthiazol-2-yl)-2,5-diphenyl tetrazolium bromide

NRPS – Non-ribosomal peptide synthetase

PBS – Phosphate-buffered saline

PI – Propidium Iodide

PKS – Polyketide synthetase

PMA – Phosphomolybdic acid

R_f – Retention factor

R_f – Retention factor

SPE – Solid phase extraction

SRB - Sulforhodamine B

TLC – Thin Layer Chromatography

UV – Ultraviolet

VDAC 1 – voltage-dependent anion channel 1

VLC – Vacuum liquid chromatography

1. Introduction

1.1. Cancer

Cells, the building blocks of life, are the smallest unit of living organisms, each ensuring a very simple task but together forming very complex life forms, from insects and plants to humans. The human body is composed of trillions of cells, and during a human life, there are several generations of cells. Human cells keep growing and dividing, helping to balance the organism so in every moment there is the right number of cells. When a cell is incapable of continuing performing as expected, due to being either damaged or too old, they die and are replaced by new ones. These life cycles are regulated by chemical signals, by ordering cells to multiply or to die according to biological and environmental factors, in order to maintain the organisms' health (Alberts et al., 2002)

Cancer can be described as a group of diseases on which the cells of the organism divide without any control and without dying, forming masses of abnormal cells called tumours. To the process of healthy cells becoming cancerous, it's given the name of carcinogenesis. Carcinogenesis results of a deregulation between cell proliferation and cell death. When the deregulation promotes an abnormal, autonomous and uncontrollable cell proliferation, a tumour, also called a malign neoplasm, is created. They are invasive and can spread all over the body, through the lymphatic system or the bloodstream, forming secondary tumours called metastases. This way a group of cells can infect and create tumours all over the organism if left unchecked and untreated. If a tumour doesn't spread to the adjacent areas or through the body, it is considered a benign tumour, and can easily be removed as its borders are well defined - unlike malign cells, and generally, they do not come back. A tumour is only considered cancer if the neoplastic cells invade the tissues surrounding them and form metastases. The more it spreads the harder it is to treat it, (Hanahan and Weinberg, 2011) as it becomes almost impossible to remove, like benign tumours. For the metastasis to occur, tumour cells must invade other tissues and create a new colony, away from its original place. This process is very complex and not always achieved, because not all the cells manage to successfully enter and exit the circulatory system and manage to proliferate away from their primary tumour. But when it happens and in order to grow, tumour cells need space and a large amount of energy and nutrients, so they produce angiogenesis signals in order to form new blood vessels that can provide them with oxygen and nutrients directly, allowing the high growth rates of these cells and preventing hypoxia (Harris, 2002). These blood vessels can also serve as an escape for metastatic cells (Alberts et al., 2002).

Cancer cells are formed through a variety of genetic changes, triggering different types of cancer. The specific name of the disease depends on the cell type it affects; for example, if it develops on epithelial cells, cancer is called a carcinoma, which represents the most common type of cancer. On conjunctive tissues, like bones or muscles, are called sarcomas, if it develops on the bone marrow it's called leukemic and on the lymphatic system is a lymphoma (Alberts et al., 2002).

Cell's genes are responsible for cell growth, differentiation and behaviour, making sure that all cells are healthy. But the constant duplication of cells and cleaning of old and malfunctioning cells has a risk of a gene mutation to happen, either by damaging the gene, copying it more than once, or even by losing the gene. Mutations are common in cell division and happen randomly. Most of the times they are harmless or don't affect the regular functioning, but when mutations start to accumulate, or when sometimes a critical mutation is so impacting that it can affect a cell in such a way that it ignores its primary function, it is possible that a normal cell can become a cancerous cell (Hanahan and Weinberg, 2011). Even though they are usual, mutations rarely create a cancer cell, because of the mechanisms of repair of the human body. When genes get damaged cells can repair them or, in case of a great damage, the cell may die or be killed by the immune system who can recognize it as abnormal. These processes prevent that simple mutations evolve into cancer. However, if an important gene is modified or when damage builds up and the capacity of repair decreases, cells become more likely to develop additional mutations, as it is not possible to restore the genes, leading to cancer. There are a group of genes involved in the processes of cell division that are usually the ones whose damaged copies lead to the formation of tumours. The first example is the oncogenes, that when damaged will encourage the cell to multiply and divide permanently. The opposite of oncogenes, tumour suppressor genes, are responsible for stopping cell growth and, if damaged, this regulator is no longer understood by the cell, who will keep growing uncontrollably. Similar to the latter, there are the self-destruction genes, also known as apoptosis or programmed cell death. If this gene gets faulty, the cell will no longer die when damaged. Lastly, there are the DNA repair genes, whose proteins repair damages to the DNA. If impaired, DNA won't be repaired, and errors will build up (Alberts et al., 2002).

Cancer is a multistep disease, and carcinogenesis has been described in three steps: initiation, promotion and progression. Initiation consists on mutation of genes, either naturally or by exposure to a carcinogen, resulting in changes on the cell pathway of proliferation and differentiation. Then promotion, when the initial cell proliferates resulting in the accumulation of neoplastic cells and finally progression when tumour size increases and proliferates (Devi, 2004).

Even though there is a wide variety of cancer types, it is believed they do share some common ground, as (Hanahan and Weinberg, 2000) described as six alterations on cells that most if not all the types of cancer show, and that can be used as targets for cancer treatment and drug discovery: self-sufficiency in growth signals and insensitivity to antigrowth, evasion of apoptosis, potential of replication, sustained angiogenesis and capacity of tissue invasion and metastasis. In order to fight these diseases, treatments aim mostly for cell death, especially apoptosis rather than necrosis, as it is a physiological and predictable coordinated pathway that does not involve inflammation like what happens with necrosis (Han et al., 2008). Autophagy is also described as a potential target for anticancer therapeutics (Kim et al., 2012).

1.1.1. Causes of cancer

Cancer incidence grows exponentially with age, but people of all ages are susceptible to have cancer. Damage may build up and the capacity of repair decrease with ageing.

As stated previously, cancer cells are triggered by errors in the genetic material inside a cell that disrupt the normal cell cycle. Those errors can be due to intrinsic factors but also due to external factors (Devi, 2004). Although some people have more tendency to develop cancer, due to genetic factors, only a small part of cancers are from hereditary causes. Environmental and behavioural factors are the main causes of cancer. There are several risk factors that raise the chance of developing cancer, like obesity, alcohol and tobacco usage, dietary choices, sedentarism. Altogether these factors are responsible for one-third of all cancer deaths, with tobacco being responsible for around 20% of them (Gakidou et al., 2017). A carcinogen is any substance that promotes carcinogenesis. They can be direct or indirect if they need to be metabolised before, or genotoxic or not, if DNA is not affected. Biological carcinogens consist of infections, like hepatitis and human papillomavirus, for example, that can cause cancer, especially in less developed countries, contributing to 25% of cases (World Health Organization, 2018). Environmental pollutants, chemical carcinogens, and physical carcinogens like ionizing and ultraviolet radiation can also be responsible for higher cancer risk, usually causing genetic changes in cells (Alberts et al., 2002). Long exposure to such agents, by pollution or occupational hazards, are also risk factors for developing cancer.

1.1.2. Cancer Statistics

Cancer is one of the biggest causes of death for several years now, being second only to cardiovascular diseases. Even though we understand it better as the years go by, it is very hard to treat it and stop its causes, as we have several different types of cancer, a result from the wide range of genetic changes that create cancer cells.

According to this year's estimative based on data from the International Agency for Research on Cancer (IARC), there will be 18 million new cancer cases resulting in 9.6 million deaths (Bray et al., 2018). Approximately 1 in 6 deaths are due to any type of cancer. Of these deaths, a majority (about 70% of cases) occur in low and middle-income countries due to lack of accessible diagnosis and treatment (World Health Organization, 2018). The forms of cancer with most incidence are lung, breast, colorectal and prostate, but the deadliest types of cancer are lung, colorectal and stomach cancer, together killing an estimated number of 2.5 million people in 2018 (Bray et al., 2018). These types of cancers, mainly lung cancer, are usually more fatal because it occurs on organs that are harder to have a surgery on and are silent until they reach an advanced state. Developing countries are especially affected by cancer mortality due to the high cost of treatment and the ever-increasing population not getting enough cancer centre facilities and equipment to match the demand. Men are at more risk of developing cancer than women by about 20%. It is estimated that one-third of the world population will suffer from at least one type of cancer in their lifetime. This rise in incidence is due to the longevity of the population, as age is a major risk factor for cancer incidence, as cells lose their capability of regenerating and eliminating abnormal cells. Research is more and more developed and advanced, and even if the incidence is increasing, the rate of survival is expected to increase as well (World Health Organization, 2018).

1.1.3. Cancer treatment strategies and future perspectives

Treating cancer is indeed a challenging work. A tumour must be considered as a heterogeneous cell population (Khoo et al., 2016) and as cancer consists of many different diseases it is impossible to find just one universal cure. Cancer cells are also prone to develop resistance to anticancer drugs and apoptotic stimuli, making it harder to find effective treatments. Currently, many different therapies are used in fighting cancer. Improved methods of chemotherapy, radiotherapy and surgery are being combined with new treatments as hormone therapy and immunotherapy (Nicolini et al., 2016). Precision medicine is also a new technique used for cancer therapeutics. It consists on a personalized therapy on which a patient's tumour is transplanted into zebrafish (Bentley et al., 2015) or

mice (Zhang et al., 2017), in order to study and test which drugs could work. In spite of all the efforts, cancer still is one of the main causes of death worldwide, as previously discussed. The treatments currently used to treat cancer cause many unwanted side effects, especially chemotherapy, and so it is crucial that the search for anticancer treatments focus on finding drug who can more efficiently destroy cancerous cells and not affect the healthy ones, improving quality of life of patients and increasing survival rate (Feinberg et al., 2006). In recent years, the trending on natural sources for developing new drugs has been increasing, particularly in the biomedical area.

1.2. Natural products discovery

Natural products are molecules produced by a living organism, either as primary or as secondary metabolites, who can present an interesting biological activity, making them a source of potential new drugs. Although the isolation of natural compounds might be a complex method of drug discovery, according to a study by (Bade et al., 2010), 10% of the compounds that passed phase I of clinical trials were unchanged natural products, and 29% were derived from natural products. From 2008 to 2011, 5 new natural products and 20 natural product-derived drugs were approved for medical usage, and between the years 2000 and 2013, 25% of drugs approved worldwide were from natural products (Butler et al., 2014). These numbers show the promising capability of natural products to replace or to reduce the number of synthetical drugs as treatments. For example, paclitaxel, staurosporine and doxorubicin are all anticancer drugs from natural origin, used as therapeutics for cancer treatment (Bhatnagar and Kim, 2010; Butler et al., 2014)

The search for natural products came a long way since the first results of plants (isolation of morphine by Sertürner) and fungus (discovery of penicillin by Alexander Fleming) (Beutler, 2009), as gradually other species started to be studied for the aim of isolating compounds with pharmacological or biotechnological interest, with a lot more of advances and discoveries yet to be made. An area with a big interest in what concerns natural products is marine biotechnology. The ocean takes up 70% of the Earth and is habitat for many biodiverse organisms (Ruiz-Torres et al., 2017). It is believed that the physiological adaptations of marine organisms to such a competitive and diverse environment lead to the production of unique compounds produced mainly as secondary metabolites, making the ocean a reliable and interesting source of natural compounds (Agrawal et al., 2017). Around 75% of the marine natural products described are from marine invertebrates (Hu et al., 2011). Marine microbes and sponges are amongst the most studied and the most proliferative in what concerns marine natural products (Gogineni and Hamann, 2017). Currently, there are around twenty marine drugs on the different phases of

the clinical trial, and practically all of them are being tested for anticancer purposes. There are already eight drugs originated from marine organisms, approved by both the Food and Drugs Administration (US FDA) and the European Medicines Agency (EMA). On the table below, it is represented the drugs currently used for anticancer treatment, with origin in marine.

Table 1: Marine natural drugs approved by FDA and EMA

Compound Commercial name	Origin	Activity	Year and entity
Cytarabine Cytosar-U	Sponge	Anticancer	1969, FDA
Vidarabine Vira-A	Sponge	Antiviral	1976, FDA
Ziconotide Prialt	Cone snail	Chronic pain	2004, FDA
Omega-3 acid ethyl esters Lovaza	Fish	Reduction of triglyceride levels	2004, FDA
Trabectedin Yondelis	Tunicate	Anticancer	2007, EMA
Eribulin mesylate Halaven	Sponge	Anticancer	2010, FDA
Brentuximab vedotin Adcetris	Mollusk Cyanobacteria	Antibody-drug conjugate	2011, FDA
Iota-Carrageenan Carragelose	Red seaweeds	Antiviral	2013, FDA

Cytarabine and Vidarabine were both isolated from sponges, and while one is an anticancer drug, an inhibitor of DNA polymerase, the other is an antiviral drug. Ziconotide is used for the treatment of chronic pain in cancer patients and it is known for being very potent (Mayer et al., 2010). Omega-3 acid ethyl esters are used for the treatment of hypertriglyceridemia (Dayspring, 2011). Trabectedin and Eribulin mesylate are both anticancer drugs, the first being used to treat soft tissue sarcoma and ovarian cancer, due to its inhibition of cancer cell growth and the latter for breast cancer as it interferes with microtubule formation (Bourguet-Kondracki and Kornprobst, 2014; D'incalci et al., 2014). The iota-carrageenan was already in use for food until its approval as an antiviral

compound, in 2013 (Eccles et al., 2010). Brentuximab vedotin is an antibody-drug conjugate used to treat lymphomas, being the first compound from cyanobacteria to be commercialised (Mayer, 2017; Newland et al., 2013). This highlights the potential of cyanobacteria as one of the promising groups for isolating natural products.

1.3. Cyanobacteria as a source of natural products

1.3.1. Cyanobacteria

Cyanobacteria are primordial microorganisms, previously known as blue-green algae, whose photosynthetic activity is considered to have been responsible for the release of oxygen for the atmosphere, allowing the spread of aerobic life on the planet. Fossils date these microorganisms back to 3.5 billion years ago (Schopf, 1993), but still they continue to be relevant today as they are part of the phytoplankton responsible for the primary production of organic matter, by carbon fixing (Zanchett and Oliveira-Filho, 2013), amongst possessing other interesting qualities, as it will be explored further below.

They have a worldwide geographical presence being found in the most diverse ecosystems, from fresh and marine waters to terrestrial land, and even in extreme environments like polar habitats or hot springs (Zanchett and Oliveira-Filho, 2013). It is usual for cyanobacteria to establish symbiotic relationships with plants, fungi (lichens) and marine organisms like sponges (Dvořák et al., 2017). A theory for the origin of chloroplasts suggests that cyanobacteria are the ancestors of chloroplasts, as the formation of this organelle is attributed to an endosymbiosis of cyanobacteria and a eukaryote (McFadden, 1999).

Taxonomically, cyanobacteria phylum is included in the bacteria domain. Five major groups of cyanobacteria can be identified, as shown in table 2. Cyanobacteria can be unicellular, colonial or filamentous. They do not possess flagella, but some can move by forming gas vacuoles of atmospheric nitrogen that allow them to float in the water column (Walsby, 1994). Most of them produce chlorophyll a and a phycobilin pigment, more specifically phycocyanin, whose blue-green colour is responsible for the name cyanobacteria (Whitton and Potts, 2012). Cyanobacteria reproduce by binary fission but have developed specialized ways to reproduce, such as hormogonia. A hormogonium is a cell filament, usually disperse until cell division (Castenholz et al., 2001). Is smaller than other vegetative cells, like akinetes that also work as reproductive cells and are produced by a group of cyanobacteria. They are resting cells, with a large number of stored nutrients and can resist in case of adverse conditions, such as lack of nutrients or light. Another specialized cell is heterocyte, a cell for nitrogen fixation when needed.

Table 2: Five main groups of cyanobacteria

	Characteristics
Chroococcales	Unicellular coccoid cells Reproduction by binary fusion
Pleurocapsales	Unicellular coccoid cells or aggregates
Oscillatoriales	Filamentous Do not produce heterocytes nor akinetes
Nostocales	Filamentous Divides in one plane Produce heterocytes
Stigonematales	Divides in multiple planes Produce heterocytes

These organisms are mostly known because of their negative effects, like blooms and production of toxins. Microcystin is the most studied cyanotoxin, and it is known to be prejudicial to health many species, humans included (Carmichael, 1992). However, to survive the evolutionary pressure they had to endure, they developed mechanisms of adaptation, known as secondary metabolites.

1.3.2. Cyanobacteria bioactive compounds

As mentioned, cyanobacteria are ubiquitous to various environments forcing them to come up with strategies in order to survive and reproduce (Wang et al., 2017). So, they produce an abundance of secondary metabolites who show potential as bioactive compounds, being the source for 800 chemically diverse bioactive metabolites. This diversity is due, mainly, from the biosynthesis pathway through both non-ribosomal peptide synthetase (NRPS) and polyketide synthetase (PKS), and also because they possess a lot of enzymes capable of alterations like oxidization or methylation (Costa et al., 2012).

These metabolites are studied for their bioactivities (Moosova et al., 2018) et al., 2009), such as antifouling, antialgal, antibacterial like Lyngbyoic acid that disrupts gene regulation of *Pseudomonas aeruginosa* (Kwan et al., 2009), anti-obesity such as yoshinone A, which inhibits adipogenic cell differentiation, anti-inflammatory (Koyama et al., 2016), antifungal such as hassallidin (Shishido et al., 2015) and of course, anticancer one of the most studied bioactivities.

1.3.3. Cyanobacteria anticancer compounds

One of the most studied bioactivity potentials of cyanobacteria is cytotoxic activity against cancer cells. Screening of anticancer bioactivity is frequently done using *in vitro* techniques, by exposing human cancer cell lines to cyanobacteria-derived fractions and performing anti-proliferative or cytotoxicity assays.

The screening with monolayer culture of cancer cells (2D cell culture) is commonly used due to its simplicity and reproductivity. In lung cancer cell lines, compounds like Veraguamide A, Apratoxin D, Aurilides B and C and Coibamide A showed cytotoxicity (Gutiérrez et al., 2008; Han et al., 2006; Mevers et al., 2011), while in breast cancer cells Pitipeptolides A, B and C, isolated from *Lyngbya majuscula*, exhibited anti cancerogenic potential with IC₅₀ values of 13, 11 and 73 μM, respectively (Montaser et al., 2011). Pitiprolamide isolated from the same species, also presented cytotoxicity for both adenocarcinoma breast cancer cells and colorectal carcinoma cells, but at lower values than compounds described before (Montaser et al., 2010). Apratoxin A and E, isolated from *Lyngbya majuscula* and from *Lyngbya bouillonii*, respectively, showed cytotoxicity levels in cervix carcinoma cells with IC₅₀ values of 10 and 42 nM. The former compounds were also tested in osteosarcomas cells and displayed IC₅₀ levels of 10 and 59 nM, while in rectal adenocarcinoma cells the IC₅₀ levels were of 1.4 and 21 nM (Matthew et al., 2008). Against the cervical carcinoma cells, Caylobolide B showed IC₅₀ levels of 12.2 μM while when tested on colorectal cells IC₅₀ values dropped to 4.5 μM. The compound Aurilides B when tested on renal, prostate and leukemic cancer cells had positive activity inhibiting cell growth (Han et al., 2006).

In the Blue Biotechnology and Ecotoxicology group at CIIMAR, new compounds with anticancer bioactivities were isolated and its chemical structures elucidated, such as hierridin B (Leão et al., 2013) and Portoamides (Leão et al., 2010). Hierridin B altered mitochondria's functionality, interacting with the voltage-dependent anion channel 1 (VDAC1) (Freitas et al., 2016), while Portoamides seemed to interfere with energy metabolism, decreasing ATP contents of the exposed cells (Ribeiro et al., 2017).

2. Objectives

This work was developed at CIIMAR, Interdisciplinary Centre for Marine and Environmental Research, more specifically on the Blue Biotechnology and Ecotoxicology (BBE) research group, who hosts a large collection of cyanobacteria strains, collected from the most diverse environments, forming the LEGE Culture Collection (LEGE CC). These cyanobacteria have been subject throughout the years to a lot of studies on their capability of producing primary but also secondary metabolites, with bioactivities in diverse fields, such as anti-fouling, anti-cancer and more recently, anti-obesity, etc.

The aim of this study was to screen different strains of cyanobacteria for their potential bioactivity against cancer cell lines with the aim of isolating the bioactive compounds. Traditional monolayer cultures and advanced 3D cell culture models were applied for activity screening and to identify the compounds responsible for the cytotoxicity. Bioactivity of cyanobacterial fractions was compared between both models in order to understand if the same compounds act on the advanced model for tumour spheroids compared to 2D cell culture. Monolayer cultures of MG-63 cell line were exposed to cyanobacterial-derived fractions, and the cytotoxicity was evaluated by the 3-(4,5-dimethylthiazol-2-yl)-2,5-diphenyltetrazolium bromide assay, more commonly known as MTT, to evaluate the activity of mitochondrial enzymes and, in that way define cell viability. The HCT 116 cell line was used to create 3D spheroids, as a more sensitive model for solid tumours. Spheroids were exposed to the fractions from cyanobacteria, and viability was assessed through fluorescence spectroscopy and microscopy.

A bioassay-guided fractionation approach was used for isolating bioactive compounds. Multiple techniques of fractionation and sub-fractionation were applied as column chromatography and HPLC, and techniques like ^1H NMR, LC-MS and fragmentation by ESI for the elucidation of the chemical properties of such molecules.

3. Materials and Methods

3.1. Cyanobacteria cultures

The LEGE Culture Collection (LEGE-CC), from the Blue Biotechnology and Ecotoxicology laboratory in CIIMAR, has more than 350 strains, collected from numerous environments, along many years (Ramos et al., 2018). For this work, four different strains of cyanobacteria belonging to LEGE-CC were selected. Cultures were grown at 25°C, with a light/dark cycle of 14h:10h respectively, in Z8 culture medium as described in (Kotai, 1972), and a concentration of 25 g /L of TM salt and 10 µg/mL of vitamin B12, for marine species.

Cultures were maintained in different size containers, from 1 L to 20 L, and in a 90 L sleeve bag until the amount of biomass was enough to proceed with the extraction work. For that, cultures were harvested by centrifugation, for 10 minutes at 4700 rpm and 4°C, for unicellular strains and by filtration with a 15 µm mesh for filamentous strains. The collected cells were frozen at -80°C to be then lyophilized for further extraction.

3.1.1. Biomass extraction and fractionation

Freeze dried biomass of strains LEGE 06102, 06099 and 06005 was then extracted following the BBE protocol for cyanobacterial organic extraction and fractionation, based on (Edwards et al., 2004). The biomass was immersed in a 2:1 mixture of methanol (MeOH) and dichloromethane (DCM), sonicated and stirred, so the cyanobacteria cell components could be extracted from the cells and dissolved in the solvents. The mixture was filtered multiple times, in vacuum, through a Büchner funnel with cotton and a Whatman N°1 filter paper, and collected in a round bottom flask, as shown in figure 1.



Figure 1: Organic extraction of cyanobacterial biomass

The round bottom flask was dried in a rotary evaporator to obtain a crude extract which was weighted to calculate the extraction's yield. The crude extract was then prepared for vacuum liquid chromatography (VLC), by dissolving it in DCM and adding silica gel (60 0.015-0.040 mm, Merck), and drying it, in order to obtain the crude sample preadsorbed in silica. The VLC apparatus was then assembled as shown on the figure below.

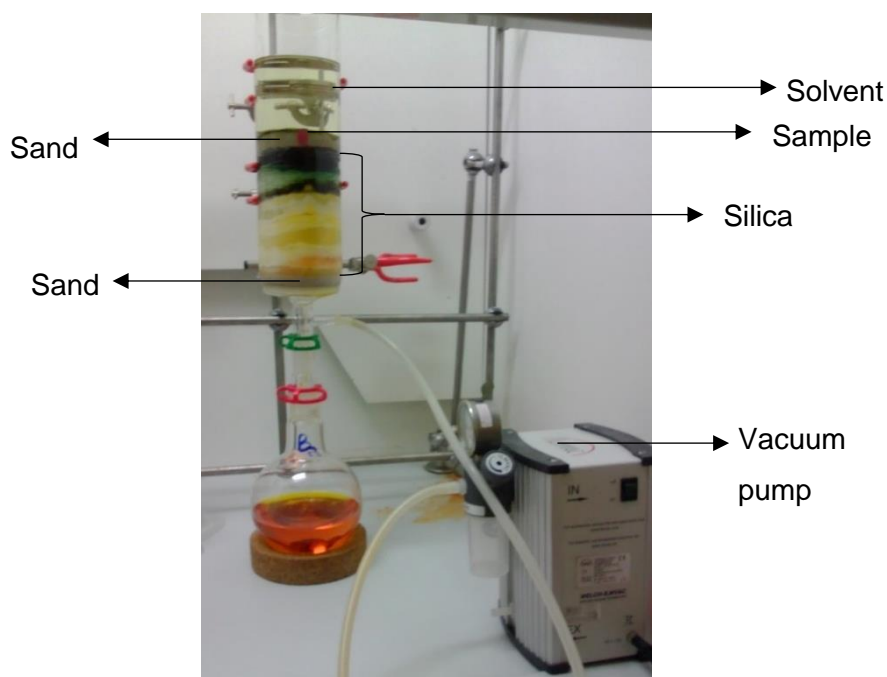


Figure 2: VLC apparatus for the fractionation of cyanobacteria crude extracts

The VLC column was packed with sand or cotton at the bottom and then was stacked with the same type of silica used as before. The quantity of silica added depends on the amount of loaded sample as it needs to be enough to separate the crude components, being 50 to 100 times the mass of the sample to be fractionated. The column was compacted using a vacuum bomb and then the dry sample of the crude was loaded on top of the silica, as levelled as possible. A paper filter was placed on the top to prevent disturbing the sample and the silica when the eluent was added. A solvent gradient, ranging from least to most polar, was used to separate the crude extract into different fractions, starting with a 9:1 mixture of hexane (Hex): ethyl acetate (EtOAc) to 100% methanol (MeOH), as shown in table 3.

Table 3: Gradients used in the VLC

Fraction	Gradient
A	90% Hex
	10% EtOAc
B	80% Hex
	20% EtOAc
C	70% Hex
	30% EtOAc
D	60% Hex
	40% EtOAc
E	40% Hex
	60% EtOAc
F	20% Hex
	80% EtOAc
G	100% EtOAc
H	25% MeOH
	75% EtOAc
I	100% MeOH

The fractions were collected on round bottom flasks and dried in a rotavapor and resuspended to 40 mL vials, previously weighted. Before completely drying the vials, a thin layer chromatography, TLC, (Silica gel 60 F₂₅₄, Merck) was performed. After drying, the vials were weighted, and the fractions were sent to proton nuclear magnetic resonance (¹H NMR) (400 MHz, Bruker Avance III). In order to test the fractions for their biological activity, stock solutions, at the concentration of 10 mg/mL, were prepared in Dimethyl Sulfoxide (DMSO).

3.2. Bioassay-guided fractionation

After testing the initial fractions for bioactivity on the osteosarcoma cancer cell line, MG-63, the ones who presented potential bioactivity were subjected to sub fractionations, with the aim of isolating the active compound. All the fractions that resulted from these processes were sent to ^1H NMR, (either 400 or 600 MHz, depending on the complexity of the fraction), and, to further continue with the bioassay-guided fractionation, a test solution was prepared for all the fractions, in DMSO, at the concentration of 4 or 10 mg/mL (depending on the amount of mass left). Some fractions used on this work were already previously fractionated and sub-fractionated (E14031 E5). In the case of E18179 DE and its subsequent sub-fractionations were performed by laboratory colleagues simultaneously to this work, with the help of the author.

3.2.1. Sub-fractioning of E14031 E5D

The sub-fraction E14031 E5D was the most active in its bioassay, so the sub-fractionation was proceeded by reverse-phase semi-preparative HPLC with a 1525 Binary HPLC pump and a 2487 dual absorbance (UV-Vis) detector (Waters). The sample was dissolved in a small volume of acetonitrile (MeCN) and the separation was carried out in a Synergi 4 μm Fusion-RP column (250 x 4.6 mm, Phenomenex), using an eluent gradient of acetonitrile and water (H_2O) (table 4), with a constant flow of 0,8 mL/min. The different fractions were collected according to the chromatogram peaks, resulting in eight new sub-fractions (E14031 E5D1-7 + \emptyset) who were dried in the rotavapor and weighted. Sub-fraction E14031 E5D2 was sent to ^1H NMR (600 MHz, Bruker Avance III) and to LC-MS (Thermo Scientific), and test solutions of all fractions were prepared at a concentration of 4 mg/mL.

Table 4: Separation conditions for the reverse phase semi-preparative HPLC of active fraction E14031 E5D

Time (min)	Gradient
0	75% MeCN 25% H_2O
20	100% MeCN
50	100% MeCN
52	75% MeCN 25% H_2O

3.2.2. Sub fractioning of E15074 B

To sub-fraction one of the active fractions of the bioassay, a solid phase extraction (SPE) was performed on a Strata SI-1 Silica SPE cartridge (55 μm , 70 \AA , 1 g / 6 mL, Phenomenex). A TLC (Silica gel 60 F₂₅₄, Merck) of the original sample was performed to better select the eluent mixture to use. Table 3 shows the conditions in which the separation was performed, and the number of tubes used to collect the products of the fractionation. After recovering 48 tubes, a TLC (Silica gel 60 F₂₅₄, Merck) was performed for each tube, in order to sort them into fractions, as shown in table 5. The fractions were then sent to ¹H NMR (400 MHz, Bruker Avance III) and test solutions were prepared at 10 mg/mL. After the bioassay, fractions E15074 B2, E15074 B3 and E15074 B4 were sent to LC-MS (Thermo Scientific).

Table 5: Conditions for the SPE of the fraction E15074 B

Tubes	Gradient	Solvent Volume (mL)
1-3	100% Hex	15
4-9	95% Hex 5% EtoAc	30
10-15	90% Hex 10% EtoAc	30
16-21	85% Hex 15% EtoAc	30
22-27	80% Hex 20% EtoAc	30
28-35	100% EtoAc	45
36-44	70% EtoAc 30% MeOH	45
45-48	100% MeOH	25

3.2.3. Sub fractioning of E15074 B4

After analysis of the NMR spectra, bioassay results and LC-MS data, sub-fraction E15074 B4 was chosen to be sub fractionated. The sample was dissolved in a mixture of ethyl acetate and hexane and separated using the same semi-preparative HPLC, as

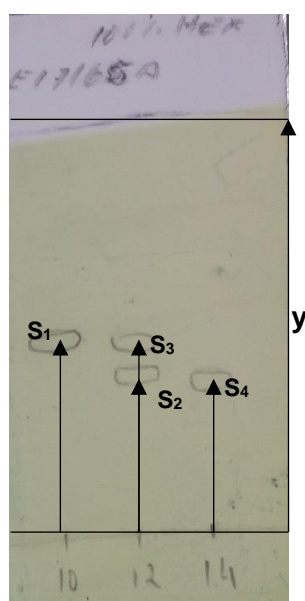
previously used. To optimize the compound's separation, the optimal separation conditions were established with injections of small sample amounts, on a Luna 5 μm Silica normal-phase column (100A, 250 x 4.6 mm, Phenomenex) with a flow of 1 mL/min. An isocratic condition with a mobile phase of 98% hexane and 2% ethyl acetate was chosen. Eight fractions were collected in round bottom flasks and then a last fraction was collected during elution with 100% ethyl acetate. After the separation was concluded, all sub-fractions were sent to ^1H NMR (400 MHz, Bruker Avance III) and test solutions for all the nine fractions were prepared at 10 mg/mL.

3.2.4. Sub fractioning of E17165 A

Fraction E17165 A demonstrated a strong activity against the MG-63 cell line and so was chosen to be further fractionated. An initial TLC (Silica gel 60 F₂₅₄, Merck) of the fraction was performed before to determine the conditions of the separation. Due to the amount of mass and the characteristics of the sample, a column chromatography was the method used for this separation. A 2.5 x 40 cm column was used and packed with silica gel 60 (0.015 – 0.040 mm, Merck) to work as the stationary phase. Mobile phase started with 100% hexane, and then a mixture of hexane and ethyl acetate (9:1) was used until the end of the chromatography. The eluted solutions were collected into test tubes and then, to sort the tubes into fractions, TLC (Silica gel 60 F₂₅₄, Merck) of the tubes was made, and the retention factor was calculated to identify the tubes with similar composition and pool them into different fractions, in round bottom flasks which were dried and then transferred to preweighed vials. All the obtained fractions were sent to ^1H NMR (600MHz, Bruker Avance III) and test solutions were prepared, at the concentration of 10 mg/mL.



Figure 3: Sub-fractionation of E17165 A



$$Rf(Sx) = \frac{Sx \text{ (mm)}}{y \text{ (mm)}}$$

Figure 4: TLC procedure and retention factor calculation

3.2.5. Sub fractioning of E17165 A7

After a positive result on the bioassay, sub-fraction E17165 A7 was sub fractioned by flash chromatography, in a 2.5 x 30 cm column packed with silica gel 60 (0.015-0.040 mm, Merck). As in the previous sub-fractionation, the initial eluent is hexane, followed by

mixtures of hexane and ethyl acetate, according to the gradient seen on table 6. The separation resulted in 125 tubes and their contents were assessed by TLC (Silica gel 60 F₂₅₄, Merck) and sorted into 15 fractions (table 7), who were then prepared for ¹H NMR (400 MHz, Bruker Avance III). The test solutions were prepared at a concentration of 10 mg/mL.

Table 6: Conditions for the sub-fractionation of E17165 A7

Eluent	Gradient (%)	Volume (ml)
Hexane	100	200
Hex:EtOAc	99:1	200
Hex:EtOAc	98:2	100
Hex:EtOAc	97:3	100
Hex:EtOAc	96:4	100
Hex:EtOAc	95:5	100
Hex:EtOAc	94:6	100
Hex:EtOAc	92:8	100
Hex:EtOAc	90:10	100
EtOAc	100	60

Table 7: Sub-fractions obtained after sub-fractioning of E17165 A7

Tubes	Fraction
1-23	E17165 A7A
24-26	E17165 A7B
27	E17165 A7C
28-29	E17165 A7D
30-60	E17165 A7E
61-68	E17165 A7F
69-85	E17165 A7G
86-95	E17165 A7H
96-101	E17165 A7I
102-111	E17165 A7J
112	E17165 A7K
113	E17165 A7L
114	E17165 A7M
115-120	E17165 A7N
121-125	E17165 A7O

3.2.6. Sub fractioning of E17165 A7O

As the process of fractionation continued and the samples were simplified, active sub-fraction E17165 A7O was further sub-fractionated by normal-phase HPLC, on a Luna 5 μm Silica (250 x 4.6 mm, Phenomenex) column, and as eluent, a solvent gradient as shown in table 8, with a flow of 1 mL/min. Nine sub-fractions were obtained by collecting the chromatography products in round bottom flasks and then transferred to weighted vials. Samples were sent to ^1H NMR (400 MHz, Bruker Avance III) and test solutions were prepared, at the concentration of 10 mg/mL. From this sub-fractionation, samples E17165 A7O2 and E17165 A7O5 were sent to MS/MS (Thermo Scientific), subsequent of the results of the bioassay.

Table 8: Conditions for the HPLC separation of E17165 A7O

Time (min)	Gradient
0	85% Hex
	15% EtOAc
40	100% EtOAc
53	85% Hex
	15% EtOAc

3.2.7. Sub fractioning of E17165 A7O8

After the final bioassay, E17165 A7O8 was sub-fractionated by HPLC again, with the same equipment as before, flow of 1 mL/min and the mobile phase as shown in table 9. Seven new sub-fractions were separated and sent to ^1H NMR (400 MHz, Bruker Avance III) and test solutions were prepared, at the concentration of 4 mg/mL. Sub-fractions E17165 A7O8C, E17165 A7O8E and E17165 A7O8F were also sent to MS and fragmentation by MS/MS (Thermo scientific) after the biological assay.

Table 9: Optimized conditions for the HPLC separation of E17165 A7O8

Time (min)	Gradient
0	30% EtOAc 70% Hex
20	55% EtOAc 45% Hex
25	55% EtOAc 45% Hex
30	100% EtOAc
40	100% EtOAc
42	30% EtOAc 70% Hex
50	30% EtOAc 70% Hex

3.3. Cell culture and bioassays

For the bioactivity screening of the cyanobacteria fractions, two cell lines were cultured throughout the period of work. Osteosarcoma cell line, MG-63 was cultured with Dulbecco's Modified Eagle Medium (DMEM, Gibco) complemented with 10% fetal bovine serum (FBS, Biochrom), 1% of penicillin-streptomycin (Pen-Strep, Biochrom, at concentrations of 100 IU/mL and 10 mg/mL, respectively) and 0.1% of amphotericin B (GE Healthcare). Colon colorectal carcinoma cell line, HCT 116, was cultured with McCoy's medium modified with the same complements as DMEM. Cell cultures were maintained with 5% CO₂ and at 37°C in an 8000 DH incubator (Thermo Scientific).

To maintain the cultures, every 2 to 3 days cell medium was renewed and every week, depending on cell growth, cells were split. The cell medium was removed, and cells washed with a phosphate-buffered saline solution (PBS), before incubating with Tryplex (Life Technologies) for 5 minutes for cell detachment. After centrifugation and dilution, cells were seeded in fresh medium. Cell density was calculated in a Countess Automated Cell Counter (Thermo Scientific), using trypan blue as cell dye.

3.3.1. MTT assays

To access the cytotoxicity of the previously obtained fractions, the 3-(4,5-dimethylthiazol-2-yl)-2,5-diphenyltetrazolium bromide assay (MTT assay) was performed on the MG-63 cell line. For this assay, cells were seeded in 96-well plates at a concentration of 3.3×10^4 cells per mL and allowed to adhere overnight. After 24 hours, the cells were exposed to triplicates of each fraction, at concentrations ranging from 20 to 50 µg/mL. DMSO was used as a solvent control (0.5%) and positive control (20% of DMSO). After 24 and 48 hours, 20 µL of MTT solution, at 1 mg/mL, was added to the wells and the plates

were left to incubate for 2 to 3 hours. Medium was removed and 100 μ L of DMSO was added to dissolve the purple formazan crystals. To measure the absorbance, a Biotek Synergy HT spectrophotometer, at 550 nm. The results were averaged, the standard deviation was calculated, and to get the percentage of cell viability, equation 1 was used.

$$\% \text{ cell viability (to solvent control)} = \frac{\bar{x} (\text{Absorbance}_{\text{sample}})}{\bar{x} (\text{Absorbance}_{\text{solvent control}})} \times 100$$

Equation 1: Calculation of % cell viability after MTT Assay

3.3.2. Spheroids assays

For the assays using 3D cell models, the HCT 116 cell line was chosen because of its relative ease in forming spheroids, as it was previously tested on other studies within the laboratory. In order to form these structures, cells were seeded in Corning Colstar Ultra Low Attachment 96 well plates, at a concentration of 1×10^4 cells per well, to obtain one spheroid per well. The culture medium used for the seeding was previously filtrated, to prevent any particle from interfering with the spheroid formation. The plate was left at room temperature for 30 minutes, before incubation, so the cells could agglomerate easier. After 5 days, when the spheroid was fully formed, cells were exposed to triplicates of the fractions, at a concentration of 30 μ g/mL, and to solvent (DMSO) and positive (Doxorubicin, Paclitaxel, Mitomycin C) controls according to (Sirenko et al., 2015). After 48 hours of exposure, 3 fluorescent stainings were added to the culture medium, Hoechst 33342 (5 μ g/mL), Propidium Iodide (5 μ g/mL) (Sigma- Aldrich) and Calcein AM (3 μ M) (Life Technologies). After 1 hour of incubation, spheroids were washed twice with PBS and fixed with 4% formaldehyde for 1 hour, before washing with PBS twice again. The fluorescence was measured by fluorescence spectroscopy using a Fluoroskan Ascent (Labsystems) fluorescence plate reader, and by fluorescence microscopy, using an Olympus BX41 fluorescent microscope and cell^b software to obtain the spheroids images, who were then analysed using Cell Profiler software (Carpenter et al., 2006).

4. Results

4.1. Biomass collection and fractionation

The cyanobacteria strains used on this work were cultured by scaling up the original cultures, first in round bottom flasks of 4 L, until they were transferred to a larger scale. For this, either multiple Nalgene flasks of 20 L were used, or for one of the strains, a sleeve bag with 90 L. This last method of culture is semi-continuous and more effective as it permits the renewing of culture medium every time a volume of culture was collected for harvesting. After the extraction process of the cyanobacterial biomass, the crude extract was fractionated using vacuum liquid chromatography, an easy and commonly used method because of its efficiency on separating a large amount of a complex crude extract. In table 10, the biomass collection and the extraction data are represented.

Table 10: Extraction and fractionation data for the strains used on this work

Strain ID	Dry biomass (g)	Extract ID	Crude (g)	Yield (%)	Mass after fractionation (g)	Yield (%)
<i>Nodosilinea nodulosa</i> LEGE 06102	37.796	E17165	10.8	28.5	6.89	63.8
<i>Synechocystis salina</i> LEGE 06099	31.46	E18179	6.965	22.1	4.86	69.8
	28.3	E15074	3.9679	14	3.05	77
<i>Synechocystis</i> sp. LEGE 06005	77.9153	E18184	13.8	17.7	8.50	61.6
<i>Synechocystis</i> sp. LEGE 07211	24.634	E14031	4.4792	18	3.64	85

Extracts and fractions of E15074 and E14031 were prepared previously to this work, from colleagues of the laboratory.

4.2. Bioassay-guided fractionations

The fractionations previously mentioned followed the results of the MTT assays, performed on the MG-63 cancer cell line grown as monolayer culture. This *in vitro* model for testing cell viability of fractions is widely used, mainly because it's a simple and quick process to access toxicity, working as an early process of screening potential bioactive complex fractions.

The results of this work are organized by the extraction ID of the cyanobacteria products. Data for the graphs were calculated as previously mentioned, using equation 1 to calculate the percentage of cell viability, according to solvent control results.

4.2.1. Screening and sub-fractionation of E14031 E5

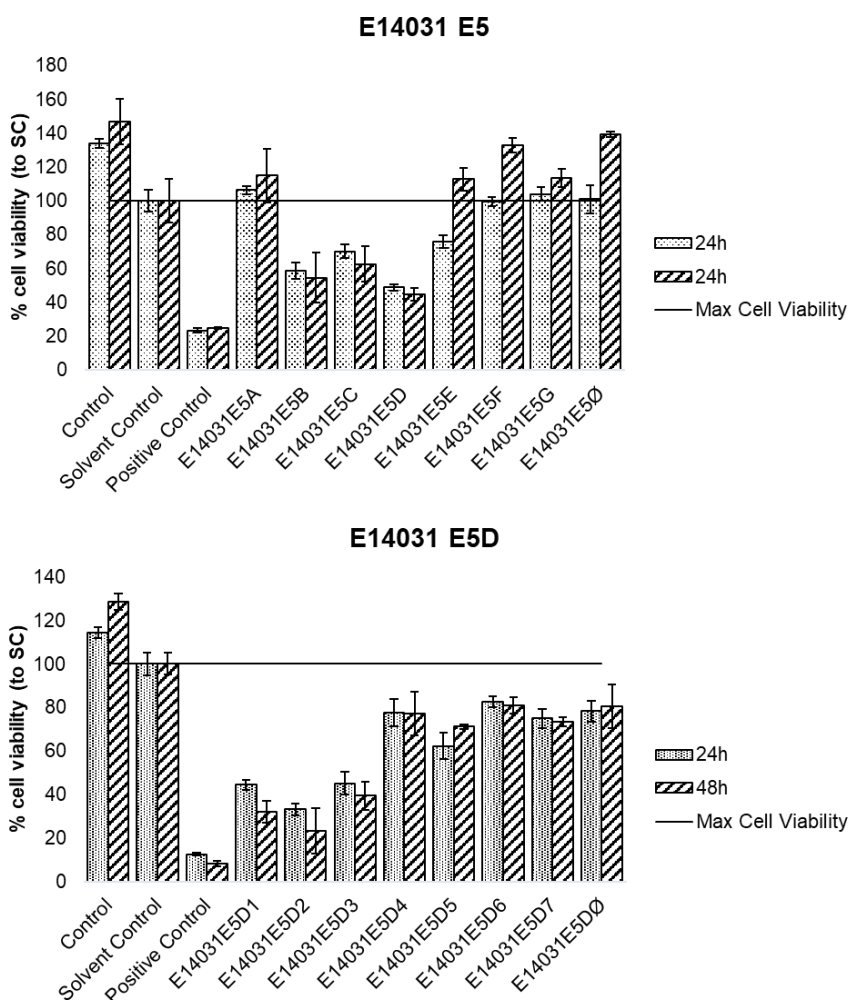


Figure 5: Cell viability after 24 and 48 hours of exposure to sub-fractions of E14031 E5 (top) and E14031 E5D (bottom), at a concentration of 20 $\mu\text{g}/\text{mL}$. Cells on Solvent Control were exposed to 0.5% DMSO, on Positive Control to 20% DMSO and on Control to culture medium only. All sub-

fractions were exposed to at least 3 replicates and controls in 6 replicates, data are shown as mean +/- standard deviations.

Previous screening done by colleagues of the laboratory identified the E14031 E fraction as bioactive with cytotoxic activity towards MG63 cells, and sub-fractions of E14031 E were prepared. Here, cells exposed to sub-fraction E14031 E5D had the least viability, (48.7% at 24 h and 47.7% at 48 h) so this sub-fraction was selected for sub-fractionation, by reverse-phase HPLC. The chromatogram is represented in the figure below.

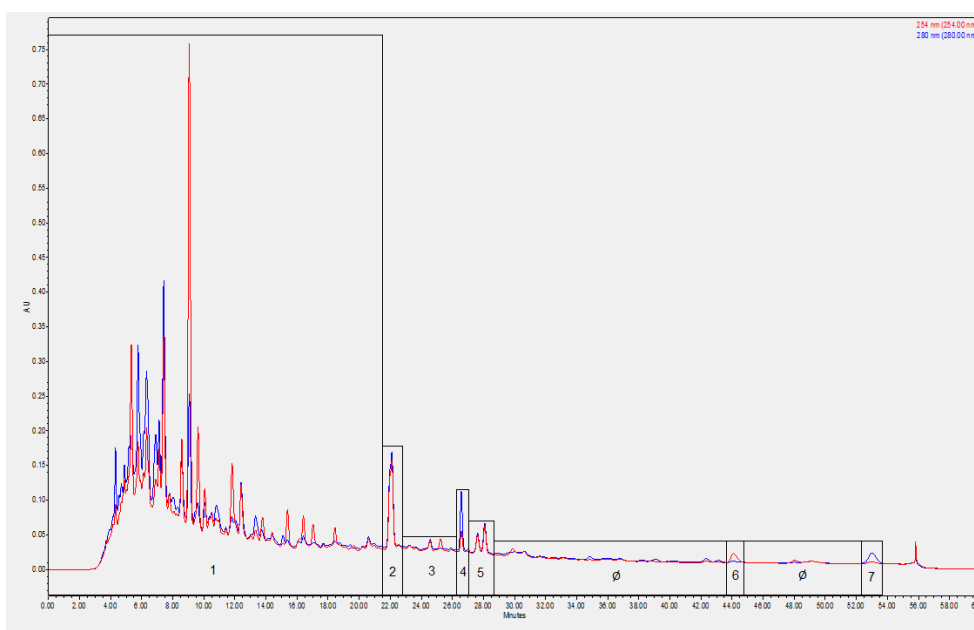


Figure 6: HPLC chromatogram of E14031 E5D

Eight different fractions were obtained, and fraction E14031 E5D∅ was a collection of the chromatogram areas where no significant peak appeared.

Table 11: Sub-fractions obtained after the separation of E14031 E5

Sub-fraction	Mass (mg)
E14031 E5D1	1,75
E14031 E5D2	0,29
E14031 E5D3	0,29
E14031 E5D4	~0
E14031 E5D5	0,2
E14031 E5D6	~0
E14031 E5D7	~0
E14031 E5D∅	0,76

As seen in figure 6, sub-fraction E14031 E5D2 corresponded to an isolated peak, with minor impurities, with a mass of only 0.29 mg (table 2). After the bioassay, this sub-fraction proved to be the most bioactive against the cells (33.2% viability at 24 h, 23.2% at 48 h) and was sent to ^1H NMR and to LC-MS. The LC-MS data showed a peak at retention time 13.024 minutes, who corresponded to a peak of $[\text{M} + \text{H}]^+ = 623.289 \text{ m/z}$.

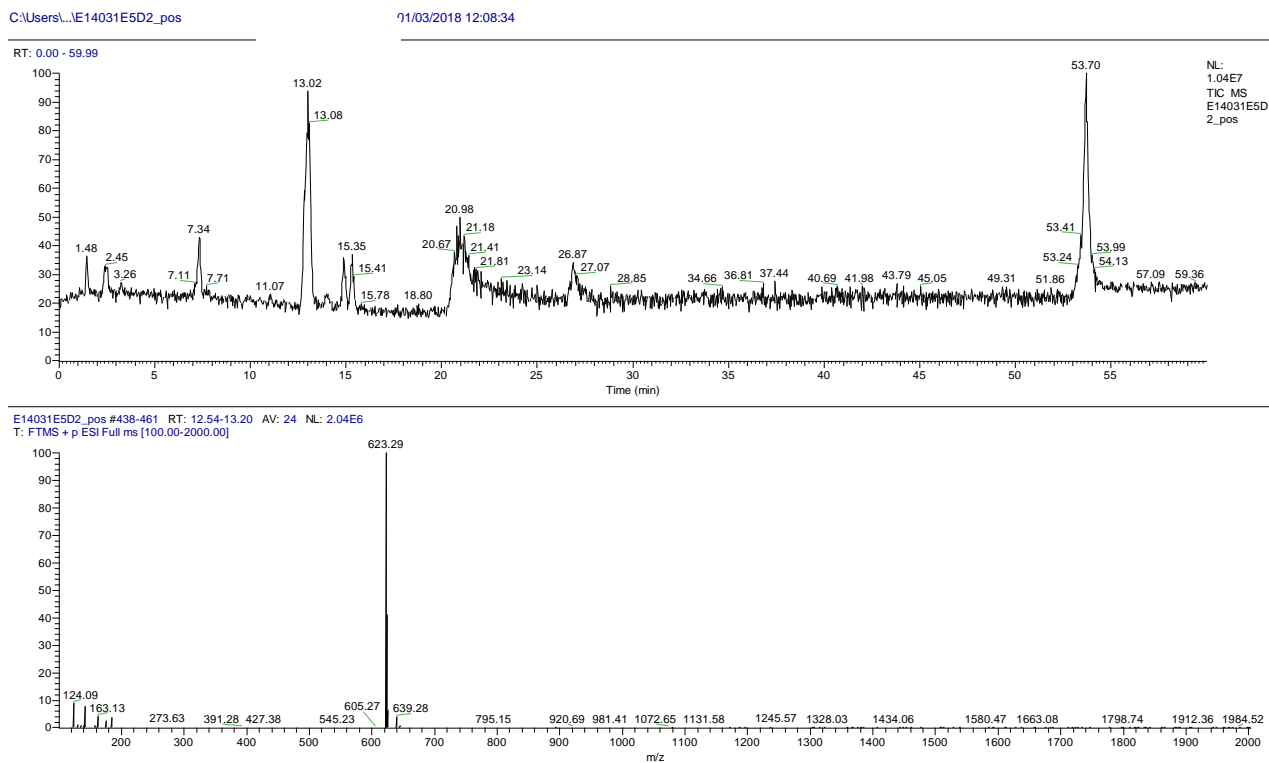


Figure 7: LC-MS data of sub-fraction E14031 E5D2. Sample was solubilized in MeOH. Peak at $R_t = 13.02$ minutes and the corresponding MS peak of $[\text{M} + \text{H}]^+ = 623.289 \text{ m/z}$.

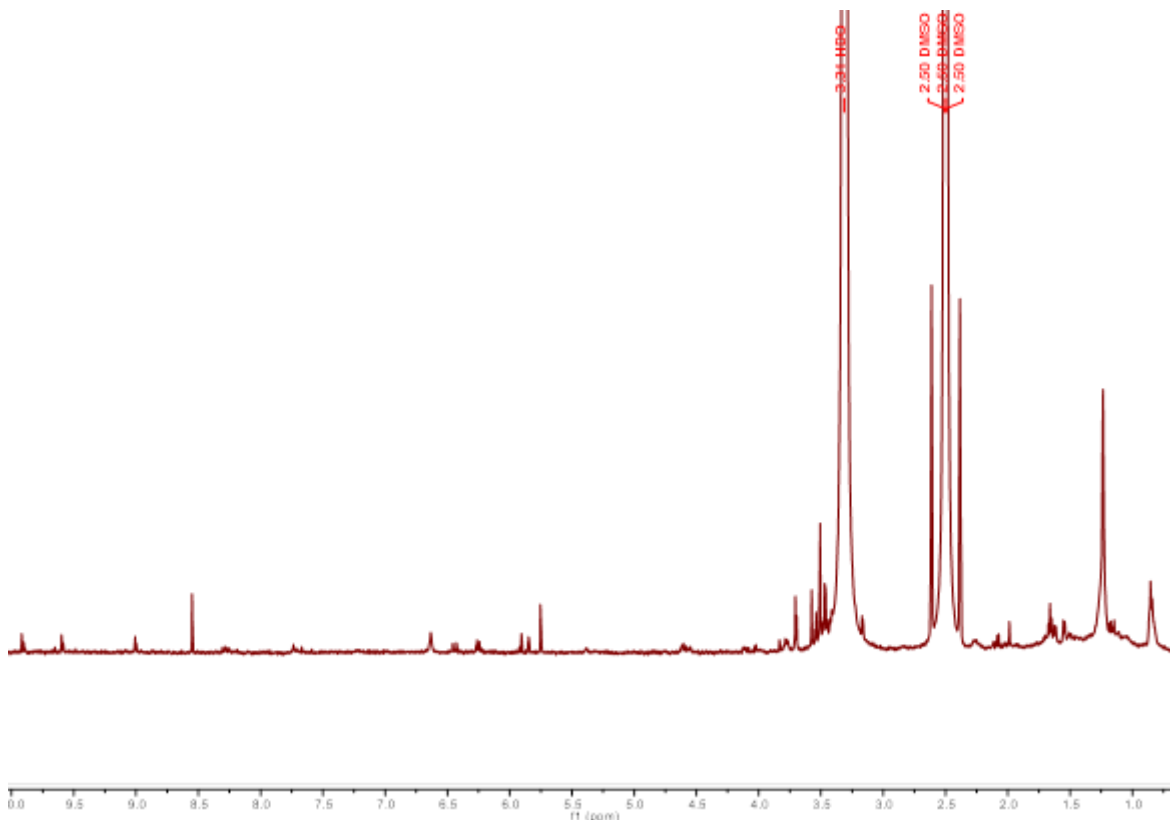


Figure 8: ^1H NMR spectrum of E14031 E5D2 at 600 MHz. Sample diluted in deuterated DMSO

This fraction, E14031 E5D2, results from the continuation of previous work within the laboratory, where bioactivity of *Synechocystis* sp. LEGE 07211, was discovered. E14031 E5D2 was obtained by reverse-phase HPLC, at 21.5 minutes of retention time. The chromatogram represented on Figure 6 shows that this fraction corresponds to an isolated peak that absorbs at both wavelengths of the UV detector. After reducing the viability of MG-63 cells to 23% after 48h of exposure, the remaining mass of this sample was sent to LC-MS. Figure 7 shows both the LC chromatogram, with a major peak at 13.02 minutes of retention time, and its respectively mass spectrum with a peak considered to be $[\text{M} + \text{H}]^+ = 623.289$ m/z. No more major MS peaks were found for this retention time, as we had a small amount of sample left (around 0.2 mg) and because the fraction is almost pure, so only one peak is expected to be found. Regarding the same retention time at negative ionization, no peaks were encountered. Using the software available for the LC-MS data analysis, molecular formulas of $\text{C}_{25}\text{H}_{39}\text{O}_9\text{N}_{10}$ and $\text{C}_{26}\text{H}_{45}\text{O}_{14}\text{N}_3$ were suggested. When searching for a possible molecular formula on ChemCalc (Institute of chemical sciences and engineering ISIC, 2014), multiple formulas were proposed; we decided to exclude any that contained chlorine or bromine as we did not find the characteristic isotopic signature for the presence of these elements, due to their usual isotopic abundance. The second more accurate formula from ChemCalc suggested $\text{C}_{32}\text{H}_{46}\text{O}_{10}\text{S}$, followed by $\text{C}_{31}\text{H}_{40}\text{O}_3\text{N}_7\text{S}$. All these

suggestions were searched on online databases for compounds, such as Spectral Database for Organic Compounds (National Institute of Advanced Industrial Science and Technology, 2018), ChemSpider (Royal Society of Chemistry, 2015), IBScreening (Interbioscreen, 2017) and Dictionary of Natural Products (CRC Press, 2018), but no hits were found. When searching for the mass values obtained from the LC-MS on ChemSpider, multiple hits were found, making it harder to compare them all with our sample, meaning that more information it is needed in order to easily dereplicate this fraction. This mass value was also searched on the MarinLit database, but non-significant and accurate results were found. From the NMR spectra (Figure 8), besides the usual peaks, like the deuterated DMSO peak around 2.50 ppm, water at 3.30 ppm, and some other minor solvent impurities, some characteristics peaks, at 9.92, 9.90, 9.60, 9.59, 9.01 and 9.00 ppm were identified as belonging to a chlorophyll, as their profile matches the one described by (Abraham and Rowan, 1991). However, the molecular mass of chlorophylls is usually greater than the one from this compound. Future perspectives to possible identify this compound is to try to send the remaining mass to fragmentation and search those results on databases for MS and MS-MS data in order to obtain a match or more information about the sample, and to start the process of growing the biomass all over again, and follow a more objective fractionation, and sending to more conclusive tests, like carbon NMR, for example.

4.2.2. Screening and sub-fractionation of E15074

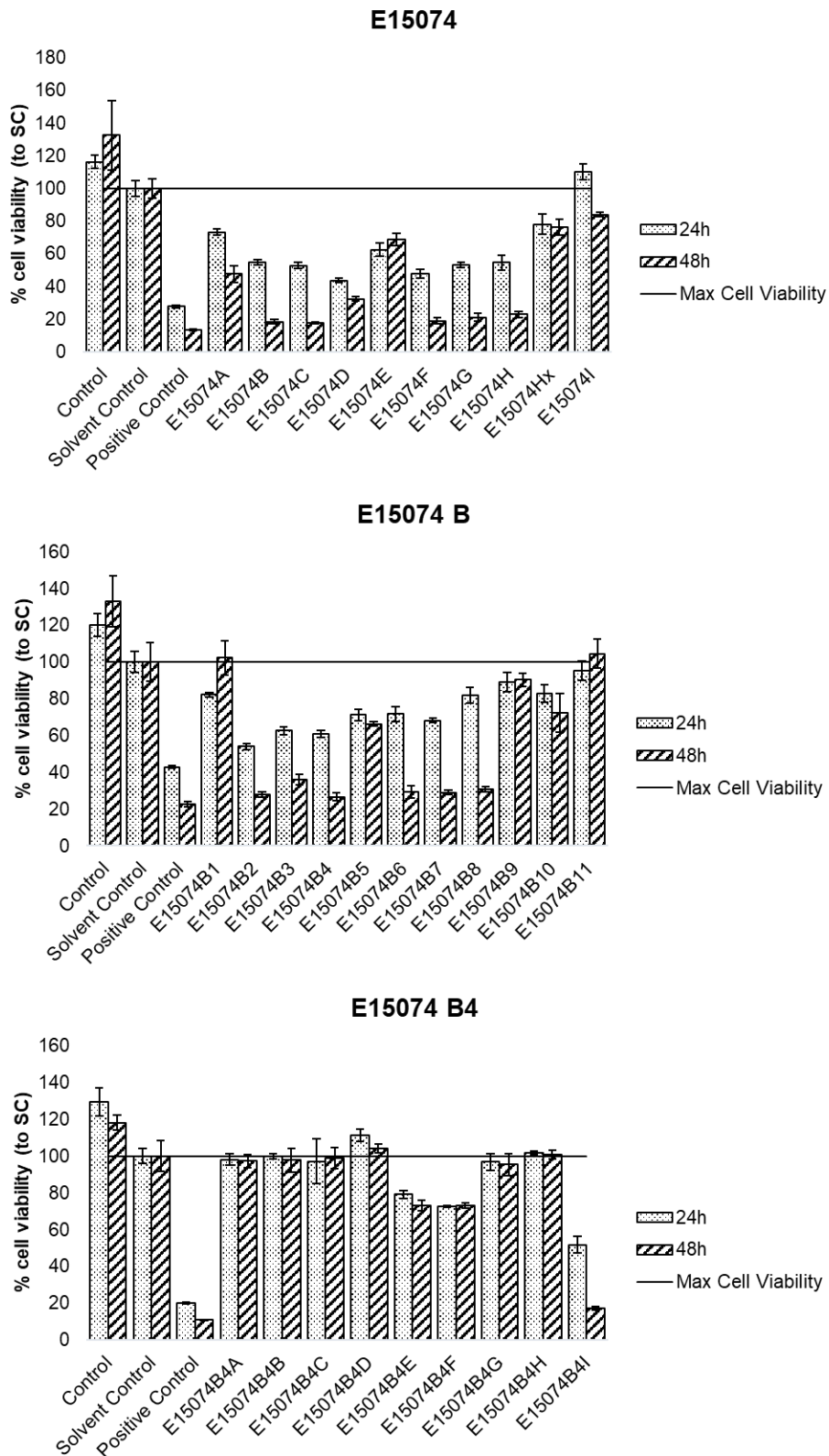


Figure 9: Cell viability and standard deviation after 24 and 48 hours of exposure to VLC fractions of E15074 (top), sub-fractions of E15074 B (middle) and sub-fractions of E15074 B4 (bottom) at a concentration of 50 µg/mL. Cells on Solvent Control were exposed to 0.5% DMSO, on Positive

Control to 20% DMSO and on Control to culture medium only. All sub-fractions were exposed to at least 3 replicates and controls in 6 replicates.

Many VLC fractions from this extraction were bioactive against the MG-63 cell line. Fraction E15074 B was then further fractionated by SPE as described in the previous section. Tubes with similar bands in TLC were combined to yield a particular sub-fraction (Figure 10). The results of the sub-fractionation are shown below.

Table 12: Sub-fractions obtained after SPE of E15074 B

Tubes	Fraction	Mass (mg)
1-4	E15074 B1	0.67
5	E15074 B2	1.61
6	E15074 B3	6.15
7-8	E15074 B4	6.11
9-13	E15074 B5	3.06
14-17	E15074 B6	1.52
18-27	E15074 B7	1.82
28	E15074 B8	2.21
29-35	E15074 B9	1.14
38-44	E15074 B10	1.77
45-48	E15074 B11	0.67

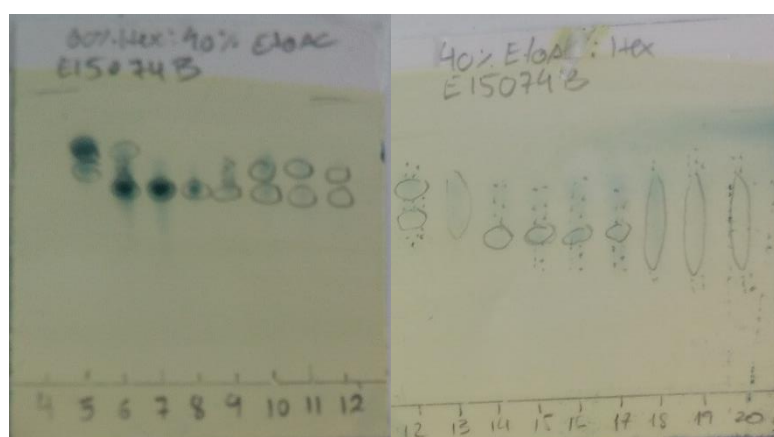


Figure 10: Example of TLC of the collection tubes, to separate the sub-fractions

As seen on the second graph of Figure 9, sub-fractions E15074 B2, E14074 B3, E15074 B4, E15074 B6, E15074 B7 and E15074 B8 caused a decrease in cell viability, particularly after 48 hours of exposure (26 to 36% viability). Fraction E15074 B4 was sent

to LC-MS, and after analysing the data (Figure 12), the sub-fractionation was proceeded by normal-phase HPLC (Figure 13). The chemical data from both the ^1H NMR and LC-MS of sample E15074B4 are represented below.

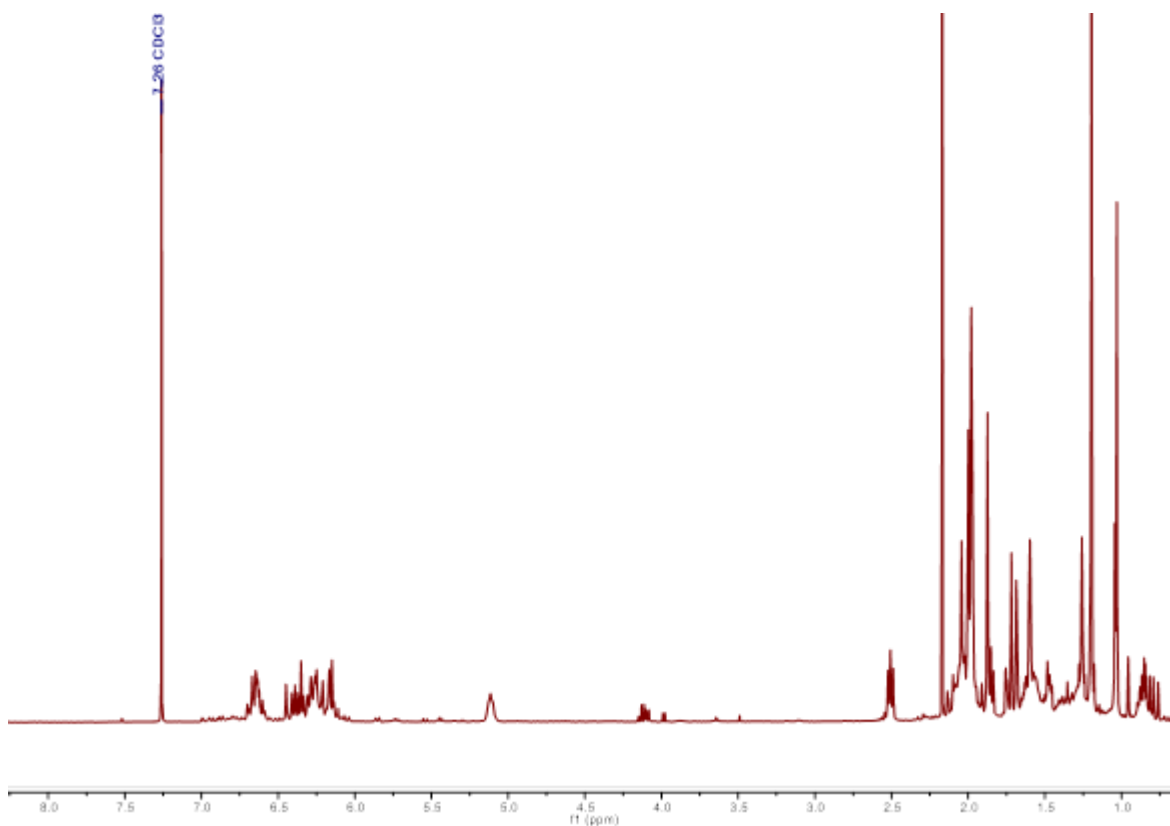


Figure 11: NMR spectrum of E15074 B4 at 400 MHz. Sample diluted in deuterated chloroform.

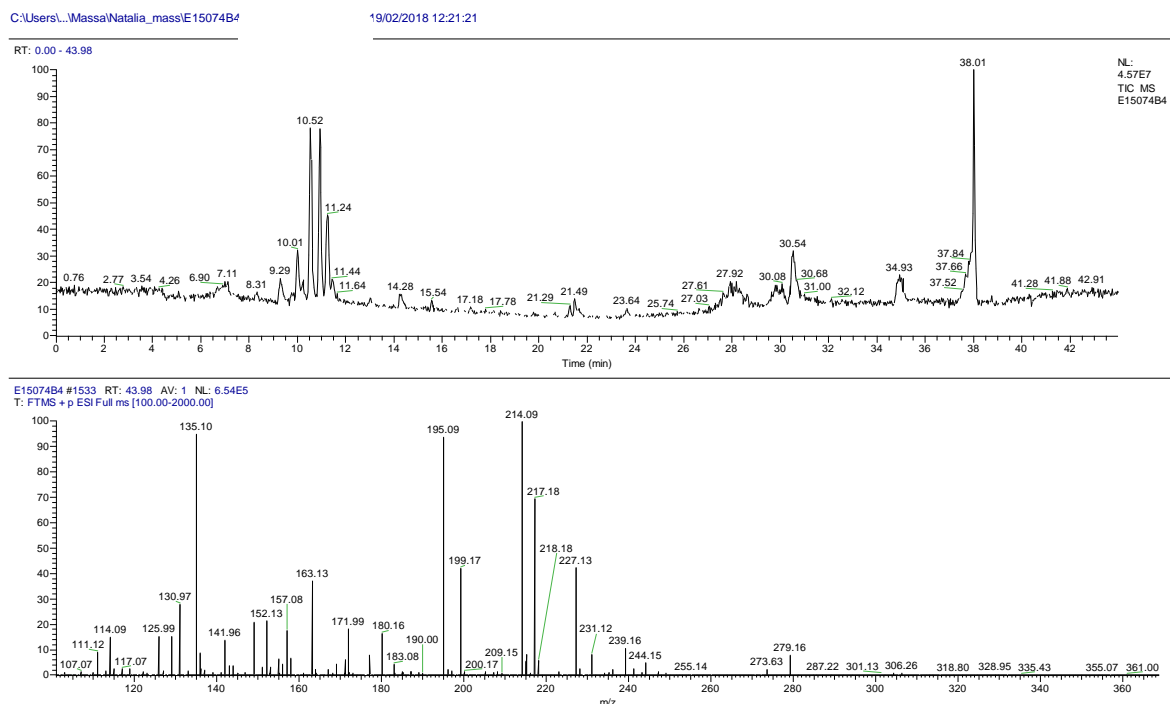


Figure 12: LC-MS data from sample E15074 B4. Sample diluted in a mixture of CHCl_3 : MeOH

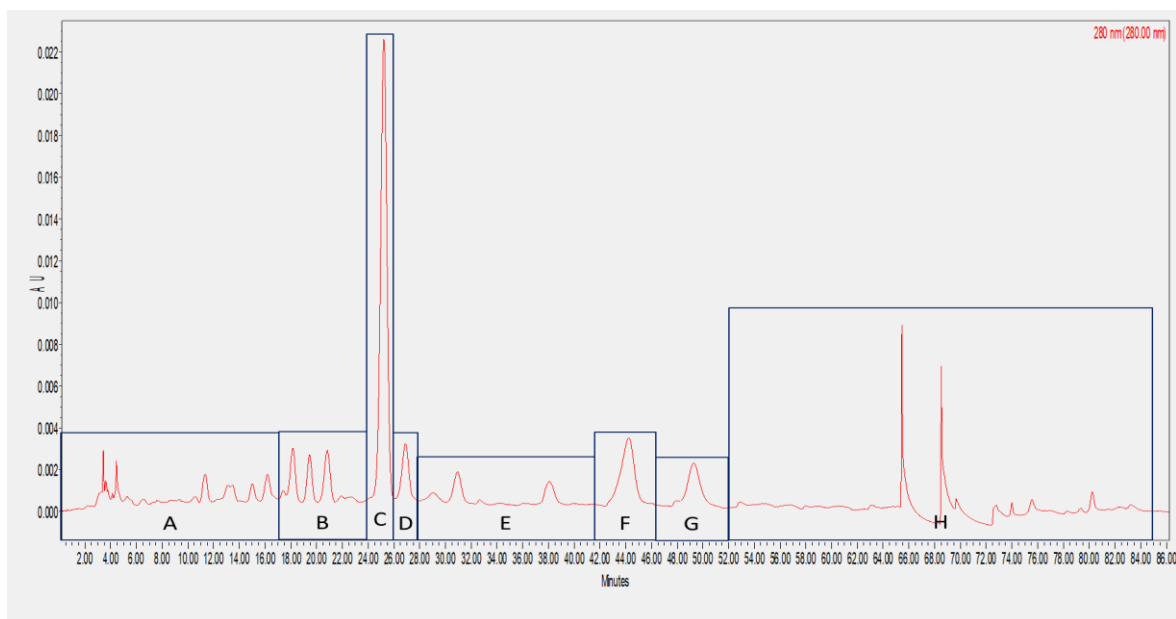


Figure 13: Chromatogram of the sub-fractionation of E15074 B4

Besides the fractions represented in Figure 11, a last sub-fraction (E15074 B4I), was collected while eluting the chromatographic column with 100% EtOAc (Table 13).

Table 13: Sub-fractions obtained after HPLC of E15074 B4

Sub-fraction	Mass (mg)
E15074 B4A	0.89
E15074 B4B	0.65
E15074 B4C	0.26
E15074 B4D	0.16
E15074 B4E	0.86
E15074 B4F	0.13
E15074 B4G	0.54
E15074 B4H	1.8
E15074 B4I	5.67

The last sub-fraction, E18074 B4I, was the most bioactive (17.3% cell viability after 48 h). Due to lack of time, it was impossible to continue with the fractionation for isolating the compound responsible for such activity.

Fractions E15074 B4 and E15074 B4I were two of the fractions from this strain with biological activity against the MG-63 cell line, causing a decrease in cell viability of 74 and 83%, respectively (Figure 9). E15074 was sent to LC-MS and later was fractionated, originating fraction E15074 B4I. From the MS of E15074 B4, numerous peaks were found,

as shown in Figure 12, and some of them look to be mass isomers. Some peaks, their respective mass and some suggested formulas are shown below.

Table 14: Data from the MS of fraction E15074 B4 and suggested hits for identification

Retention Time	m/z	Suggested Formula	Database hits
10.01	[M + H] ⁺ = 195.088	C ₈ H ₁₀ N ₄ O ₂	10 hits on IBScreen
	[M + Na] ⁺ = 217.180		7 hits on DNP
10.52	[M + H] ⁺ = 340.261	C ₂₀ H ₃₅ O ₄	2 hits on ChemSpider
	[2M + H] ⁺ = 679.516	C ₁₈ H ₃₃ N ₃ O ₃	>1000 hits on ChemSpider
	[2M + Na] ⁺ = 701.497		
11.24	[M + H] ⁺ = 453.346	C ₂₆ H ₄₇ NO ₅	17 hits on ChemSpider
	[M + Na] ⁺ = 475.326		2 on DNP
30.54	[M + H] ⁺ = 427.380	C ₂₇ H ₄₆ N ₄	4 hits on ChemSpider
	[M + Na] ⁺ = 449.362		
	[2M + Na] ⁺ = 875.736		

More ways of dereplication need to be employed in order to identify the compounds and describe their bioactivity, if they are already known, or to confirm that it is, in reality, a new compound. As this fraction, E15074 B4 was already sub fractionated, and fraction E15074 B4I is still complex, this data could be useful for further identify the peak corresponding to the bioactive compound.

4.2.3. Screening and sub-fractionation of E18179

This extraction was performed on additional biomass from another growth period of the same cyanobacterial strain (LEGE 06099) as used in 3.2.2, in order to obtain more mass for an active compound isolation. The results of the bioassays are represented in Figure 14.

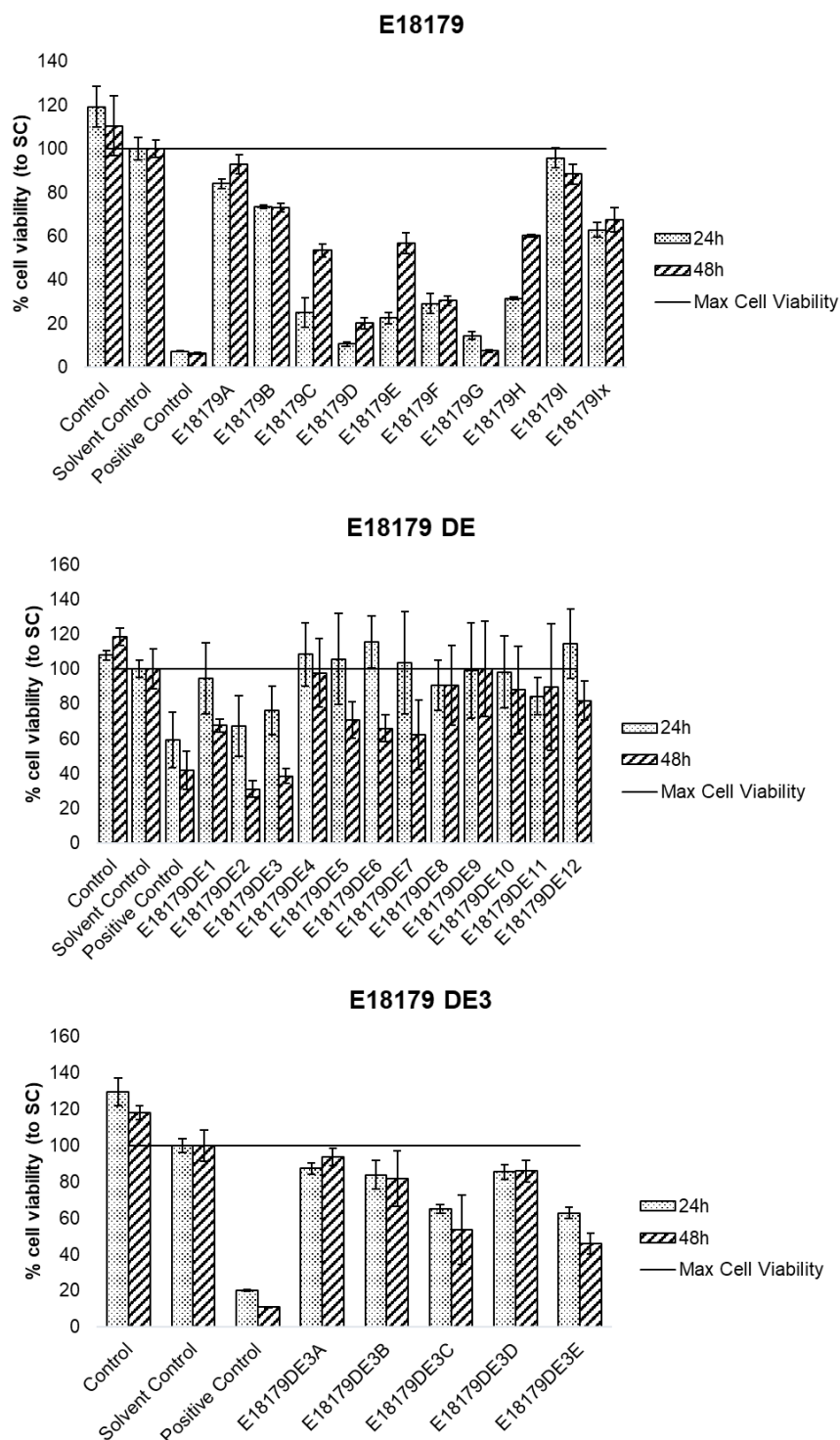


Figure 14: Cell viability after 24 and 48 hours of exposure to VLC fractions of E18179 (top), sub-fractions of E18179 DE (middle) and sub-fractions of E18179 DE3 (bottom) at a concentration of 50 µg/mL. Cells on Solvent Control were exposed to 0.5% DMSO, on Positive Control to 20% DMSO

and on Control to culture medium only. All sub-fractions were exposed to at least 3 replicates and controls to 6 replicates, and data are shown as mean +/- standard deviations.

In the fractions of the repeated biomass extraction, the compound responsible for the activity was contained in fraction E18179 D (10.6 % after 24 h and 20.1% after 48 h), instead of observing the bioactivity in fractions B and C as for the extract E15074, even though the cyanobacteria strain was the same. This can happen due to different variables of the VLC process, and some variability is normal, which enables that some compounds get distributed in adjacent fractions.

After analysis of the ¹H NMR of all fractions, it was decided that to obtain more mass, fractions E18179 D and E18179 E should be joined and then sub-fractionated by flash chromatography. After another bioassay, sub-fraction E18179 DE3 (cell viability of 38.4% after 48 h) was further sub-fractionated by HPLC. These sub-fractions were performed by lab colleagues. As seen on the two last graphs on Figure 14, the fractions did not induce a considerable decrease in cell viability, as the previous fraction had caused in the beginning. The discrepancies in our results could be due to using a different solvent to the formazan crystals, isopropanol, instead of the usual DMSO. Isopropanol does not dissolve the crystals with the same efficiency as DMSO (Twentyman and Luscombe, 1987) which can explain the higher error bars obtained on that assay. However, these sub-fractions were also tested for another work, on zebrafish embryos for the screening of anti-obesogenic compounds. The loss of activity was also observed on the zebrafish assays, and this may be due to loss of the active compound during the HPLC sub-fractionation.

4.2.4. Screening and sub-fractionation of E17165

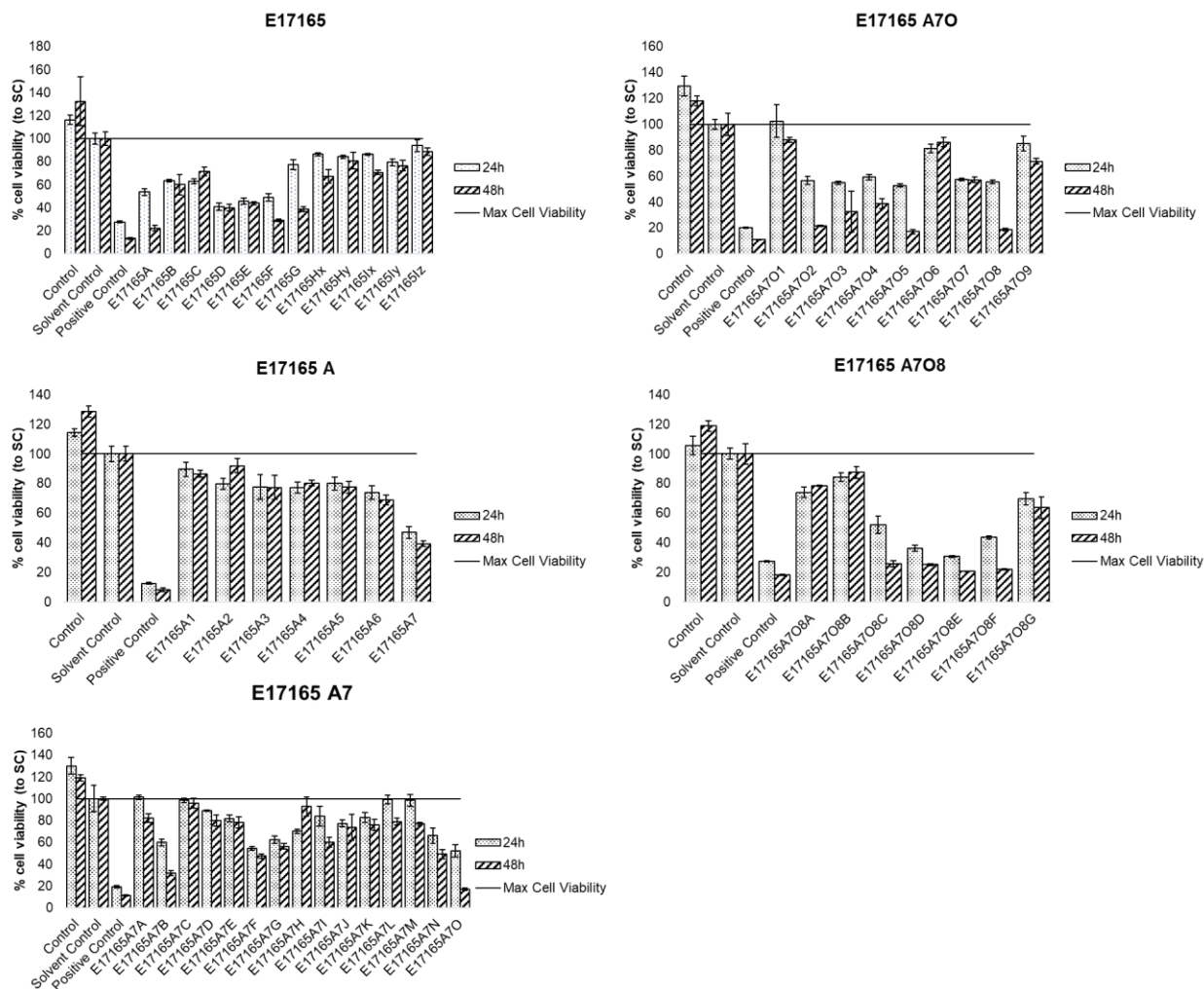


Figure 15: Cell viability after 24 and 48 hours of exposure to VLC fractions of E17165 (top, left), sub-fractions of E17165 A (top, right), sub-fractions of E17165 A7 (middle, left), E17165 A70 (middle, right) and E17165 A708 (bottom) at a concentration of 50 $\mu\text{g}/\text{mL}$. Cells on Solvent Control were exposed to 0.5% DMSO, on Positive Control to 20% DMSO and on Control to culture medium only. All sub-fractions were exposed to at least 3 replicates and controls to 6 replicates, and data are shown as mean \pm standard deviations.

Regarding this extract obtained from *Nodosilinea nodulosa* LEGE 06102 biomass, the first VLC fraction was the most bioactive on its bioassay (22.3% after 48 h). Following sub-fractionation of E17165 A by column chromatography, the obtained fractions, shown in Table 14, were subjected to another bioassay. Here, the last sub-fraction was the most active one (48 h exposure to E17165 A7 resulted in a cell viability of 39.3%).

Table 15: Column chromatography results of the fractionation of E17165 A

Tubes	Rf	Fractions	Mass (mg)
3 - 4	0.86	E17165 A1	4.14
5 - 6	0.74	E17165 A2	1.99
7 - 8	0.57	E17165 A3	1.65
9 - 11	0.47	E17165 A4	1.3
12 - 17	0.39	E17165 A5	1.81
18 - 27	0.21	E17165 A6	1.82
28 - 30	-	E17165 A7	56.6

Sub-fraction E17165 A7 was further sub-fractionated by flash chromatography (Table 15), and once again, the last sub-fraction showed higher activity, diminishing the activity of mitochondrial enzymes (16.8% after 48h).

Table 16: Sub-fractionation of E17165 A7

Tubes	Fraction	Mass (mg)
1-23	E17165 A7A	1.15
24-26	E17165 A7B	20.27
27	E17165 A7C	2.01
28-29	E17165 A7D	0.88
30-60	E17165 A7E	11.6
61-68	E17165 A7F	0.93
69-85	E17165 A7G	2.33
86-95	E17165 A7H	0.79
96-101	E17165 A7I	0.85
102-111	E17165 A7J	1.84
112	E17165 A7K	0.51
113	E17165 A7L	0.84
114	E17165 A7M	1.04
115-120	E17165 A7N	1.13
121-125	E17165 A7O	11.89

E17165 A7O was fractionated by normal-phase HPLC (Figure 16), and the resulting fractions submitted to activity tests.

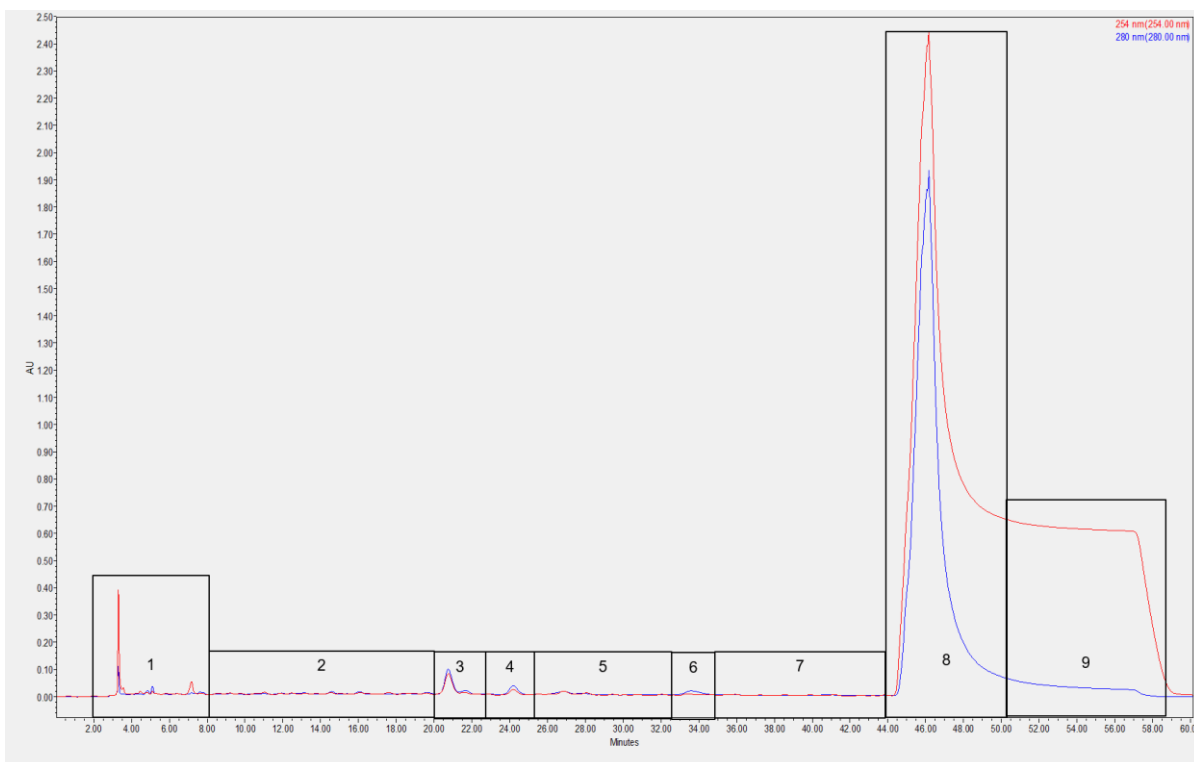


Figure 16: HPLC chromatogram of E17165 A7O

Table 17: Sub-fractions after sub-fractionation of E17165 A7O

Sub-fraction	Mass (mg)
E17165 A7O1	1.78
E17165 A7O2	1.17
E17165 A7O3	0.46
E17165 A7O4	0.52
E17165 A7O5	0.38
E17165 A7O6	0.58
E17165 A7O7	0.81
E17165 A7O8	9.92
E17165 A7O9	1.45

Sub-fractions E17165 A7O2, E17165 A7O5 and E17165 A7O8 showed a decrease in cell viability (21.5%, 17% and 18.7%, 48 h of exposure), and the first two were sent to MS/MS due to the low amount of mass, while sub-fraction E17165 A7O8 was fractionated using HPLC (Figure 19). The ^1H NMR and MS/MS of fraction E17165 A7O2 are represented below.

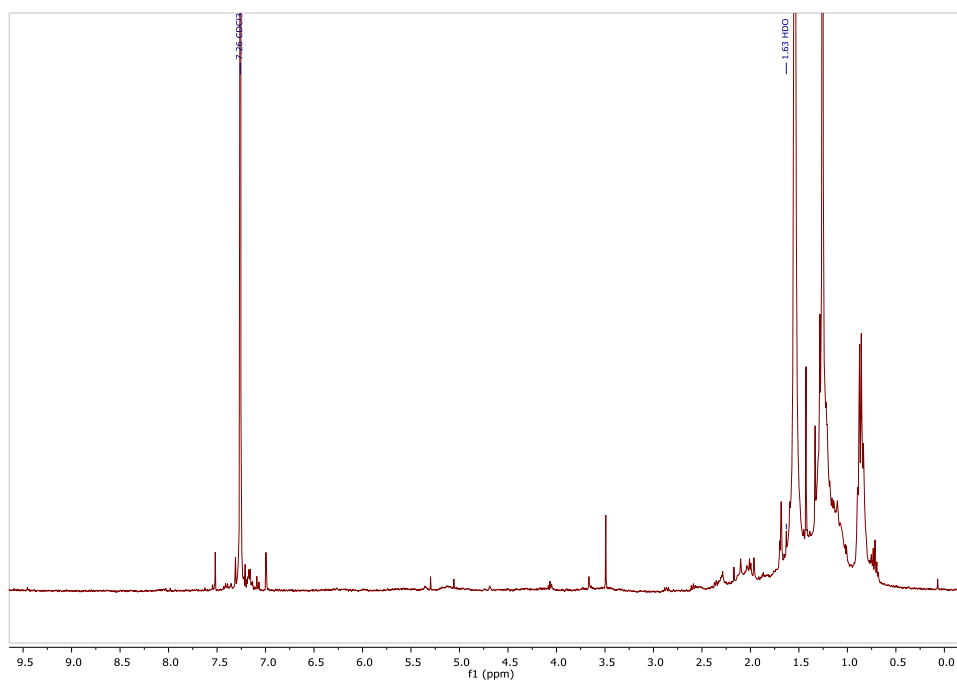


Figure 17: ^1H NMR of E17165 A7O2 at 400 MHz. Sample was diluted in deuterated chloroform

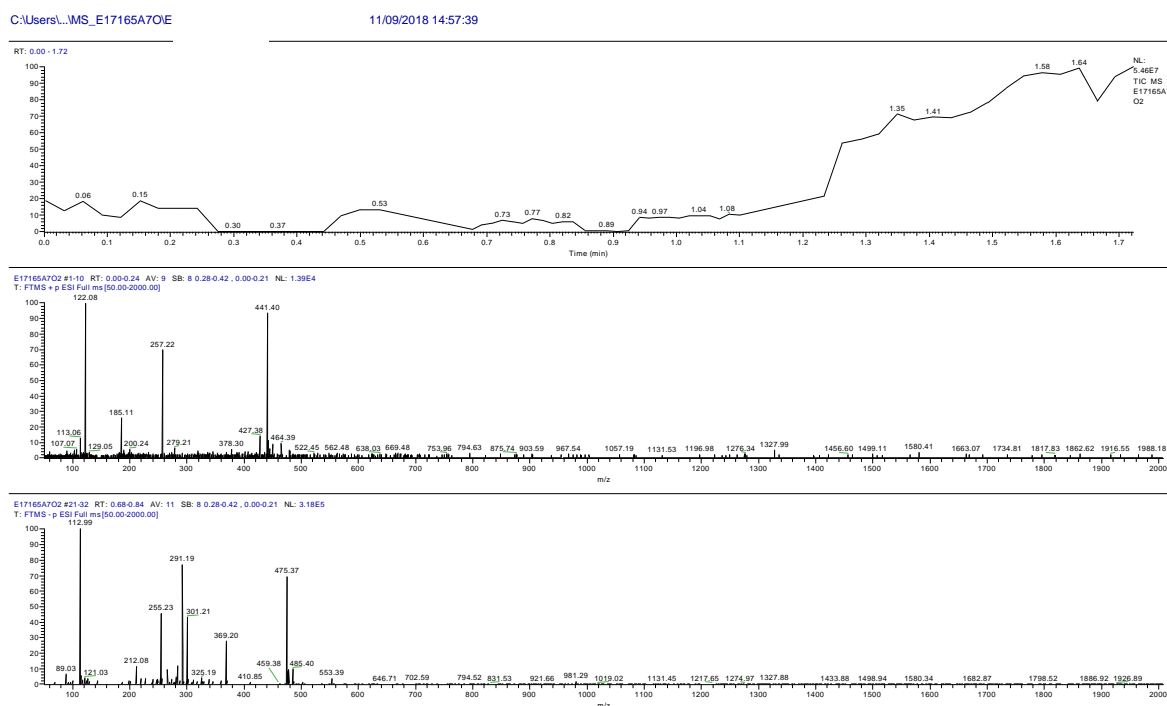


Figure 18: MS and MS/MS of E17165 A7O2. Sample was diluted in DCM. Peaks observed $[M + H]^+$ = 441.405 m/z on the positive ionisation and $[M + Cl]^-$ = 475.369 m/z on the negative ionization.

The results from the mass spectrometry of E17165 A7O5 did not show any major peaks worth elaborating on, so that data was not included.

After four fractionations of the extract of *Nodosilinea nodulosa* LEGE 06102, fraction E17165 A7O2 was isolated. When exposed to the MG-63 cell line, it drastically decreased cell viability to 21% after 48 hours of exposure (Figure 15). The last fractionation was performed by normal-phase HPLC, and this sample was eluted at 85% hexane and 15% ethyl acetate. Fraction E17165 A7O2 did not absorb at the two wavelengths supported by the UV detector, 254 and 280 nm, as verified in the chromatogram in Figure 16. After biological tests, we were left with approximately 1 mg of fraction that was sent for MS and fragmentation analysis. From these spectra, as visible in Figure 18, peaks of the MS data were identified as $[M + H]^+ = 441.405$ m/z and as $[M + Na]^+ = 463.387$ m/z, corresponding to a suggested chemical formula of $C_{26}H_{52}O_3N_2$, by both the program used to analyse the data, Thermo Xcalibur Qual Browser and the online database ChemCalc (Institute of chemical sciences and engineering ISIC, 2014). This formula suggestion was further corroborated by a peak at negative fragmentation, $[M + Cl]^- = 475.369$ m/z (Figure 18). The 1H NMR data of this fraction, performed at 400 MHz, sample dissolved using deuterated chloroform, was inconclusive due to the small amount of sample that was left. In the NMR spectra, Figure 17, peaks at 7.26 ppm, 5.30 ppm, 3.49 ppm, 2.17 ppm and 2.04 ppm corresponded to solvents and contaminations, and corresponded, respectively, to deuterated chloroform, used to dissolve the sample and to dichloromethane, methanol, acetone and water, solvent contamination from the NMR tubes. The sample was very diluted, so the peaks that correspond to our sample weren't very visible. However, besides the intense signals at the upfield of the spectra (2.5 – 0.5 ppm) that correspond to primary and secondary carbons, we can only assume that peaks around 7.5 – 7 ppm, compatible with the aromatic hydrogen atoms, may belong to the active compound.

With this information, we searched numerous online databases to see if any could indicate us if this chemical formula corresponded to any known molecule. No matches were found on AIST (National Institute of Advanced Industrial Science and Technology, 2018), Dictionary of Natural Products (CRC Press, 2018), ChemNetBase (Informa UK Limited, 2018) or IBScreen (Interbioscreen, 2017). When searching for the molecular formula on ChemSpider, eighteen molecules corresponded to our search. Comparing the information of those eighteen compounds to our data, mainly by predicting the NMR of the eighteen matches, none seemed to correspond to our fraction. However, it needs to be noted that this method may not be the most precise, because as much as we try to predict the NMR spectra as close to the same conditions to ours as possible, it isn't the most accurate way to compare and make conclusions, as the predicted spectra may be divergent from the actual spectrum. Also, as our proton spectrum was not very detailed due to the sample's dilution, some peaks may have been hidden by the impurities presented in the sample.

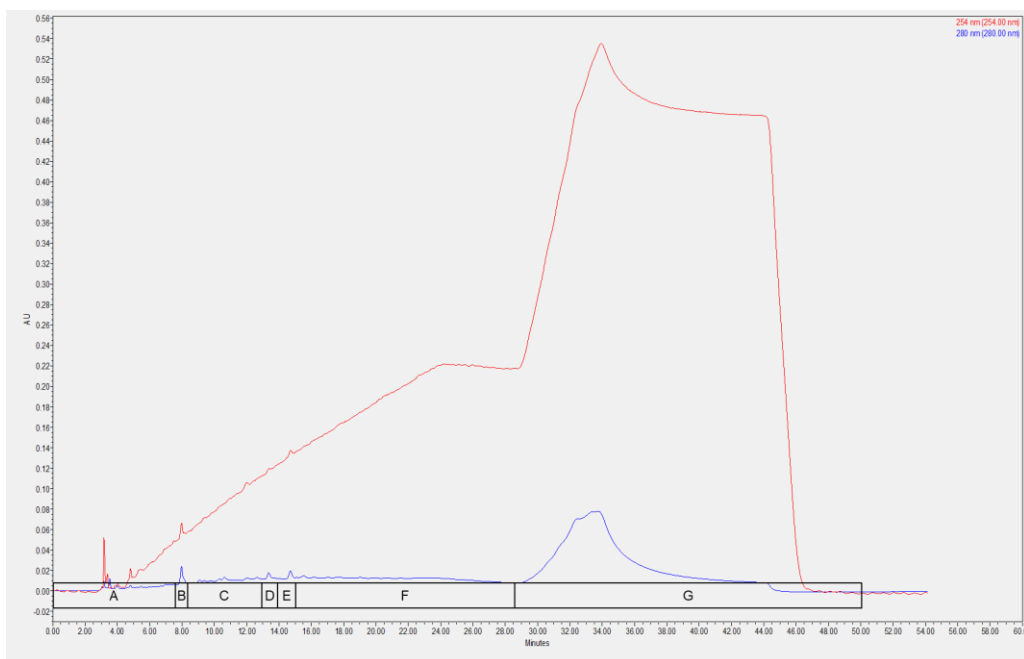


Figure 19: HPLC chromatogram of E17165 A7O8

Table 18: Sub-fractions after sub-fractionation of E17165 A7O8

Sample	Mass (mg)
E17164 A7O8A	1.84
E17164 A7O8B	~0
E17164 A7O8C	0.77
E17164 A7O8D	0.06
E17164 A7O8E	0.24
E17164 A7O8F	1.98
E17164 A7O8G	5.52

The sub-fractions were tested on the bioassay on MG-63 cells, and E17165 A7O8C to E17165 A7O8F had strong cytotoxic activities after 48 hours of exposure (25.9%, 25.3%, 20.6% and 21.9%, respectively). From those active sub-fractions, only E17164 A7O8D wasn't sent to MS/MS, due to lack of mass, since all the remaining was used on the bioassay. The mass spectrometry results showed some peaks that were transversal to all the fractions but no significant peaks that could lead to an identification were found, so the data is not shown.

4.2.5. Screening and sub-fractionation of E18184

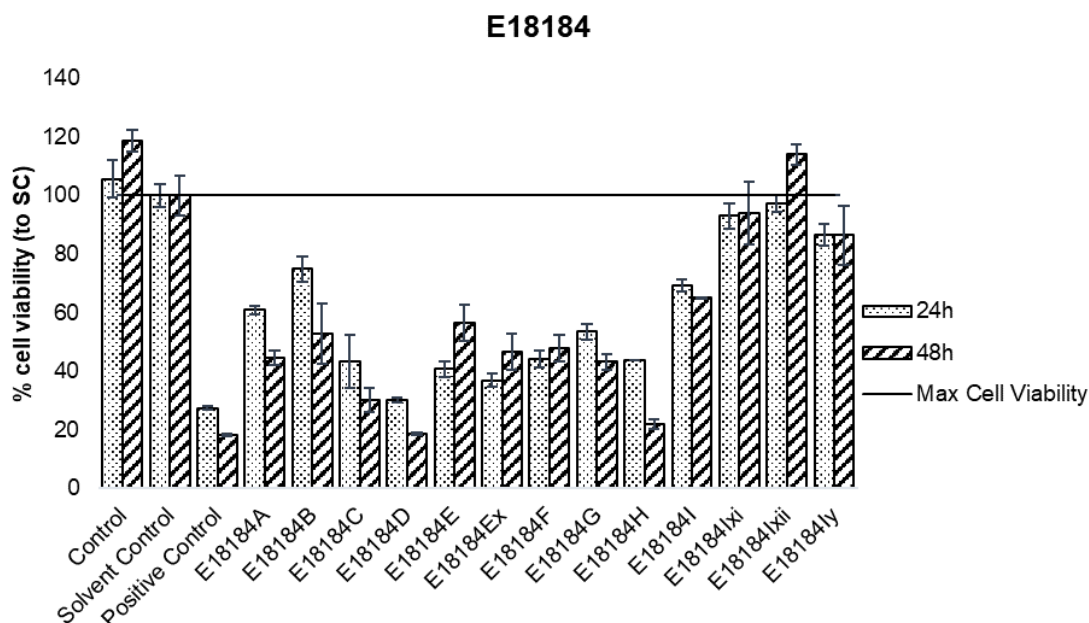


Figure 20: Cell viability after 24 and 48 hours of exposure to VLC fractions of E18184 at a concentration of 50 µg/mL. Cells on Solvent Control were exposed to 0.5% DMSO, on Positive Control to 20% DMSO and on Control to culture medium only. All fractions were exposed to at least 3 replicates and controls to 6 replicates, and data are shown as mean +/- standard deviations.

The last extraction was from biomass of the *Synechocystis* sp. LEGE 06005 strain, in which only the VLC fractions were tested on the MG-63 cell line. Multiple fractions showed an interesting decrease in cell viability (cells exposed to E18184 D displayed a viability of 18.6% and the ones exposed to E18184 H of 21.8%). This is an interesting strain to continue working on, since the total mass obtained after VLC is far superior to the mass obtained in extraction and fractionation before, due to the growth in a sleeve bag of 90 L. The ¹H NMR data is represented in Figure 21.

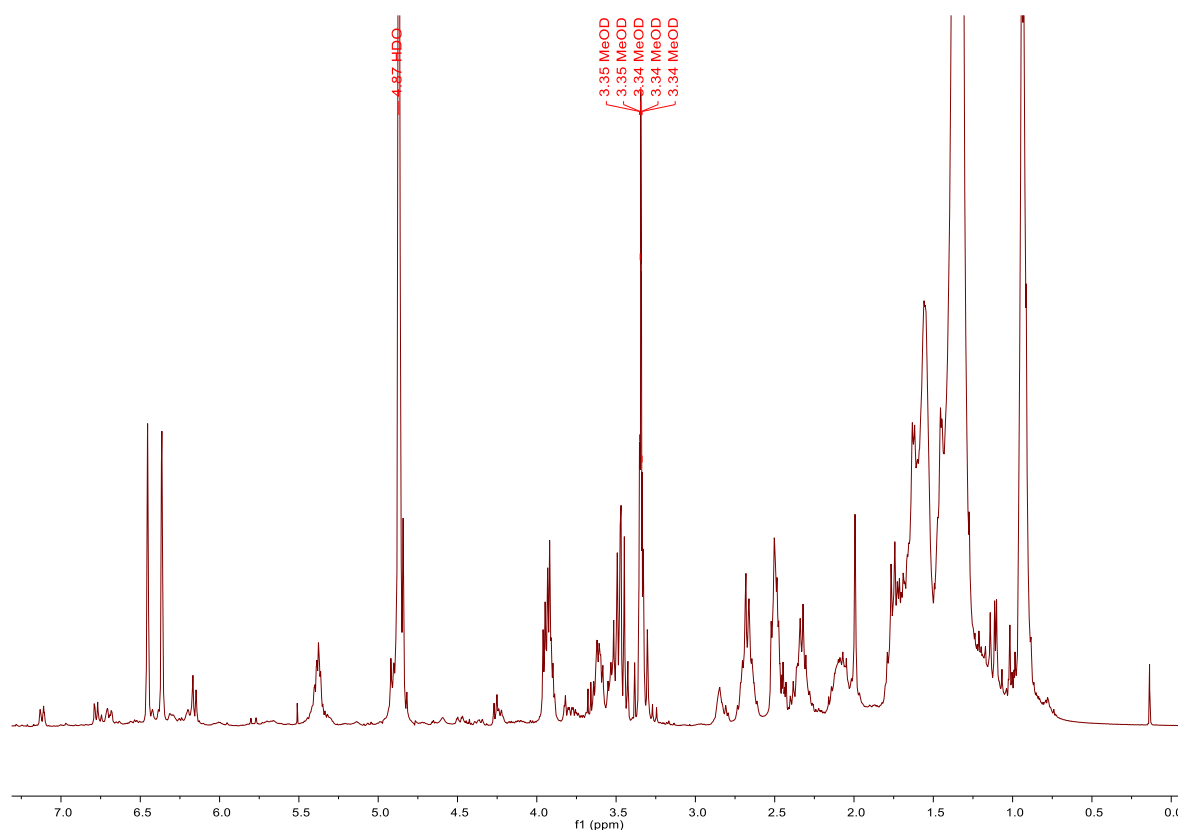


Figure 21: ^1H NMR of E18184 H at 400 MHz. Sample was diluted in deuterated MeOH

These fractions were the last ones to be tested and fraction E18184 D was the most bioactive on 2D, presenting a cell viability of 18% after 48h of exposure, followed by fraction E18184 H with 21%. As this last fraction was considered the most bioactive on the 3D bioassay, future work is going to be more focused on this fraction. So far, there isn't a lot of information regarding the chemical characterisation of this sample as the work is very preliminary, but we have a ^1H NMR spectra (Figure 21) who shows that it's still very complex, as there are a lot of signals around the high field (2.5 – 0 ppm) as well as some signals on the low field (around 7ppm), compatible with aromatic compounds.

4.3. Spheroids of HCT-116 Cell Line – 3D cell model assays

2D monolayer cultures are often criticised to be a simplistic model for anti-cancer drug discovery. To compare the results obtained on the 2D cell model and to apply an advanced, physiologically relevant method of bioactivity screening, a 3D cell culture model was developed to test the same cyanobacteria-derived fractions. For that, spheroids of the HCT 116 cell line were exposed to fractions used in the 2D assays and the results were analysed by both fluorescence spectroscopy and microscopy. The blue dye, Hoechst 33342

was used for nucleus staining of living cells and monitored the nuclear condensation, a process common to apoptosis. A red staining, Propidium Iodide, was used as an indicator for dead cells, as the dye cannot penetrate the membrane of viable cells. The green Calcein AM dye was not used for all assays, but it was added as it is as a good indicator of cell viability, which is based on the activity of cellular esterases in the cytoplasm.

4.3.1. Screening of E15074

Fractions E15074 A to E15074 H were tested on the spheroids for 48 h until fluorescent stains were added to the wells. The readings from the fluorescence plate reader and from the imaging approach with CellProfiler quantifications are shown in Figure 22.

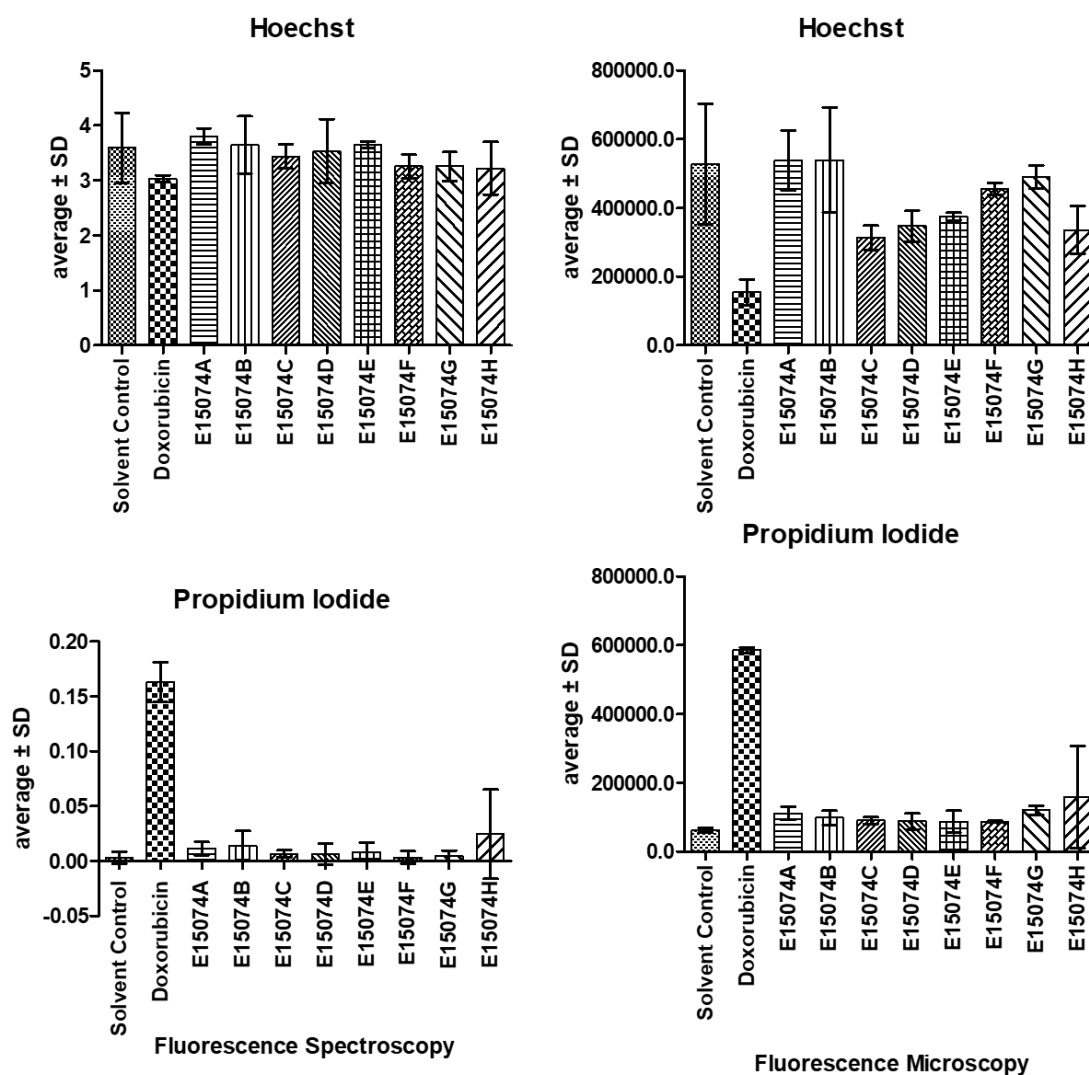


Figure 22: Data analysis of the spheroids assay after 48 h exposure of E15074 fractions (30 µg/mL) to HCT 116 spheroids. For the fluorescence readings (left), a bottom read of the plate with an integration time of 500 ms at 340Ex/280Em for Hoechst 33342 and 535Ex/586Em for Propidium iodide was used. For the microscopy imaging (right), filters for DAPI (for Hoechst 33342) and TRITC

(for propidium iodide) were chosen at an integration time of 2 and 30 ms respectively. Solvent Control was 0.5% of DMSO and Doxorubicin (4 μ M) served as positive control. All tests were performed, at least, with triplicates.

On Figure 23, images of the spheroids from the fluorescence microscopy are shown for the solvent control, positive control (Doxorubicin), and fraction E15074 H. The fraction E15074 H decreased slightly the nucleus staining and increased the staining for dead cells, however, replicates were not consistently resulting in a high standard deviation.

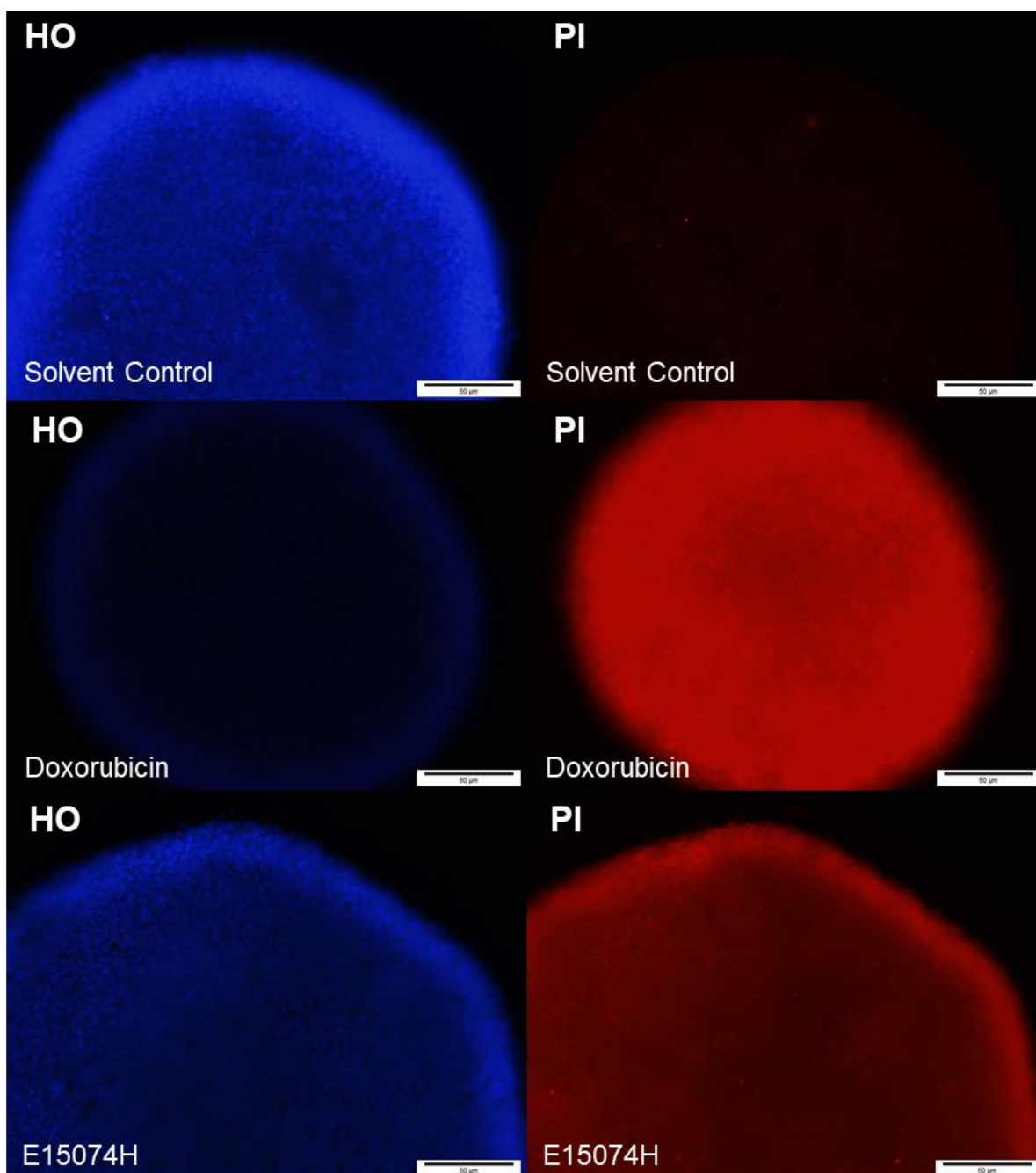


Figure 23: Microscopy imaging of HCT 116 spheroids after exposure to fraction E15074 H, Solvent Control (0.5% of DMSO) and Doxorubicin (4 μ M), as positive control. Filters for DAPI (for Hoechst

33342) and TRITC (for propidium iodide) were chosen, at an integration time of 2 and 30 ms respectively and 10x objective. All tests were performed, at least, with triplicates.

4.3.2. Screening of E18179

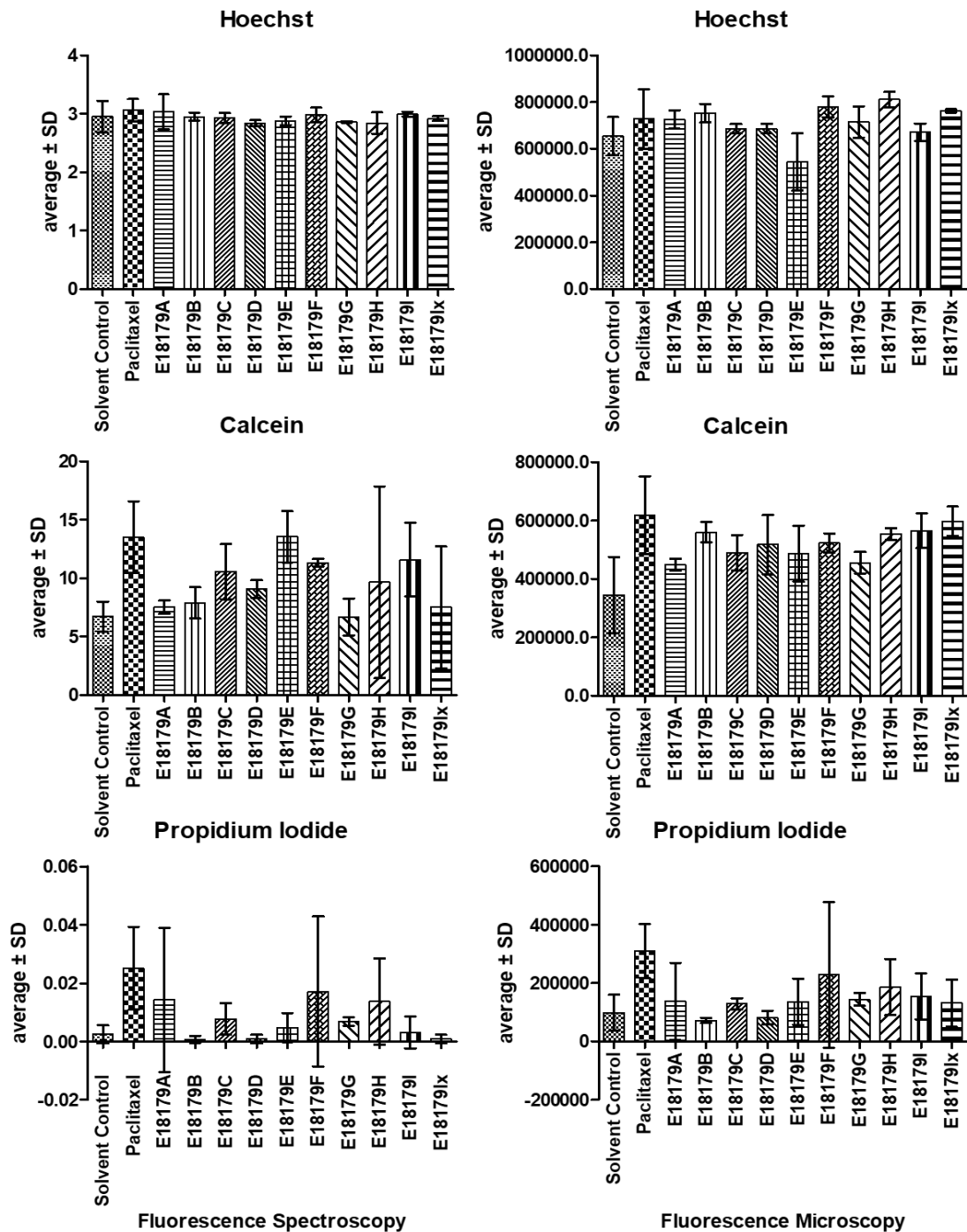


Figure 24 Data analysis of the spheroids assay after 48 h exposure of E18179 fractions (30 µg/mL) to HCT 116 spheroids. For the fluorescence readings (left), a bottom read of the plate with an integration time of 500 ms at 340Ex/280Em for Hoechst 33342, 485 Ex/538 Em for Calcein, and 535Ex/586Em for Propidium iodide was used. For the microscopy imaging (right), filters for DAPI (for Hoechst 33342), FITC (for Calcein) and TRITC (for propidium iodide) were chosen, at an integration

time of 1, 1 and 15 ms respectively. Solvent Control was 0.5% of DMSO and Paclitaxel (400 nM) served as positive control. All tests were performed, at least, with triplicates.

The fractions A-Ix from the extracts E18179 were screened on cancer spheroids using HO, PI and calcein dyes (Figure 24). No effects on the number of viable cells were observed, but some fractions seemed to increase the PI staining, however, with a high variation between the replicates. In Figure 25, the comparison is demonstrated between the solvent control, positive control, and the most bioactive fraction E18179 F.

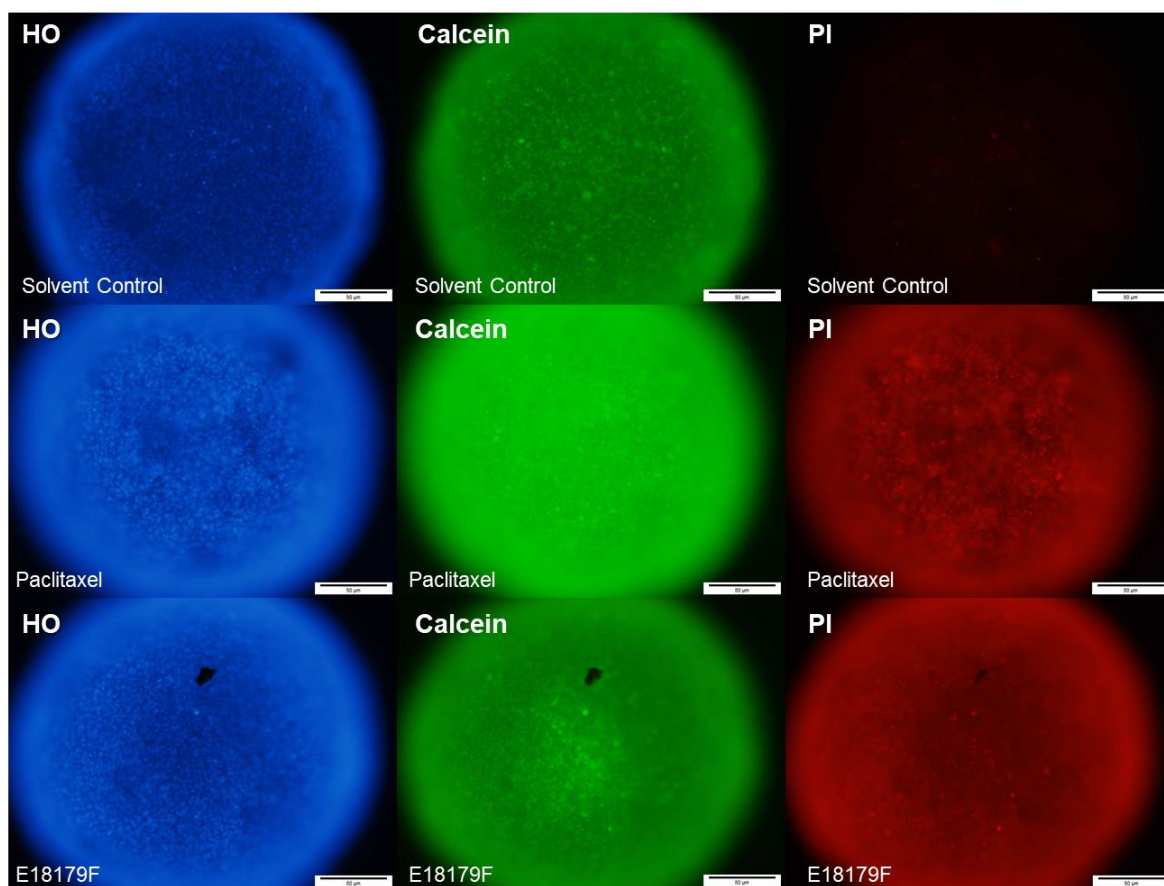


Figure 25: Microscopy imaging of HCT 116 spheroids after exposure to fraction E18179 F, Solvent Control (0.5% of DMSO) and Paclitaxel (400 nM) as positive control. Filters for DAPI (for Hoechst 33342), FITC (for Calcein) and TRITC (for propidium iodide) were chosen, at an integration time of 1, 1 and 15 ms respectively and 10x objective. All tests were performed, at least, with triplicates.

4.3.3. Screening of E17165

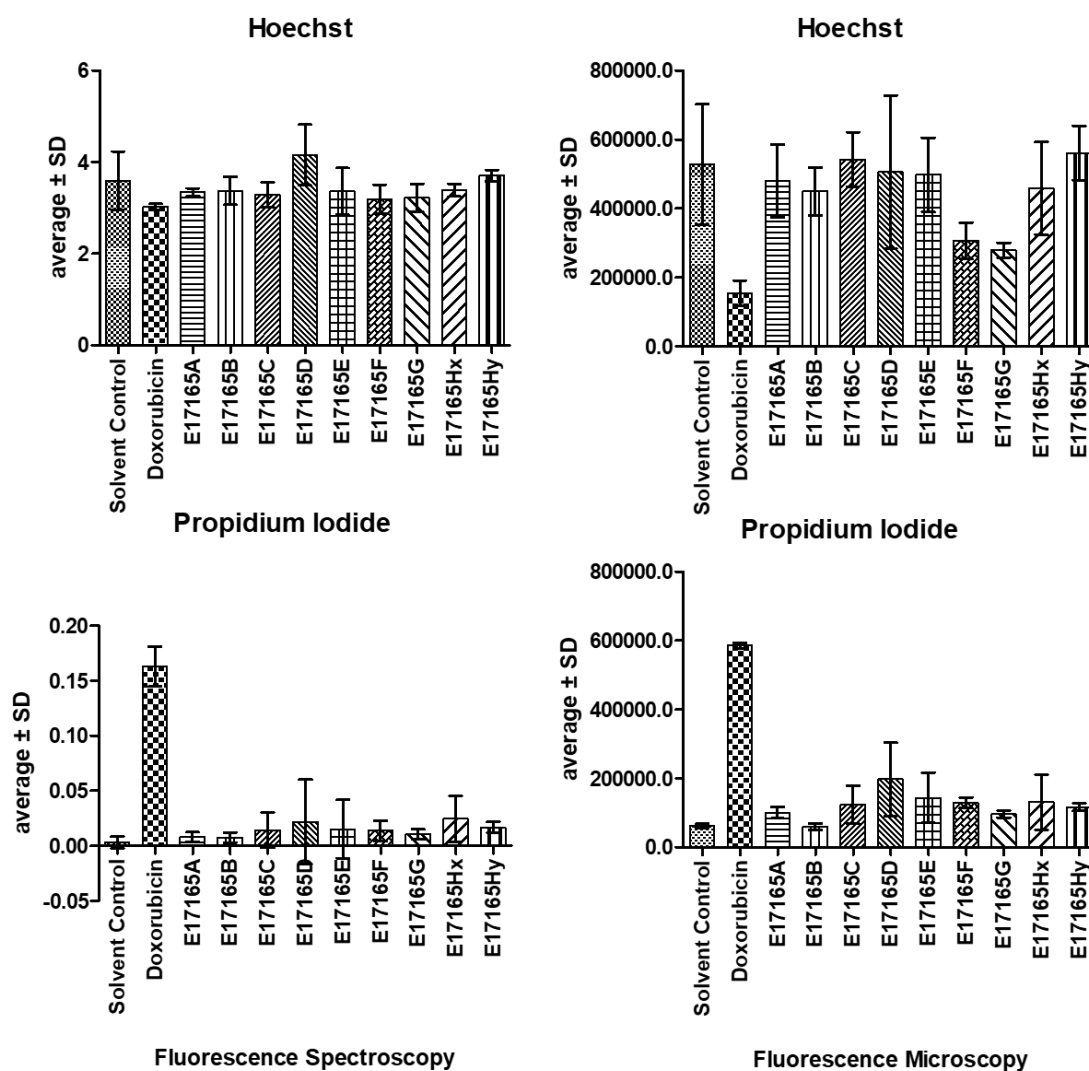


Figure 26: Data analysis of the spheroids assay after 48 h exposure of E17165 fractions (30 $\mu\text{g/mL}$) to HCT 116 spheroids. For the fluorescence spectroscopy readings (left), a bottom read of the plate with an integration time of 500 ms at 340Ex/280Em for Hoechst 33342, and 535Ex/586Em for Propidium Iodide was used. For the microscopy imaging (right), filters for DAPI (for Hoechst 33342) and TRITC (for propidium iodide) were chosen, at an integration time of 2 and 30 ms respectively. Solvent Control was 0.5% of DMSO and Doxorubicin (4 μM) served as positive control. All tests were performed, at least, with triplicates.

The results of the bioactivity screening of E17165 A to Hy sub-fractions on cancer spheroids is shown in Figure 26. Fractions E17165 F, G decreased the HO staining, while E17165 D increased the PI staining indicative of a higher number of dead cells. In this assay, the replicates were consistent. On figure 27 microscopic images of the spheroids are shown for the solvent control and positive control, and the bioactive sub-fraction E17165 D.

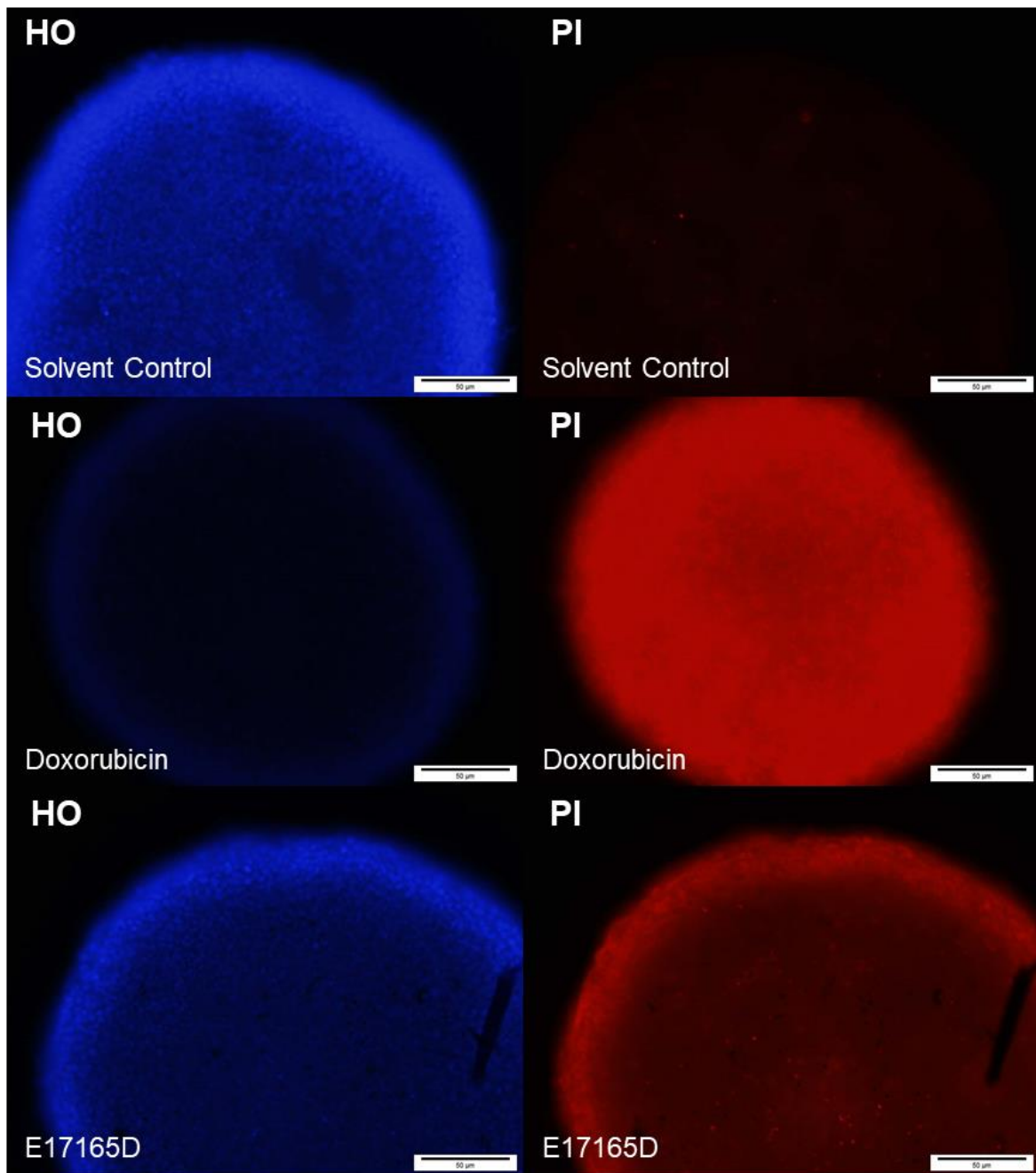


Figure 27: Microscopy imaging of HCT 116 spheroids after exposure to fraction E17165 D, Solvent Control (0.5% of DMSO) and Doxorubicin (4 μ M) as positive control. Filters for DAPI (for Hoechst 33342) and TRITC (for propidium iodide) were chosen, at an integration time of 2 and 30 ms respectively and 10x objective. All tests were performed, at least, with triplicates.

4.3.4. Screening of E18184

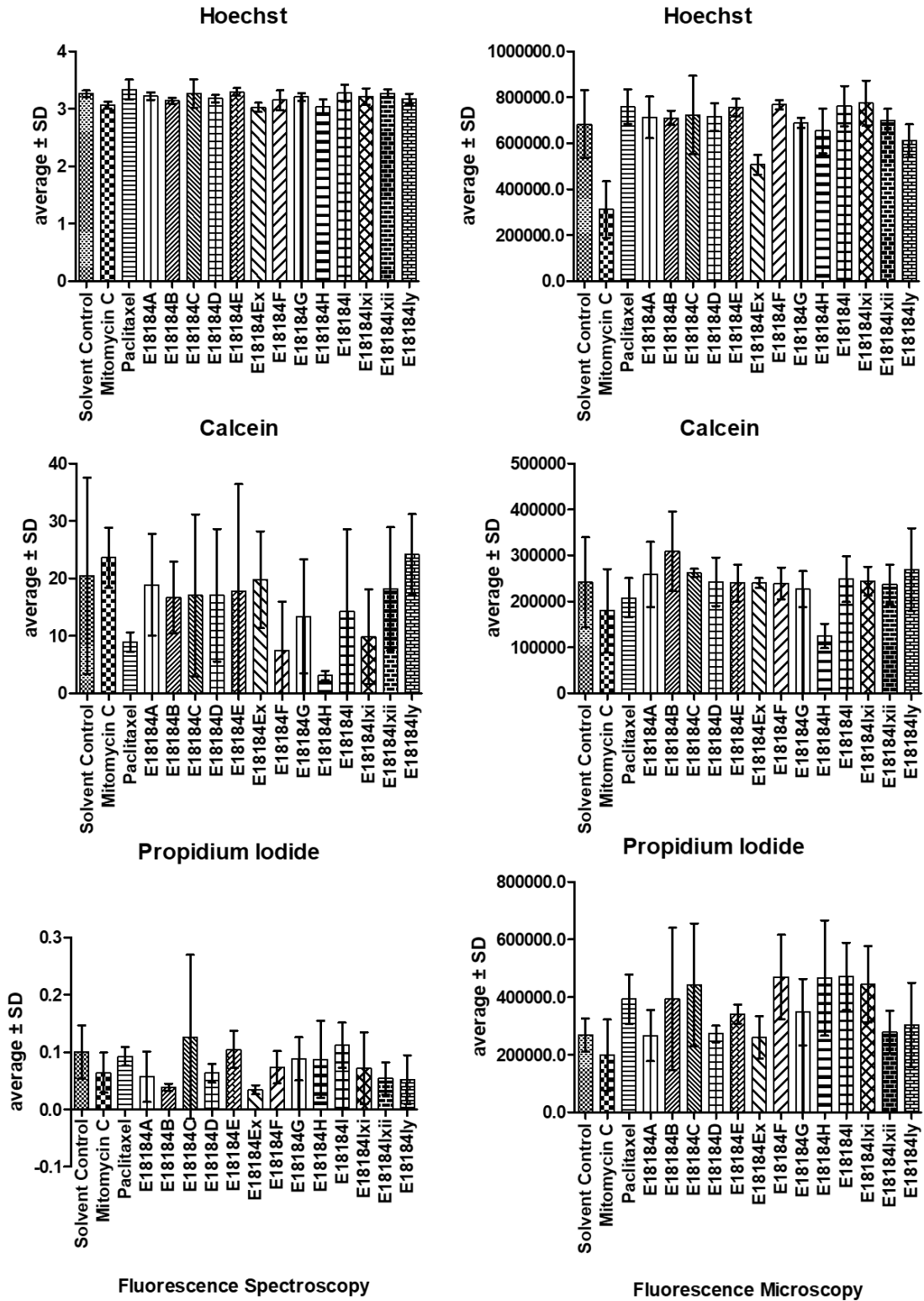


Figure 28 Data analysis of the spheroids assay after 48 h exposure of E18184 fractions (30 µg/mL) to HCT 116 spheroids. For the fluorescence readings (left), a bottom read of the plate, with an integration time of 500 ms, at 340Ex/280Em for Hoechst 33342, 485 Ex/538 Em for Calcein, and 535Ex/586Em for Propidium Iodide were used. For the microscopy imaging (right), filters for DAPI (for Hoechst 33342), FITC (for Calcein) and TRITC (for propidium iodide) were chosen, at an

integration time of 0.5, 2 and 5 ms respectively. Solvent Control was 0.5% of DMSO and Paclitaxel (400 nM) and Mitomycin C (4 μ M) worked as positive control. All tests were performed, at least, with triplicates.

The screening of fractions E18184 A – Iy is shown in Figure 28 and revealed sub-fraction E18184 H as an interesting one since it decreased the calcein signals (less viable cells) and increased the PI signal on the same time (more dead cells). The spheroids exposed to solvent control and the two positive controls are represented in Figure 29, as well as the bioactive sub-fraction E18184 H. Generally, this assay would need a repetition in order to confirm the results, since the solvent control had higher PI values as usual, as well as Paclitaxel exposure, did not result in a strong increase of PI.

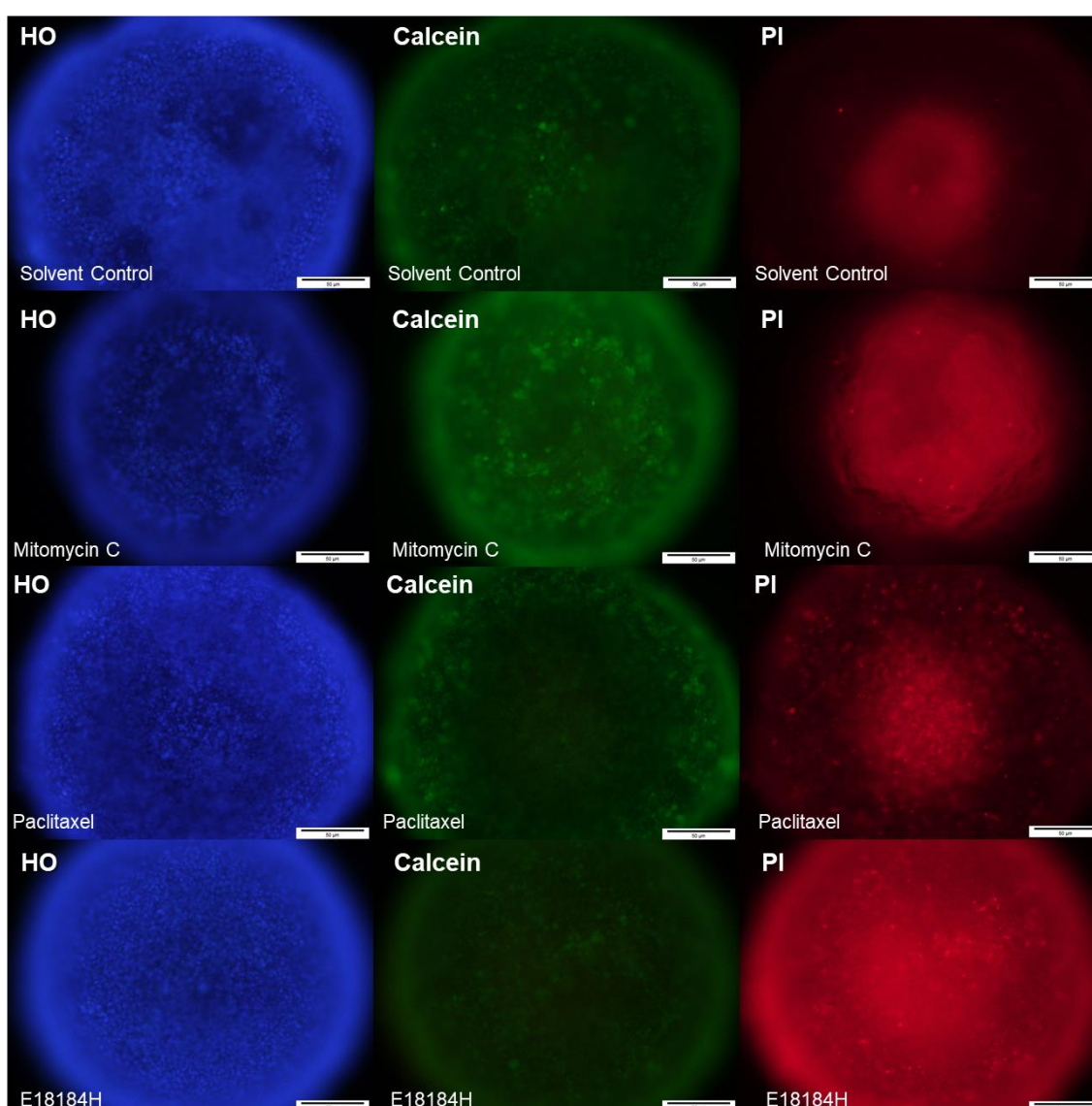


Figure 29: Microscopy imaging of HCT 116 spheroids after exposure to fraction E18184 H and to Solvent Control (0.5% of DMSO), and as positive controls, Paclitaxel (400 nM) and Mitomycin C (4 μ M). Filters for DAPI (for Hoechst 33342), FITC (for Calcein) and TRITC (for propidium iodide) were chosen, at an integration time of 0.5, 2 and 5 ms respectively and 10x objective. All tests were performed, at least, with triplicates.

5. Discussion

5.1. Bioactivity screening of cyanobacteria fractions

Earlier studies revealed promising bioactivities of the cyanobacteria belonging to the LEGE CC, using tests with crude extracts and some initial fractions of biomass for different applications and activities (Costa et al., 2013).

Synechocystis salina LEGE 06099 had already shown its potential as a producer of bioactive compounds, as (Brito et al., 2015) confirmed that this strain had encoding genes for two pathways thought to be responsible for the production of diverse secondary metabolites, NRPS and PKS. Its interest in anticancer was further proved by Costa et al., 2014, as LEGE 06099 was among one the most interesting strains regarding the isolation of bioactive compounds, proving to be bioactive against four different cancer cell lines, including the MG-63, where it displayed moderate toxicity, by both MTT and LDH (lactic dehydrogenase release) assays. Using ¹H NMR spectra of VLC fractions of LEGE 06099, (Costa et al., 2016) detected that this strain is a producer of dehydroabietic acid, compounds used as biomarkers for conifers in palaeobotany and organic geochemistry.

Nodosilinea nodulosa LEGE 06102 had already shown to have potential as a producer of bioactive compounds. Bartoloside A, an aromatic glycolipid, was isolated from crude extracts of LEGE 06102 (Leão et al., 2015) and fractions of this strain showed bioactivity against five cancer cell lines, MG-63 included (Costa et al., 2013). This strain produces its secondary metabolites mainly by the PKS biosynthesis pathway, as it has encoding genes for this pathway (Brito et al., 2015).

Synechocystis sp. LEGE 06005 also showed to be bioactive against the MG-63 cell line, the same used on this work, and on experiments on 3D cell spheroids (Sousa, 2017).

These strains were selected for this work, based on their promising results during these screenings. The cyanobacteria VLC fractions were all initially tested on 2D models and their potential for interfering with mitochondrial viability was measured. As this method is faster, easier and a cheaper process than 3D culture, as well as having a more defined protocol, the guided fractionation was made using the results from these assays. Nevertheless, all the initial VLC fractions were also tested on cell spheroids.

5.1.1. Bioactivity in 2D

The screening tests were carried out using two models to evaluate cell viability after exposure to cyanobacteria fractions, 2D and 3D cell culture models. For the monolayer cell culture model, cell viability was measured using an MTT assay, a very popular method

being widely used for this type of testing, as it is an easy and rather inexpensive method for analysing cell viability. MTT is short for 3-(4,5-dimethylthiazol-2-yl)-2,5-diphenyltetrazolium bromide, that when in contact with cells is reduced to formazan in the mitochondria of viable cells. Therefore, it is possible to access cell viability as it is directly proportional to the amount of formazan, meaning that the higher number of viable cells, more purple crystals will be present. MTT is broadly used for accessing bioactive fractions and as a guide for the fractionation of natural extracts not necessarily only from cyanobacteria, like from fungi (Alves et al., 2015), for example.

In earlier studies from the BBE group, two compounds with anticancer properties were isolated from the cyanobacteria from LEGE CC, and their mechanism of action studied. Portoamides are cyclic peptides with antiproliferative properties on cancer cells. In a work developed by (Ribeiro et al., 2017), it was shown that this compound affects energy metabolism, reducing ATP cellular content, and also affects the mitochondria's structure and function. Portoamides showed toxicity towards different cell lines, including MG-63 and HCT 116. Another isolated compound was Hierridin B, for being cytotoxic to cancer cells. Proteomics showed an increase in VDAC-1, a protein often used as a target for cancer treatment, as it is important for the regulation of mitochondrial functions (Freitas et al., 2016).

Monolayer cultures, although offering an easy and swift information towards cytotoxic compounds, are not the most representative model of cancer, thus extrapolation to *in vivo* models are often failing (Fayad et al., 2011). New models are developed to overcome these limitations and deliver more sensitive and accurate information.

5.1.2. Bioactivity in 3D

The other model chosen for this work was a 3D culture where cells were seeded into forming spheroid structures. This type of structure is more physically relevant than monolayer cultures, as it simulates both the real solid tumour as well as its microenvironment (Zhang et al., 2014). This microenvironment is very important to the tumour cells as it impacts drug sensitivity. Tumour morphology gives the cells a particular environment, such as pH content, access to O₂ or nutrients, cell-cell contact and signalization. Spheroids cells differ from monolayer cells, as they include cells in different stages, depending on their position on the spheroid. As oxygen, nutrients, and growth factors are limited in the spheroid's core, cells tend to be in a quiescent, hypoxic or even necrotic state, while the cells on the outer layer are usually proliferating cells. This diversity is analogous to what happens to tumours *in vivo*, reinforcing once more the relevance of this method (Edmondson et al., 2014). The spheroid model has been used with positive

results in what concerns the isolation and identification of bioactive compounds. Whether it is by searching for compounds that induce tumour cell apoptosis (Herrmann et al., 2008) or by studying the mitochondrial function (Zhang et al., 2014), this type of test is increasingly more and more used. (Zhang et al., 2014), was able to identify a compound, VLX600, after screening using HCT 116 spheroids, and even describe its mode of action – reduction of mitochondrial oxidative phosphorylation. On this work, we used a typical approach for evaluating the results of the exposure of fractions to cell spheroids, of staining and fluorescence reading and imaging. However, there are multiple ways to access the effect of drugs on spheroids. (Sirenko et al., 2015), for example, using the same type of staining as used on this work, but instead used an automatic imaging system, simplifying data acquisition. Other works preferred already available kits, like ELISA for example, in order to analyse not only the effects but the molecular action as well, as those kits targeted apoptosis (Herrmann et al., 2008; Zhang et al., 2014). Data analysis can also vary from work to work, depending on the preferred software. (Karlsson et al., 2012), for example, also used CellProfiler for their results.

The results from the 3D spheroids assay were assessed by microscopy and spectroscopy of fluorescence. After exposure, stains were added according to the parameters chosen to be analysed. Hoechst and Propidium Iodide were the two dyes primarily chosen, as they are widely used for identifying apoptosis. They both bind to DNA but while Hoechst is a live cell-permeable dye that stains the nuclei, propidium iodide is not permeant to live cells, so it's used as an indicator for dead cells. Calcein is a stain useful for the identification of cell viability because live cells have active esterases, who convert the nonfluorescent calcein into a green fluorescent calcein by hydrolysis. After staining, cells were fixed, and data obtained from both the spectroscopy and microscopy methods. Overall, the latter seemed more accurate for analysing the results, as we could define better the needed integration time, and control the quality of the images. One problem we kept encountering when we were reading the plate by spectroscopy was the necessity of having the spheroids always centred in the well or else the reading for that specific well wouldn't work.

When observing the graphs on Figures 22, 24, 26 and 28 it is possible to note that, on this assay, high variability was observed between replicates, especially on propidium iodide. However, a similar variability of replicates was observed by microscopy. Between the staining and fixation step, if the wells are not properly washed, some residue of staining can be left and interfere with the cell fixation. Diminishing the washing and improve the staining process are essential steps to diminish the variability (Sirenko et al., 2015). This protocol should be altered in order to obtain a more accurate reading, to shift from the 2D

cell assays to the 3D. To achieve this, it is needed to assure the reproducibility and increase the efficiency of the assay and standardize the protocol.

Overall, the results of the 3D assays were different from the results on the 2D assays, with an exception for one of the strains. This difference may be due to cell line selectivity – for 2D, osteosarcoma cells were used, while on 3D the cells were from colon carcinoma. However, some compounds will have differences in their chemical properties, as some drugs may have some difficulty to penetrate the tumour masses (Kobayashi et al., 1993). Their easiness or not into to interfere in such different cell models and their surrounding environment is due to mechanisms of resistance developed by the spheroids. Penetration of compounds along the spheroid is different being often less available on necrotic areas of the spheroid, and penetrations efficiency is also affected by the hydrophobicity of compounds, which can happen to be effective in monolayer but not in spheroids. This highlights the need to use advanced, physiologically relevant models for the discovery of novel cancer drugs from marine resources. The results from our comparative screening from 2D and 3D cancer models are in line with the previously mentioned results and confirm that the isolation of compounds should be guided by relevant screening tools.

5.1.3. Bioactive fractions in 2D vs 3D

The results obtained from both methods are summarized in the table below:

Table 19: Summary of the bioactive fractions after all the assays on both models. 2D refers to the assays on cultures of MG-63, PI refers to propidium iodide and Cal to calcein, stains used on 3D cultures of HCT 116. Bioactivity is characterized as decrease in cell viability, assessed by three levels: +++ strong bioactivity, ++ medium bioactivity, + low bioactivity or – no bioactivity.

Strain		LEGE 06099							
Extract		E15074							
Fraction		A	B	C	D	E	F	G	H
2D		+	+++	+++	++	-	+++	++	++
3D	PI	+	+	-	-	-	-	+	++
	Cal	Not tested with calcein staining							

Strain		LEGE 06099									
Extract		E18179									
Fraction		A	B	C	D	E	F	G	H	I	Ix
2D		-	-	-	+++	-	++	+++	-	-	-
3D	PI	-	-	-	-	-	++	-	+	+	-
	Cal	-	-	-	-	-	-	-	-	-	-

Strain		LEGE 06102									
Extract		E17165									
Fraction		A	B	C	D	E	F	G	Hx	Hy	
2D		++	-	-	++	+	++	++	-	-	
3D	PI	+	-	++	+++	++	++	+	++	+	
	Cal	Not tested with calcein staining									

Strain		LEGE 06005												
Extract		E18184												
Fraction		A	B	C	D	E	Ex	F	G	H	I	Ixi	Ixii	Iy
2D		+	-	++	+++	-	+	+	+	+++	-	-	-	-
3D	PI	-	-	+	-	-	-	+	-	+	+	+	-	-
	Cal	-	-	-	-	-	-	-	-	++	-	-	-	-

Overall, the fractions we considered the most bioactive in 2D also presented some bioactivity against 3D, but the most active of each did not coincide with each other, as expected.

From the same cyanobacterial strain, LEGE 06099, the results between different extractions and different models were diverse. Fraction E15074 B showed a strong 2D activity and was further fractionated, but it didn't work so strong on the 3D, where fraction E15074 H was the most interesting. This fraction also showed some bioactivity on 2D, so it could be a more interesting fraction to follow. Regarding the second extraction from different biomass of the same strain, fraction E18179 D was chosen as the most bioactive on 2D, while on the 3D, fraction E18179 F was the only one to increase more significantly the signal of PI.

For the strain LEGE 06102, fractions E17165 A and E17165 D were considered the most bioactive on 2D and 3D, respectively. Even if not very strong, E17165 A also showed some increase in PI and E17165 D displayed a moderate bioactivity on the MG-63 cell line, so although they are not directly coincident, they do share some characteristic bioactivity.

On the fractions from E18184, many showed some degree of toxicity on monolayer culture of MG-63, and in the 3D culture fractions E18184 C, E18184 F and E18184 H were all coincident with the results on 2D. Still, only fraction E18184 H showed a decrease in cell viability, as demonstrated by the calcein decrease, associated with the increase on the propidium iodide signal, so it was considered the most bioactive from this assay. As these results are coincident with the 2D results, where this fraction decreased cell viability around 80%, work will be progressed on sub-fractionating fraction H. Therefore, this fraction is the most promising to isolate a compound who is bioactive against a model of a solid tumour and a much more sensitive and relevant result.

Other works have also presented a difference for 2D and 3D screening results. (Barbone et al., 2008) observed that mesothelioma cells, when grown in monolayer, displayed various stimuli that were related to apoptosis that were not observed when the cells were grown as spheroids, as these structures developed resistance to those apoptosis signals. Sensitivity to the anti-cancer drug paclitaxel was also different when tested on spheroids, as they showed a higher percentage of survival than 2D cells (Loessner et al., 2010). Cytotoxic drugs used as a treatment for colorectal cancer, like 5-FU, oxaliplatin and irinotecan, were tested on monolayer and 3D cultures of HCT116 cell lines. The results of the monolayer exposure showed a high cytotoxicity to all the drugs, while the testing on cell spheroids showed resistance to those drugs (Karlsson et al., 2012). Cisplatin, 5-azacytidine, mitoxantrone and 5-FU again, all drugs used on chemotherapy, also induced a much stronger apoptosis response on monolayer culture than on HCT 116 spheroids. On the other hand, drugs like pimozide and tamoxifen, induced strong apoptosis on both models (Herrmann et al., 2008). In a study that compared a library of 10,000 compounds on 2D and 3D cell culture models for cancer, it was demonstrated that bioactive compounds on 2D did not correspond to bioactive compounds on 3D and that the chemical properties of bioactive compounds were different between both models (Fayad et al., 2011).

These results further confirm that in order to obtain compounds more suitable to work as therapeutics for cancer, new and more relevant models for screening should be used. The 3D cell culture of spheroids is a promising model to replace the ones currently used as a standard for isolation of bioactive compounds. To achieve that, however, the methodology still needs some improvement, to minimize errors and to speed up the work.

5.2. Difficulties in using the bioassay-guided fractionation of cyanobacteria fractions

Following a bioassay-guided fractionation for screening and isolating natural compounds is a process that is widely used, including in our lab, because is a helpful and consistent method that allows the isolation of compounds whose bioactivity is already identified (Freitas et al., 2016). In this work, this method was applied successfully as we were able to separate and simplify many fractions and to obtain some information on their chemical nature. However, this method takes a long time and a risk exists that the isolated molecule could have been previously discovered and structurally elucidated. But, in this work, the biggest disadvantage was that this methodology is sample-consuming; in each step part of the original mass is lost, whether during the sub-fractionation processes or by preparing test solutions. In the end, fractions were almost isolated, but in such a small quantity that it was impossible to continue the isolation process, or to perform more tests. Therefore, it was not possible to chemically elucidate the structure of molecules responsible for the anticancer activities that were observed in this work.

One way to surpass these obstacles is to start with a greater amount of biomass, by growing the cyanobacteria cultures on a larger scale. As mentioned, one of the strains used on this work was cultured in a sleeve bag with a capacity up to 90 L. It occupies less space than multiple flasks of cultures and requires less replication. As soon as the cyanobacteria growth reached its peak, 20 to 40 L of culture were recollected, and the same volume was replaced by new culture medium, allowing to have, in a shorter time, a greater amount of biomass. It has, of course, its disadvantages, because it requires material and place to do the setup, cultures are more susceptible to contamination, leaks or holes can cause some loss of culture, and the biomass will take longer to dry as there is more quantity. As seen on table 10 on the results, the cyanobacteria strain *Synechocystis* sp. LEGE 06005 had approximately 80 g of dry biomass at the start of the extraction, and both the extraction and fractionation yields were lower than the yields of the extraction and fractioning of smaller amounts of biomass. As the amount to work with is much larger, the method used may not be as efficient as it is with smaller amounts, so it is necessary to use a lot more of solvents, more sonication time, or even more stirring, to extract the maximum of crude. The extraction protocol needs a few adaptations when working with larger amounts of biomass, nevertheless, even though there was a slight decrease in yield, in the end, we still obtained a larger amount of crude extract and a large quantity of mass after VLC fractionation, as it was expected. Even though there was not enough time to proceed with sub-fractioning these fractions, future work will include isolation of compounds, hopefully in a quantity that could be possible to chemically elucidate completely.

6. Conclusion and future work

The aim of this work was to identify new molecules, produced by cyanobacteria as secondary metabolites, with potential bioactivity towards anticancer cells. Four different strains were screened for activity using two different *in vitro* models for testing cell viability.

The 2D bioactivity assays on MG-63 cell line successfully lead to identifying ten bioactive fractions, from which E17165 A7O2 and E14031 E5D2 are practically isolated. No hits were found during dereplication what could mean that we have potential new compounds. In order to identify the molecule, whether already known or not, future data analysis of the MS and the fragmentation data, using new and advanced dereplication techniques, like chemical networking, for example, will be necessary so we can process the information about our fractions, and achieve a chemical structure with a well-defined bioactivity. Other chemical techniques could be employed in order to obtain more information about the compounds, but more quantity of sample would be needed, to, for example, send the fraction for carbon NMR. This new information, together with the MS data we already have, could lead to the identification of the molecule.

For the fractions who still need more purifications, the bioassay-guided fractionation will be continued. E15074 B4I is promising for isolating new compounds due to its strong bioactivity. Fraction E18184 H showed potential bioactivity on both methodologies tested, 2D and 3D cell culture models. This sub-fraction is very promising as its purification could lead to the isolation of a compound active against cell spheroids, which are a more accurate representation of a solid tumour.

Different fractions showed different activities on the 2D and 3D cellular models, due to selectivity towards the cell line or to the different chemical efficacies either on monolayer or a 3D culture. Although the methodology to evaluate cell viability on 3D assays still needs improvement, to decrease the variability observed in the results, this model is a promising replacement for other assays that are not so physiologically relevant, provided the protocols are standardized.

Finally, testing these compounds on other cell lines, cancerous and not, would be interesting, as well as deciphering the mechanisms of actions behind the bioactivity.

Cyanobacteria are indeed a very interesting source of compounds, as seen from all the work that has been developed with them so far, and the more that it is yet to come, as they are just simple primordial microorganisms but an endless source of new possibilities for scientific progress.

7. References

- Abraham RJ and Rowan A (1991) Nuclear magnetic resonance spectroscopy of chlorophyll. *797-834*.
- Agrawal S, Acharya D, Adholeya A, Barrow CJ and Deshmukh SK (2017) Nonribosomal peptides from marine microbes and their antimicrobial and anticancer potential. *Frontiers in Pharmacology* **8**:1-26.
- Alberts B, Johnson A, Lewis J, Walter P, Raff M and Roberts K (2002) *Molecular Biology of the Cell 4th Edition: International Student Edition*, Routledge.
- Alves R, Preto M, Vasconcelos V, Oliveira RS and Martins R (2015) Cytotoxicity Induced by Extracts of *Pisolithus tinctorius* Spores on Human Cancer and Normal Cell Lines—Evaluation of the Anticancer Potential. *Journal of Toxicology and Environmental Health, Part A* **78**:840-847.
- Bade R, Chan H-F and Reynisson J (2010) Characteristics of known drug space. Natural products, their derivatives and synthetic drugs. *European Journal of Medicinal Chemistry* **45**:5646-5652.
- Barbone D, Yang T-M, Morgan JR, Gaudino G and Broaddus VC (2008) Mammalian target of rapamycin contributes to the acquired apoptotic resistance of human mesothelioma multicellular spheroids. *Journal of Biological Chemistry* **283**:13021-13030.
- Bentley VL, Veinotte CJ, Corkery DP, Pinder JB, LeBlanc MA, Bedard K, Weng AP, Berman JN and Dellaire G (2015) Focused chemical genomics using zebrafish xenotransplantation as a pre-clinical therapeutic platform for T-cell acute lymphoblastic leukemia. *Haematologica* **100**:70-76.
- Beutler JA (2009) Natural products as a foundation for drug discovery. *Current Protocols in Pharmacology* **46**:9-11.
- Bhatnagar I and Kim S-K (2010) Immense essence of excellence: marine microbial bioactive compounds. *Marine Drugs* **8**:2673-2701.
- Bourguet-Kondracki ML and Kornprobst JM (2014) Promising Marine Molecules in Pharmacology. *Outstanding Marine Molecules*:243-264.

- Bray F, Ferlay J, Soerjomataram I, Siegel RL, Torre LA and Jemal A (2018) Global Cancer Statistics 2018: GLOBOCAN Estimates of Incidence and Mortality Worldwide for 36 Cancers in 185 Countries, in *CA: a Cancer Journal for Clinicians*.
- Brito Â, Gaifem J, Ramos V, Glukhov E, Dorrestein PC, Gerwick WH, Vasconcelos VM, Mendes MV and Tamagnini P (2015) Bioprospecting Portuguese Atlantic coast cyanobacteria for bioactive secondary metabolites reveals untapped chemodiversity. *Algal Research* **9**:218-226.
- Butler MS, Robertson AA and Cooper MA (2014) Natural product and natural product derived drugs in clinical trials. *Natural Product Reports* **31**:1612-1661.
- Carmichael W (1992) Cyanobacteria secondary metabolites—the cyanotoxins. *Journal of Applied Bacteriology* **72**:445-459.
- Carpenter AE, Jones TR, Lamprecht MR, Clarke C, Kang IH, Friman O, Guertin DA, Chang JH, Lindquist RA and Moffat J (2006) CellProfiler: image analysis software for identifying and quantifying cell phenotypes. *Genome Biology* **7**:R100.
- Castenholz RW, Wilмотte A, Herdman M, Rippka R, Waterbury JB, Iteman I and Hoffmann L (2001) Phylum BX. cyanobacteria, in *Bergey's Manual® of Systematic Bacteriology* pp 473-599, Springer.
- Costa M, Costa-Rodrigues J, Fernandes MH, Barros P, Vasconcelos V and Martins R (2012) Marine cyanobacteria compounds with anticancer properties: A review on the implication of apoptosis. *Marine Drugs* **10**:2181-2207.
- Costa M, Garcia M, Costa-Rodrigues J, Costa MS, Ribeiro MJ, Fernandes MH, Barros P, Barreiro A, Vasconcelos V and Martins R (2013) Exploring bioactive properties of marine cyanobacteria isolated from the Portuguese coast: high potential as a source of anticancer compounds. *Marine Drugs* **12**:98-114.
- Costa MS, Rego A, Ramos V, Afonso TB, Freitas S, Preto M, Lopes V, Vasconcelos V, Magalhães C and Leão PN (2016) The conifer biomarkers dehydroabietic and abietic acids are widespread in Cyanobacteria. *Scientific Reports* **6**:23436.
- CRC Press TFG, an Informa Group company, (2018) Dictionary of Natural Products 27.1. <http://dnp.chemnetbase.com/faces/chemical/ChemicalSearch.xhtml>, September 2018

- D'incalci M, Badri N, Galmarini C and Allavena P (2014) Trabectedin, a drug acting on both cancer cells and the tumour microenvironment. *British Journal of Cancer* **111**:646.
- Dayspring TD (2011) Understanding hypertriglyceridemia in women: clinical impact and management with prescription omega-3-acid ethyl esters. *International Journal of Women's Health* **3**:87.
- Devi PU (2004) Basics of carcinogenesis. *Health Administration* **17**:16-24.
- Dvořák P, Casamatta DA, Hašler P, Jahodářová E, Norwich AR and Poulíčková A (2017) Diversity of the Cyanobacteria, in *Modern Topics in the Phototrophic Prokaryotes: Environmental and Applied Aspects* (Hallenbeck PC ed) pp 3-46, Springer International Publishing, Cham.
- Eccles R, Meier C, Jawad M, Weinmüllner R, Grassauer A and Prieschl-Grassauer E (2010) Efficacy and safety of an antiviral Iota-Carrageenan nasal spray: a randomized, double-blind, placebo-controlled exploratory study in volunteers with early symptoms of the common cold. *Respiratory Research* **11**:108.
- Edmondson R, Broglie JJ, Adcock AF and Yang L (2014) Three-dimensional cell culture systems and their applications in drug discovery and cell-based biosensors. *Assay and Drug Development Technologies* **12**:207-218.
- Edwards DJ, Marquez BL, Nogle LM, McPhail K, Goeger DE, Roberts MA and Gerwick WH (2004) Structure and biosynthesis of the jamaicamides, new mixed polyketide-peptide neurotoxins from the marine cyanobacterium *Lyngbya majuscula*. *Chemistry & Biology* **11**:817-833.
- Fayad W, Rickardson L, Haglund C, Olofsson MH, D'arcy P, Larsson R, Linder S and Fryknäs M (2011) Identification of agents that induce apoptosis of multicellular tumour spheroids: enrichment for mitotic inhibitors with hydrophobic properties. *Chemical Biology & Drug Design* **78**:547-557.
- Feinberg AP, Ohlsson R and Henikoff S (2006) The epigenetic progenitor origin of human cancer. *Nature Reviews Genetics* **7**:21.
- Freitas S, Martins R, Costa M, Leão PN, Vitorino R, Vasconcelos V and Urbatzka R (2016) Hierridin B isolated from a marine cyanobacterium alters VDAC1, mitochondrial activity, and cell cycle genes on HT-29 colon adenocarcinoma cells. *Marine Drugs* **14**:158.

- Gakidou E, Afshin A, Abajobir AA, Abate KH, Abbafati C, Abbas KM, Abd-Allah F, Abdulle AM, Abera SF and Aboyans V (2017) Global, regional, and national comparative risk assessment of 84 behavioural, environmental and occupational, and metabolic risks or clusters of risks, 1990–2016: a systematic analysis for the Global Burden of Disease Study 2016. *The Lancet* **390**:1345-1422.
- Gogineni V and Hamann MT (2017) Marine natural product peptides with therapeutic potential: Chemistry, biosynthesis, and pharmacology. *Biochimica et Biophysica Acta (BBA)-General Subjects*.
- Gutiérrez M, Suyama TL, Engene N, Wingerd JS, Matainaho T and Gerwick WH (2008) Apratoxin D, a potent cytotoxic cyclodepsipeptide from Papua New Guinea collections of the marine cyanobacteria *Lyngbya majuscula* and *Lyngbya sordida*. *Journal of Natural Products* **71**:1099-1103.
- Han B, Gross H, Goeger DE, Mooberry SL and Gerwick WH (2006) Aurilides B and C, Cancer Cell Toxins from a Papua New Guinea Collection of the Marine Cyanobacterium *Lyngbya majuscula*. *Journal of Natural Products* **69**:572-575.
- Han SI, Kim Y-S and Kim T-H (2008) Role of apoptotic and necrotic cell death under physiologic conditions. *BMB Reports* **41**:1-10.
- Hanahan D and Weinberg RA (2000) The hallmarks of cancer. *cell* **100**:57-70.
- Hanahan D and Weinberg RA (2011) Hallmarks of cancer: the next generation. *cell* **144**:646-674.
- Harris AL (2002) Hypoxia—a key regulatory factor in tumour growth. *Nature Reviews Cancer* **2**:38.
- Herrmann R, Fayad W, Schwarz S, Berndtsson M and Linder S (2008) Screening for compounds that induce apoptosis of cancer cells grown as multicellular spheroids. *Journal of Biomolecular Screening* **13**:1-8.
- Hu G-P, Yuan J, Sun L, She Z-G, Wu J-H, Lan X-J, Zhu X, Lin Y-C and Chen S-P (2011) Statistical research on marine natural products based on data obtained between 1985 and 2008. *Marine Drugs* **9**:514-525.
- Informa UK Limited (2018) Chemical Search Engine.
<http://www.chemnetbase.com/faces/search/SimpleSearch.xhtml>, September 2018

- Institute of chemical sciences and engineering ISIC (2014) Molecular Formula from Monoisotopic Mass. <http://www.chemcalc.org/>, September 2018
- Interbioscreen (2017) Chemical Search Engine. <http://mastersearch.chemexper.com/misc/hosted/ibscreen/>, September 2018
- Karlsson H, Fryknäs M, Larsson R and Nygren P (2012) Loss of cancer drug activity in colon cancer HCT-116 cells during spheroid formation in a new 3-D spheroid cell culture system. *Experimental Cell Research* **318**:1577-1585.
- Khoo BL, Chaudhuri PK, Ramalingam N, Tan DSW, Lim CT and Warkiani ME (2016) Single-cell profiling approaches to probing tumor heterogeneity. *International Journal of Cancer* **139**:243-255.
- Kim M-K, Suh DH, Seoung J, Kim HS, Chung HH and Song Y-S (2012) Autophagy as a target for anticancer therapy and its modulation by phytochemicals. *Journal of Food and Drug Analysis* **20**:241-245.
- Kobayashi H, Man S, Graham CH, Kapitain SJ, Teicher BA and Kerbel RS (1993) Acquired multicellular-mediated resistance to alkylating agents in cancer. *Proceedings of the National Academy of Sciences* **90**:3294-3298.
- Kotai J (1972) Instructions for preparation of modified nutrient solution Z8 for algae. *Norwegian Institute for Water Research, Oslo* **11**:5.
- Koyama T, Kawazoe Y, Iwasaki A, Ohno O, Suenaga K and Uemura D (2016) Anti-obesity activities of the yoshinone A and the related marine γ -pyrone compounds. *The Journal of Antibiotics* **69**:348.
- Kwan JC, Taori K, Paul VJ and Luesch H (2009) Lyngbyastatins 8–10, elastase inhibitors with cyclic depsipeptide scaffolds isolated from the marine cyanobacterium *Lyngbya semiplena*. *Marine Drugs* **7**:528-538.
- Leão PN, Costa M, Ramos V, Pereira AR, Fernandes VC, Domingues VF, Gerwick WH, Vasconcelos VM and Martins R (2013) Antitumor activity of hierridin B, a cyanobacterial secondary metabolite found in both filamentous and unicellular marine strains. *PloS one* **8**:e69562.
- Leão PN, Nakamura H, Costa M, Pereira AR, Martins R, Vasconcelos V, Gerwick WH and Balskus EP (2015) Biosynthesis-Assisted Structural Elucidation of the Bartolosides,

Chlorinated Aromatic Glycolipids from Cyanobacteria. *Angewandte Chemie International Edition* **54**:11063-11067.

Leão PN, Pereira AR, Liu W-T, Ng J, Pevzner PA, Dorrestein PC, König GM, Vasconcelos VM and Gerwick WH (2010) Synergistic allelochemicals from a freshwater cyanobacterium. *Proceedings of the National Academy of Sciences* **107**:11183-11188.

Loessner D, Stok KS, Lutolf MP, Hutmacher DW, Clements JA and Rizzi SC (2010) Bioengineered 3D platform to explore cell–ECM interactions and drug resistance of epithelial ovarian cancer cells. *Biomaterials* **31**:8494-8506.

Matthew S, Schupp PJ and Luesch H (2008) Apratoxin E, a cytotoxic peptolide from a Guamanian collection of the marine cyanobacterium *Lyngbya bouillonii*. *Journal of Natural Products* **71**:1113-1116.

Mayer A (2017) Marine pharmaceuticals: the clinical pipeline.
http://marinepharmacology.midwestern.edu/clinical_pipeline.html, September 2018

Mayer AM, Glaser KB, Cuevas C, Jacobs RS, Kem W, Little RD, McIntosh JM, Newman DJ, Potts BC and Shuster DE (2010) The odyssey of marine pharmaceuticals: a current pipeline perspective. *Trends in Pharmacological Sciences* **31**:255-265.

McFadden GI (1999) Endosymbiosis and evolution of the plant cell. *Current Opinion in Plant Biology* **2**:513-519.

Mevers E, Liu W-T, Engene N, Mohimani H, Byrum T, Pevzner PA, Dorrestein PC, Spadafora C and Gerwick WH (2011) Cytotoxic veraguamides, alkynyl bromide-containing cyclic depsipeptides from the marine cyanobacterium cf. *Oscillatoria margaritifera*. *Journal of Natural Products* **74**:928-936.

Montaser R, Abboud KA, Paul VJ and Luesch H (2010) Pitiprolamide, a proline-rich dolastatin 16 analogue from the marine cyanobacterium *Lyngbya majuscula* from Guam. *Journal of Natural Products* **74**:109-112.

Montaser R, Paul VJ and Luesch H (2011) Pitipeptolides C–F, antimycobacterial cyclodepsipeptides from the marine cyanobacterium *Lyngbya majuscula* from Guam. *Phytochemistry* **72**:2068-2074.

- Moosova Z, Hrouzek P, Kapuscik A, Blaha L and Adamovsky O (2018) Immunomodulatory effects of selected cyanobacterial peptides in vitro. *Toxicon* **149**:20-25.
- National Institute of Advanced Industrial Science and Technology (2018) AIST: Spectral Database for Organic Compounds, SDBS. https://sdb.sdb.aist.go.jp/sdb/cgi-bin/direct_frame_top.cgi, September 2018
- Newland AM, Li JX, Wasco LE, Aziz MT and Lowe DK (2013) Brentuximab Vedotin: A CD 30-Directed Antibody-Cytotoxic Drug Conjugate. *Pharmacotherapy: The Journal of Human Pharmacology and Drug Therapy* **33**:93-104.
- Nicolini A, Carpi A, Ferrari P, Mario Biava P and Rossi G (2016) Immunotherapy and hormone-therapy in metastatic breast cancer: A review and an update. *Current Drug Targets* **17**:1127-1139.
- Ramos V, Morais J, Castelo-Branco R, Pinheiro Â, Martins J, Regueiras A, Pereira AL, Lopes VR, Frazão B, Gomes D, Moreira C, Costa MS, Brûle S, Faustino S, Martins R, Saker M, Osswald J, Leão PN and Vasconcelos VM (2018) Cyanobacterial diversity held in microbial biological resource centers as a biotechnological asset: the case study of the newly established LEGE culture collection. *Journal of Applied Phycology* **30**:1437-1451.
- Ribeiro T, Lemos F, Preto M, Azevedo J, Sousa ML, Leao PN, Campos A, Linder S, Vitorino R and Vasconcelos V (2017) Cytotoxicity of portoamides in human cancer cells and analysis of the molecular mechanisms of action. *PloS one* **12**:e0188817.
- Royal Society of Chemistry (2015) ChemSpider Advanced Search. <http://www.chemspider.com/FullSearch.aspx>, September 2018
- Ruiz-Torres V, Encinar JA, Herranz-López M, Pérez-Sánchez A, Galiano V, Barrajon-Catalán E and Micol V (2017) An updated review on marine anticancer compounds: The use of virtual screening for the discovery of small-molecule cancer drugs. *Molecules* **22**:1037.
- Schopf JW (1993) Microfossils of the Early Archean Apex chert: new evidence of the antiquity of life. *Science* **260**:640-646.
- Shishido T, Humisto A, Jokela J, Liu L, Wahlsten M, Tamrakar A, Fewer D, Permi P, Andreote A and Fiore M (2015) Antifungal compounds from cyanobacteria. *Marine Drugs* **13**:2124-2140.

- Sirenko O, Mitlo T, Hesley J, Luke S, Owens W and Cromwell EF (2015) High-content assays for characterizing the viability and morphology of 3D cancer spheroid cultures. *Assay and Drug Development Technologies* **13**:402-414.
- Sousa ML (2017) Cyanobacterial bioactive metabolites for anticancer drug discovery: Characterization of new compounds and molecular mechanisms in physiologically relevant 3D cell culture, in *8th International Conference on Marine Biotechnology*.
- Twentyman PR and Luscombe M (1987) A study of some variables in a tetrazolium dye (MTT) based assay for cell growth and chemosensitivity. *British Journal of Cancer* **56**:279.
- Walsby AE (1994) Gas vesicles. *Microbiological Reviews* **58**:94-144.
- Whitton BA and Potts M (2012) Introduction to the cyanobacteria, in *Ecology of Cyanobacteria II* pp 1-13, Springer.
- World Health Organization (2018) Cancer. <https://www.who.int/cancer/en/>, September 2018
- Zanchett G and Oliveira-Filho EC (2013) Cyanobacteria and cyanotoxins: from impacts on aquatic ecosystems and human health to anticarcinogenic effects. *Toxins* **5**:1896-1917.
- Zhang X, Fryknäs M, Hernlund E, Fayad W, De Milito A, Olofsson MH, Gogvadze V, Dang L, Pålman S and Schughart LAK (2014) Induction of mitochondrial dysfunction as a strategy for targeting tumour cells in metabolically compromised microenvironments. *Nature Communications* **5**:3295.
- Zhang Y-J, Wen C-L, Qin Y-X, Tang X-M, Shi M-M, Shen B-Y and Fang Y (2017) Establishment of a human primary pancreatic cancer mouse model to examine and investigate gemcitabine resistance. *Oncology Reports* **38**:3335-3346.

8. Appendix


Appendix I – Poster presentation – “Bioactivity screening of cyanobacteria for the isolation of novel anticancer compounds using 2D and 3D cell culture models.” presented at the *IMMR - International Meeting on Marine Research*, 5 and 6th of July 2018, Peniche, Leiria, Portugal

Bioactivity screening of cyanobacteria for the isolation of novel anticancer compounds using 2D and 3D cell culture models

Leonor Ferreira^{1,2,3,*}, Maria Lígia Sousa^{1,3}, Marco Preto¹, Vítor Vasconcelos^{1,3}, Ralph Urbatzka^{1,*}

¹ CIIMAR, Centro Interdisciplinar de Investigação Marinha e Ambiental; ² ICBAS, Instituto de Ciências Biomédicas Abel Salazar (Universidade Porto); ³ FCUP, Faculdade de Ciências da Universidade do Porto

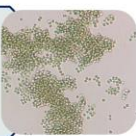
*Correspondence: Leonor Ferreira, leonor.amaral.s.f@gmail.com; Ralph Urbatzka, rurbatzka@ciimar.up.pt



Introduction

Cyanobacteria

- Photosynthetic prokaryote microorganisms
- Ubiquitous in diverse types of ecosystems
- Production of biologically active secondary metabolites
 - Antibacterial
 - Antifouling
 - Anticancer
- Major interest for marine biotechnology
- Source of new drugs




Cancer

- Second biggest cause of mortality in the world
- Number of new cases expected to rise by 70%

Cell models for bioactivity assays


2D Cell Culture

- Easier and less expensive work
- Previously established protocols
- Cell line used: MG-63 human osteosarcoma

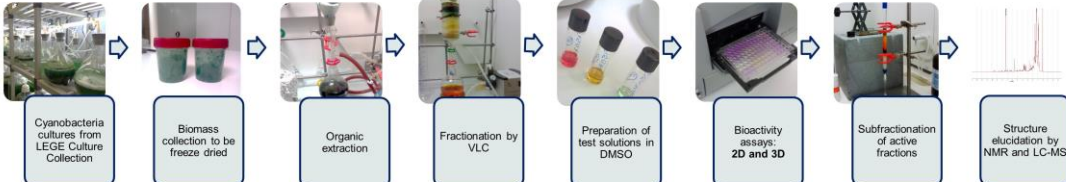


3D Cell Culture

- More sensitive and accurate representation of tumour tissue
- Physiologically more relevant
- Techniques are still being improved
- Cell line used: HCT 116 human colon carcinoma



Methodology




Results

2D

Nodosilinea nodulosa LEGE 06102

% Cell viability (vs Solvent Control) after 48h of exposure - MTT Assay




3 subfractionations

Structure elucidation by NMR and LC-MS techniques

Future subfractionation by HPLC for isolation of active compound

Synechocystis salina LEGE 06099

% Cell viability (vs Solvent Control) after 48h of exposure - MTT Assay



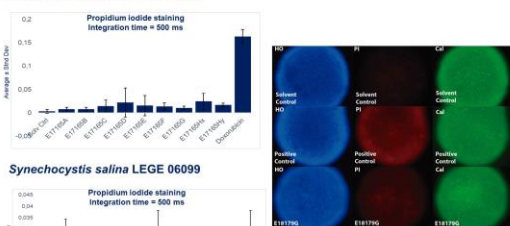
2 subfractionations

Analysis of the NMR spectra to decide next step

3D

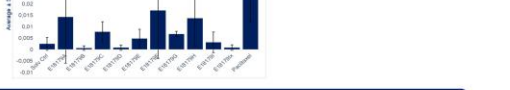
Nodosilinea nodulosa LEGE 06102

Propidium iodide staining
Integration time = 500 ms



Synechocystis salina LEGE 06099

Propidium iodide staining
Integration time = 500 ms



Final Remarks

- Compounds were successfully isolated using the 2D bioactivity assays
- 3D methodology needs to be improved in order to reduce the variability in the results
- Different fractions show different activities on the 2D and 3D cellular model
- Selectivity or chemical properties of compounds may be different towards cells grown as monolayer or as spheroid
- Ongoing work is being developed using these two methods to validate the bioactivity of potential isolated compounds

Strain	06102										06099									
	Fractions										Fractions									
2D	MTT										MTT									
	PI										PI									
3D	HO										HO									
	Cal										Cal									

Stainings: PI - Propidium iodide; HO - Hoechst; Cal - Calcein

References

Cancer. (2018, February 15). Retrieved July 1, 2018, from <http://www.who.int/cancer/>

Cotella, G., Fracchi, F., Gallo, M., Chiara, A. D., Aprea, G., Rusci, C., Nigro, F. D. (2018). Serrania Spheroids and Organoids—Promising Tools in the Era of Personalized Medicine. *International Journal of Molecular Sciences* 19(2), 615. doi:10.3390/ijms19020615

Leão, P. N., Engene, N., Antunes, A., Gewick, W. H., & Vasconcelos, V. (2012). The chemical ecology of cyanobacteria. *Natural Product Reports*, 29(3), 372–391. <http://dx.doi.org/10.1039/c2np00079f>

Ramos, V., Moraes, J., Castelo-Branco, R., Pinheiro, A., Martins, J., Regueiras, A., Pereira, A.L., Lopes, V., Frazão, B., Gomes, D., Moreira, C., Costa, M.S., Brde, S., Faustino, S., Martins, R., Saker, M., Oswald, J., Leão, P.N., Vasconcelos, V.M. (2018). Cyanobacterial diversity held in mBRCs as a biotechnological asset: the case study of the newly established LEGE Culture Collection. *Journal of Applied Phycology*. DOI: 10.1007/s10811-018-1369-y

Acknowledgments & Funding sources

This work was supported by the project INNOVMAR - Innovation and Sustainability in the Management and Exploitation of Marine Resources (reference NORTE-01-0145-FEDER-000035, within the research line NOVELMAR, supported by North Portugal Regional Operational Program (NORTE 2020), under the PORTUGAL 2020 Partnership Agreement, through the European Regional Development Fund (ERDF).

Leonor Ferreira would also like to thank ICBAS for funding the author's presence in IMMR'18